University of South-Eastern Norway
Faculty of Technology, Natural Sciences, and Maritime Sciences
—
Master Thesis in Systems Engineering with Embedded Systems
Department of Science and Industry Systems
May 28, 2021

Jan Ali

Power Grid Noise Analysis Using Empirical Mode Decomposition Method

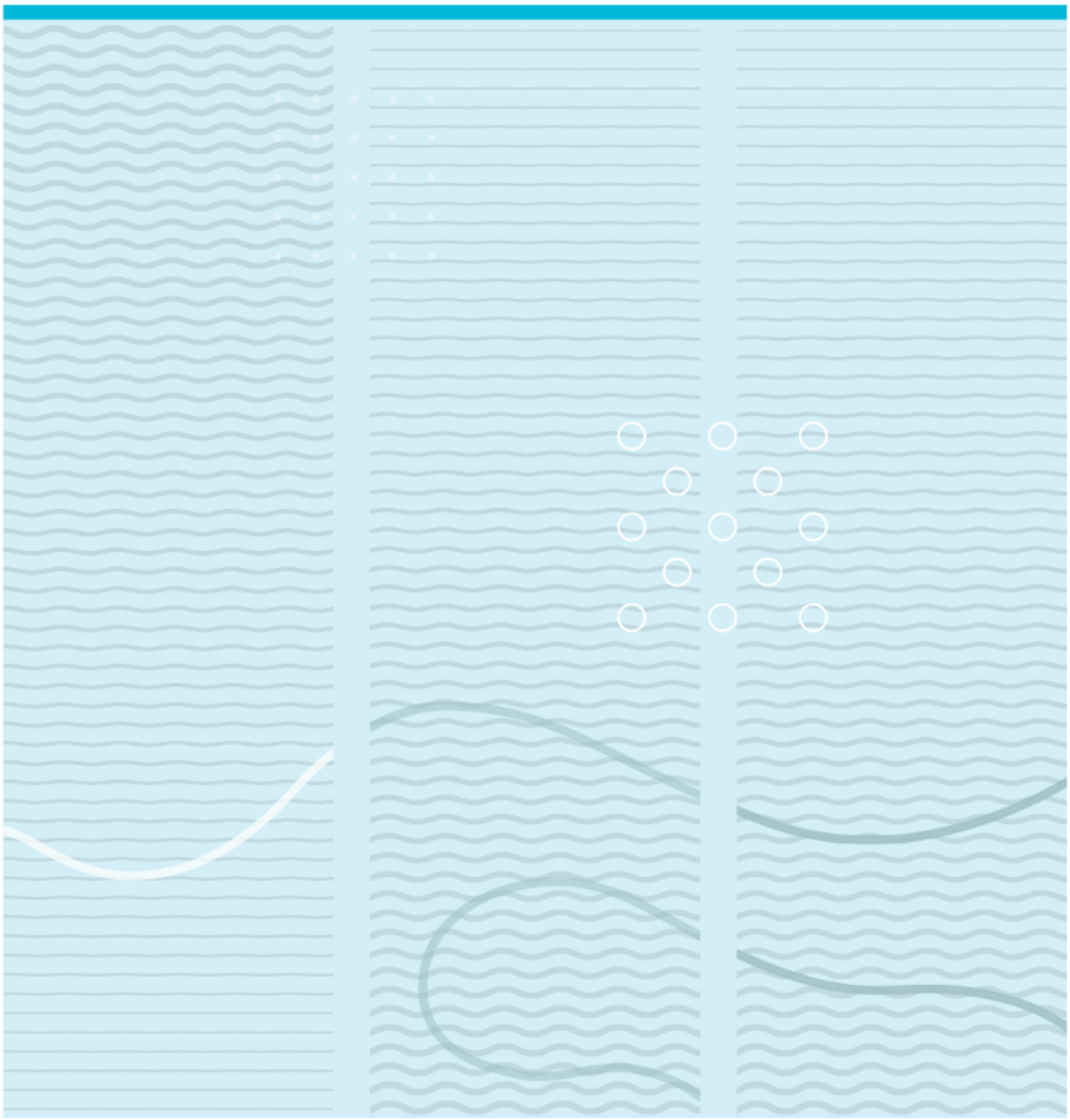

University of South-Eastern Norway
Faculty of Technology, Natural Sciences, and Maritime Sciences
Department of Science and Industry Systems
PO Box 235
NO-3603 Kongsberg, Norway

http://www.usn.no

This thesis is worth 30 study points

The undersigned have examined the thesis entitled ***Power Grid Noise Analysis Using Empirical Mode Decomposition Method*** presented by *Jan Ali*, a candidate for the degree of *Master in Systems Engineering with Embedded Systems* and hereby certify that it is worthy of acceptance.

Date	Head of Department
Date	Supervisor's name
Date	Committee member's name
Date	Committee member's name

Abstract

Due to the increasing consumption of electrical load and growth in the use of sensitive devices connected to power grid, Power quality (PQ) has become a subject of interest. PQ disturbances (PQDs) that affect voltage or current in the power system, may introduce some technical problems; hence, detection and mitigation of these PQDs are necessary. Recently, several techniques and methods for PQ analysis have been developed. Since most of the PQ events are non- stationary, proper time-frequency analysis techniques are required that can accurately identify and analyze events and disturbance in the power system. One of the recently developed tools that can be used for decomposition and analysis of any complex signal, is the Empirical Mode Decomposition (EMD) method. It is an adaptive time-frequency method for analyzing transient, nonlinear, and non-stationary signals.

In this thesis the EMD, Short Time Fourier Transform (STFT) and Continuous Wavelet Transform (CWT) are studied and applied to analyze a PQ event related to single phase low voltage power grid. Then their effectiveness and performance are evaluated. The STFT can provide the time–frequency domain information, but a compromise between time and frequency resolution has to be established because it is using a fixed window. To overcome this shortcoming, the CWT is used which utilizes variable sized windowing technique in order to maintain time and frequency resolution simultaneously. The WT yields high frequency resolution but low time resolution in the low frequency components, while low frequency resolution but high time resolution in the high frequency components. It needs to select a certain wavelet as primary function. Moreover, it encounters difficultly in noisy conditions.

The EMD decomposes the signal into a sum of intrinsic oscillatory components, known as *Intrinsic Mode Functions* (IMFs). Each IMF has different frequency components, which are extracted through sifting processes in a way from the highest frequency to the lowest. Once the IMFs are obtained, the Hilbert Transform (HT) can then be applied to calculate the instantaneous frequency and amplitude of each IMF. The combination of the EMD and the HT is known as the Hilbert–Huang Transform (HHT). The EMD is a fully data-driven signal analysis method which does not need any a priori defined basis function. The empirical nature of EMD presents the advantage over other signal analysis methods. Although EMD has demonstrated to be an effective method for analyzing non-stationary signals, it experiences some shortcomings. Mode mixing is one of the major problem to the EMD method. In order to overcome the mode mixing issue, a noise-assisted data analysis method referred to as the Ensemble EMD (EEMD) is implemented. The added white noise will be averaged out with sufficient number of trials; the only persistent part that survives the averaging process is the component of the original signal.

Acknowledgement

I would like to express my sincere appreciation and gratitude to my thesis supervisor, professor Sigmund Gudvangen for his guidance, patience and useful comments throughout the duration of the thesis work. His attention to details was always remarkable and quite helpful that has influenced my work and personal development.

I would also like to express my gratitude to my lecturers and faculty members at the University of South-Eastern Norway for sharing their valuable knowledge, guidance and expertise. I take this opportunity to express my gratitude to all my classmates for their friendship, specially my lab-mates for their discussion and sharing knowledge.

Special thanks to the administrator of Laboratory for Innovation and Technology in University of Technology Paraná in Brazil for providing datasets and making them accessible for researchers so that I could utilized for this thesis work.

Last but not least, I must express my very deep gratitude to my family for their ultimate encouragement and providing me with unfailing support and for all the sacrifices they have made for my behalf. Especially my wife who tolerated the life hardship and took care of my kid all the time while I studied. They have played an important role in helping me to reach this stage.

Contents

List of Figures

List of Tables

List of Abbreviations

COI	Cone Of Influence
CWT	Continuous Wavelet Transform
DFT	Discrete Fourier Transform
EEMD	Ensemble Empirical Mode Decomposition
EMD	Empirical Mode Decomposition
FFT	Fast Fourier Transform
FSST	Fourier SynchroSqueezed Transform
FT	Fourier Transform
FVI	Frequency Variation Interval
HAS	Hilbert Spectral Analysis
HHT	Hilbert Huang Transform
HT	Hilbert Transform
IFT	Inverse Fourier Transform
IMF	Intrinsic Mode Functions
LIT	Laboratory for Innovation and Technology
NADA	Noise-Assisted Data Analysis
NF	Nominal Frequency
NILM	Non-Intrusive Load Monitoring
PQ	Power Quality
PQD	Power Quality Disturbance
PS	Power System
RMS	Root Mean Square
SMPS	Switched Mode Power Supplies
SAX	Symbolic Aggregate approXimation
SD	standard deviation
STFT	Short-Time Fourier Transform

WT Wavelet Transform

Chapter 1

Introduction

The electrical power consumption has been increased in the last few years due to increasing amount of electronic equipment. All electronic equipment will affect the power consumption by the way in which they are in use or standby. Electronic equipment which we use daily at home or at the office, are connected to the electric power grid continuously or during charging via regulated power supplies. Switched Mode Power Supplies (SMPS) are also becoming more popular due to continuous development in power electric and digital electronics. These SMPS use switching technology that reduces their weight, energy losses and size. However, they produce harmonics and high-frequency disturbances, which cause electromagnetic compatibility problems for the power grid and neighboring equipment connected to it. Power electronic devices produce harmonics due to their switching operations [2, 3]. Harmonics are distorted electrical waveforms that cause disturbances into electrical system. They flow into the electrical system as a result of nonlinear electronic switching devices and generate wasteful heat. The input current that contains a power frequency component of 50 Hz or 60 Hz also contains harmonic components with frequencies equal to integer multiple of the fundamental frequency [4]. The issue is non-sinusoidal current of inverters and rectifiers. Rectifiers only draw current pulses from the grid in a small time interval around the maximum amplitude of the voltage waveform. This tends to flatten the tops of the waveform, which means that the waveform contains harmonic components. The harmonic distortion of the current leads to harmonic components in the supply voltage. In a power grid, interference and unwanted currents or voltages that generate noise is one of the important factors affecting the Power System (PS) signal for a synchronous phasor measurement [5]. The voltage waveform on the power grid should ideally be sinusoidal, but in practice it is polluted by voltage spikes from lightning, industry, the power supplies in nearby equipment, radio frequency noise, etc. Noise on the power grid can leak into sensitive electronic apparatus via power supply. Modern electronic equipment is not only sensitive to voltage disturbances, it also causes disturbances for other customers. The increased use of converter driven equipment has led to a large growth of PQ disturbances (PQDs).

1.1 Power Quality

Power Quality (PQ) is the delivery of reliable and uninterrupted supply of electricity to the consumers [6,7]. It is related not only to the performance of equipment but also to the possibility of measuring and quantifying the performance of the power system. Over the last few years, the traditional framework of PS has been changed, and the electrical system can be handled as complex entity. The electricity industry is evolving into a distributed and competitive industry in which market demands drive the price of electricity and reduce the net cost due to increased competition. The change is related to the

deregulation of the electricity industry. This deregulation (privatization and liberalization) process has led to an increased need for quality indicators. Customers are getting more information on the voltage quality as they expect, and demanding the acceptable reliability and quality ranges [8]. Therefore, the responsibility of supplying a better quality of power is important for the power utility companies in order to fulfill customer's satisfaction and gain optimal profits for the company. On the other side, the increasing utilization of high technology devices has contributed to generation of PQD in the power grid. PQ has been defined as a combination of voltage quality and current quality. Voltage quality is how the network affects the customer or the load, and it is concerned with deviations of the actual voltage from the ideal voltage. Current quality is how the customer or load affects the network, and it is the equivalent definition for the current [1]. A simple and easy solution is to define the ideal voltage as a sinusoidal voltage waveform with constant frequency and amplitude equal to their nominal value. Voltage and current quality concern all deviations from the ideal voltage and current wave forms, respectively, the ideal waveform being a completely sinusoidal waveform of constant frequency and amplitude.

1.2 Motivation

The end users or electrical power consumers expect that electrical power service provider deliver optimal electricity which is undistorted sinusoidal rated voltage and current continuously at normal frequency (e.g. 50 Hz or 60 Hz). However, large penetration of electronic controllers and devices as well as development of the distributed generation and electric power industry lead to more demand on the quality of electric power [9]. Therefore, PQ is becoming an important and challenging issue due to enormous utilities of electronic equipment which introduce PQD, such as voltage variations, flicker, waveform distortion, transient, etc. [10]. Any voltage, current and/or frequency deviations that cause failure or malfunctioning to customers' equipment can be defined as a PQ problem. Power systems, especially distribution systems, have numerous non-linear loads, which affect the quality of power significantly. Apart from non-linear loads like capacitor, motor starting and switching, and unusual faults could also inflict PQ. Many problems can arise from poor PQ, especially in today's complex PS such as false operation of modern control systems.

PQD cover a broad range of frequency with significantly different magnitude variations which can be non-stationary. Thus, suitable techniques and algorithms are required to identify and analyze these events. Analysis of the PQ signal in distribution systems are important tasks for maintaining power distributed network. As most of the disturbances are non-stationary and transitory in nature [11] it requires advanced tools and techniques for the analysis of PQD. There are various methods and algorithms used for PQD analysis, each has pros and cons. Fourier Transform (FT) is a simple and good method for periodic signals to convert from the time domain to frequency domain based on assumption that the signal is linear and stationary. It does not provide information about how frequency of signal is changing with respect to time [12]. On the other hand, majority signals in real environments are non-linear and non-periodic, and multiple advanced techniques have been designed to analyze them. Short-Time Fourier Transform (STFT) and Wavelet Transform (WT) are methods for analyzing stationary and non-stationary but linear signals. To deal with non-periodic and non-linear signals, a fully data-driven, self-adaptive and unsupervised signal decomposition method is required. Hence, Empirical Mode Decomposition (EMD) is one of the methods that can attain the required conditions. This method is used to analyze non-periodic and non-linear signals in an efficient manner, and we can analyze the signal in time and frequency domain simultaneously The data is assumed that consists of multiple intrinsic modes of oscillations. Each of these modes which are called Intrinsic Mode Function (IMF) [13], added together make up the original signal. EMD also satisfies the perfect

reconstruction property, for instance superimposing all extracted IMFs together with the residual slow trend reconstructs the original signal without information loss or distortion [14]. The empirical nature of EMD offers the advantage over other empirical signal decomposition techniques like Empirical Matrix Factorization (EMF) [15] of not being constrained by conditions which often only apply approximately.

1.3 Scope

The work within the thesis focuses on investigating the methodology and implementation of Empirical Mode Decomposition (EMD) to the PQ signals, and compare its effectiveness and performance with other methods for non-stationary analysis approaches. The aim is to detect and analyze PQDs. There are numerous sources of PQD that cause deviation to sinusoidal waveform of voltage or current in the PS. EMD is used to decompose the analysed non-stationary signal into intrinsic oscillation components called Intrinsic Mode Functions (IMF) which are amplitude and frequency modulated. EMD is more effective algorithm than Fourier-based analysis to analyze signals originating from non-stationary as well as non-linear processes. It might therefore bring out new aspects of power grid pollution. The work will consist of algorithmic study and simulations in Matlab program, but real data obtained from laboratory experiments will also be analysed.

Chapter 2

Power Quality Problems

A PQ problem is manifested as a non-standard voltage, current or frequency that results in failure or mis-operation of end user's equipment [16–18]. The main causes of PQ problems can be natural or man-made. The natural causes of poor PQ are mainly faults, lightening and weather conditions which are generally transient in nature. While, the man-made causes are usually related to loads or system operations which result in both transient and steady-state types of PQ problems [7, 19, 20]. The causes of PQ problems related to the loads are nonlinear loads such as saturating transformers and other electrical machines, or loads with solid-state controllers such as PC power supplies, TVs, Uninterruptible Power Supplies (UPSs), arc furances, etc. The causes related to system operations are switching of transformers, capacitors, feeders, and heavy loads [21]. Switched capacitors can affect the PQ by generating over voltages caused by high inrush currents when closing or possible re-strike immediately after opening. Also, when mechanical switch is opened, it requires a five-minute discharge time delay before re-energizing [22]. PQ problems can be related to the voltage and current quality issue. Voltage quality concerns the effect of supply voltage on equipment, and the current quality concerns the effect of equipment current on the system [23]. Some of the voltage related PQ problems at the point of common coupling where various loads are connected, are voltage variations and waveform distortions. These problems exist in the supply system because of various disturbances in the system or the presence of various nonlinear loads such as adjustable speed drives, furnaces and UPSs. Meanwhile, PQ problems related to the current are unbalanced currents, harmonic currents, reactive power burden, etc. which cause noise, failure of capacitor banks, losses in the distribution system and electric machines, Over voltages and excessive current, signal interference and so on. PQ problems may also consist of a combination of both voltage- and current-based PQ problems in the system that affect the performance of numerous loads and other equipment in the power grid.

PQ problems affect directly or indirectly all concerned utilities, customers, and manufacturers in terms of major financial losses caused by equipment damage, wastage of raw material, interruption of process, loss of important data, production loss, etc. Some PQ problems affect protection systems and result in malfunctioning of protective devices, and interrupt many operations and processes in the industries and other systems. These problems also affect many types of measuring instruments and analyzing of the various quantities such as current, voltage, power, and energy. Furthermore, the monitoring systems are affected by these problems in many important, critical, emergency and costly equipment. Thus, the interest in the PQ has been exponentially growing recently, and some of the main reasons are as follows:

- Equipment has become more sensitive to voltage quality disturbances, production processes

have become less tolerant of improper operation of equipment, and companies have become less tolerant of production halt. The main factors are voltage dips and short interruptions.

- High-frequency transients also causes equipment malfunction. Equipment produces more current disturbances than it used to do. Both low and high power equipment is increasingly powered by simple power electronic converters which produce a broad spectrum of distortion.
- Equipment produces more current disturbances than it used to do. Both high- and low power equipment are increasingly powered by simple power electronic converters that produce a wide spectrum of distortion
- The effect of PQ disturbances to other important appliances such as telecommunication network, TVs, computers, metering, and protection systems.
- Embedded generation and renewable sources of energy create new PQ problems, such as voltage fluctuations, variations and waveform distortion [1]. Most interfaces with renewable sources of energy are sensitive to voltage disturbances.
- Energy-efficient equipment is also a significant source of PQ disturbances. Adjustable-speed drives and energy-saving lamps are both important sources of waveform distortion and are also sensitive to certain types of PQ disturbances.
- Similar to other kinds of environmental pollution such as air, the pollution of power networks with PQ problems has also become an environmental issue a long with other consequences in addition to financial issues [21].

Power distribution systems ideally should provide customers with an uninterrupted flow of energy at smooth sinusoidal voltage at the contracted magnitude level and frequency [24], but in practice, distribution systems have nonlinear loads which affects the purity of waveform of power supply. A momentary disturbance for sensitive electronic devices causes frequency deviations which results in interrupted power flow, scrambled data, unexpected plant shutdowns and equipment failure.

2.1 PQ disturbance

As described, PQ is concerned with deviations of the voltage and current from its ideal value. Any deviation of voltage or current from their ideal waveforms is a PQ phenomenon or disturbance. It can be a current disturbance a or voltage disturbance, but it is often not possible to distinguish between them [1]. Any change in current gives a change in voltage and vice versa. To distinguish be-tween voltage and current disturbances, we use the cause as a scale for distinction between them. Volt-age disturbances originate in the power network that potentially affect the customers. while current disturbances originate with a customer, potentially affect the network. However, this classification is not accurate; as instance, starting a large induction motor leads to an over current. Viewed from the network this is clearly a current disturbance. In the meanwhile, the resulting voltage dip is a voltage disturbance for a neighboring customer, but for the network operator this is a current disturbance. For PQ issues it is very common that one underlying event, for instance motor start in this case, leads to different disturbances for different customers or at different locations. This complication of distinguishing between volt-age and current disturbances is one of the reasons that the PQ term is mainly used, so our definition of PQ considers more disturbances than those that are normally considered part of PQ, such as frequency variations and disunity power factor.

There are many PQ disturbances parameters however, some of them that are still of interest today are [3]:

- Inter-harmonic: A frequency component of a periodic quantity that is not an integer multiple of the frequency at which the supply system is operating (for example, a 190-Hz component). The main sources of inter-harmonic waveform distortion are static frequency converters, induction furnaces, and arcing devices. It is generally the result of frequency conversion and is often not constant as it varies with load [25].
- Transients from opening and closing of breakers and other switch gear
- Supply voltage imbalance that creates substantial problems to electrical machines due to negative sequence currents, noise, torque pulsation, vibration, rotor heating, etc.
- Voltage interruption: The disappearance of the supply voltage on one or more phases
- Electromagnetic disturbance: Any electromagnetic phenomenon that may be superimposed on a wanted signal and degrade the performance of a device, a piece of equipment, or a system
- Over-Voltage due to lightning strokes: Over voltages can be generated by lightning currents flowing along ground conductor paths.
- Light flicker due to fast voltage fluctuations from fast load variations
- Frequency fluctuations due to unbalance between power production and consumption
- Waveform distortion (often referred to as harmonics)

PQ disturbances are often classified into variations and events. Variations are either transient or steady-state disturbances that require continuous measurements over a long period of time. While, events are sudden with a beginning and an ending that are measured with a triggering function. Such disturbances pertain to abnormalities in the system voltages or currents due to faults or some abnormal operations, where steady- state variations refer to Root Mean Square (RMS) deviations from their nominal quantities or harmonics. It is not always easy to make distinction between variations and events. For example, if we consider changes in the voltage magnitude as a PQ disturbance, it may be considered a voltage dip as an extreme case of a voltage magnitude variation. A unique way of defining events is by the triggering that is required to start their recording, but variations do not need triggering. The difference between a voltage (magnitude) variation and voltage dip is in the triggering. A voltage dip has a specific starting and ending instant, although not always uniquely defined. Both voltage dips and voltage variations use the RMS voltage as their basic measurement quantity. Nevertheless, for the further processing of voltage variations all values are important, whereas for the further processing of voltage dips only the RMS values below a certain threshold are considered. From classical power engineering point of view, the measurement of variations is similar to measurement of the energy consumption (continuous), whereas the measurement of events is similar to the functioning of a protection relay (triggered).

2.2 PQ Variations

PQ variations are slowly changing parameters such as power, voltage magnitude, frequency, harmonics, flicker, imbalance, etc. A typical example of variation is the variation of the PS frequency with nominal value of 50 Hz but the actual value always differs from nominal value by up to about 1 Hz [1]. The frequency can be measured at any moment in time and a value will be obtained. The issues when measuring PQ variations include extracting the characteristics (in this example, the frequency from the sampled voltage or current waveform), statistics to quantify the performance of the supply at

one location, and statistics to quantify the performance of a whole system. The origin of some PQ variations is described in the consecutive sections.

2.2.1 Voltage Frequency Variations

Power frequency variations are defined as the deviation of the power system fundamental frequency from its specified nominal value (e.g., 50 or 60 Hz). The power system frequency is related to the rotational speed of the generators supplying the system [1]. While the electricity cannot be stored, a balance between power generation and consumption (load) should be maintained. If the balance is violated, a power deviation will occur that will cause the system frequency deviation from its nominal value. Normally this frequency variation is very small, so its impact on end-user equipment is negligible, except some cases such as arc-furnace that both voltage and current show significant fluctuations. Since fluctuations are more severe in the current, it contains a spectrum of harmonics.

The frequency of the voltage is the repetition rate of the voltage waveform at a specific location. The voltage frequency is often very close to the frequency of the system. That is to say that the frequency assumed to be the same anywhere in the system, only during system instabilities the frequency can vary notably between different locations. Examples of measured frequency variations are shown in figures below. Figure 2.1a depicts a 1 min average frequency during a 48 hour period, whereas Figure 2.1b shows the spread in frequency during each 1 min interval. There are different patterns in variations both at longer and at shorter time scales, in different systems which are related to the size of the system and to the control methods used. As previously stated, there is no any concern of the frequency variations in the system presented here.

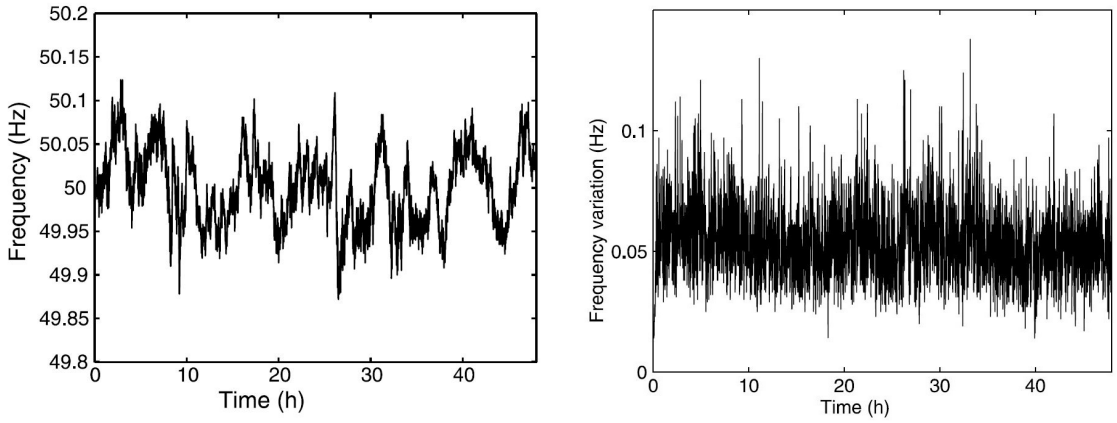

Figure 2.1: Frequency variations measured during a two-day period: (a) 1 min average frequency value, (b) Frequency variation range [1] (by permission).

In every country, a standardized frequency value called *Nominal frequency*(f_N) is decided by the design and the operating characteristics of the main components in their power system. The f_N is 50 Hz in Europe, Australia and most Asian countries, whilst 60 Hz in most parts of America. During normal operation, the frequency variation between a strict interval within a range of 50 Hz $\pm 1\%$ (i.e. 49.5 ... 50.5 Hz) [26] is allowed. This Frequency Variation Interval (FVI) is defined by every national transmission system operator, and it varies between different synchronous areas. For example, in the

Nordic area the normal frequency band (allowed FVI) is 49.9 – 50.1 Hz [27–31]. In serious contingency critical situations, the frequencies may be over the range of the normal operating conditions, but they must be within the range of the lowest to the highest critical frequencies which are indicated by Grid Codes [32–36]. The frequency variations for residential customers equipment connected to the low voltage grid is +4% and −6% [37] which for a 50 Hz system corresponds to 47 - 52 Hz. This is a wide and critical frequency range in European countries so it can reflect the technical differences between the transmission grids [38, 39]. If the system frequency reaches 47.5 Hz or 51.5 Hz, the operation of the interconnected network is at its limit and generators will be disconnected automatically. Table 2.1 indicates the allowed FVI for normal operation and critical situations in some countries with f_N of 50 Hz.

Table 2.1: Frequency Variation Interval (FVI) under normal operation and critical condition.

Country	Normal operation FVI	Critical condition FVI
Great Britain	49.5 – 50.5 Hz	47.0 – 52.0 Hz
Germany	49.5 – 50.5 Hz	47.0 – 52.0 Hz
France	49.5 – 50.5 Hz	47.0 – 52.0 Hz
Belgium	49.5 – 50.5 Hz	47.0 – 52.0 Hz
Austria	49.5 – 50.5 Hz	47.5 – 51.5 Hz
Poland	49.5 – 50.5 Hz	47.0 – 52.0 Hz
Romania	49.5 – 50.5 Hz	47.0 – 52.0 Hz
Australia	49.75 – 50.25 Hz	47.0 – 52.0/55.0 Hz
Ireland	49.8 – 50.2 Hz	47.0 – 52.0 Hz
China	49.8 – 50.2 Hz	48.0 – 51.0 Hz
Denmark	49.9 – 50.1 Hz	47.5 – 51.0 Hz
Norway	49.9 – 50.1 Hz	47.5 – 51.5 Hz
Italy	49.9 – 50.1 Hz	47.5 – 51.5 Hz

The size of the frequency shift and its duration depend on the load characteristics and the response of the generation control system to load changes. To attain power frequency control the rotor speed of generator should be regulated to synchronize with the grid frequency. The principle is to compare the measured frequency with the f_N. When the measured frequency is higher than the f_N, it indicates a surplus of rotational energy in the system. To mitigate this, the generator reduces its active power output. Further precisely, the mechanical input to the turbine generator is reduced.

2.2.2 Voltage Magnitude Variations

The voltage magnitude variation is increase or decrease of the voltage magnitude due to variation of the total load of a distribution system or part of it, actions of transformer tap changers or switching of capacitor banks or reactors [40, 41]. The actions of transformer tap changer and capacitor banks switching can normally be traced back to load variations as well. Hence, the voltage magnitude variations are mainly due to load variations which follow a daily pattern [42]. Moreover, fast variation of the voltage magnitude is referred to voltage fluctuation.

The magnitude of the voltage in the system is different for each location, so it requires a separate measurement for every location in the system. The voltage variations can affect the performance and lifetime of the equipment. Some examples of voltage variations effect are as follows:

- Over voltage will increase the risk of insulation failure, and in a long term it effects system

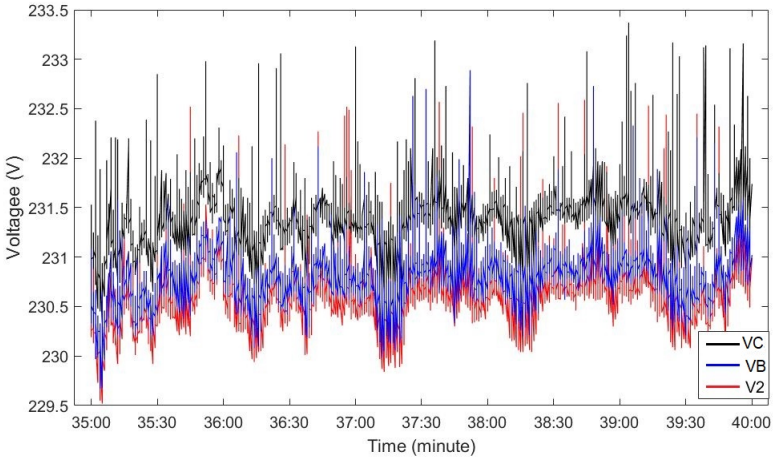

Figure 2.2: Voltage magnitude variation of a three phase electric power.

components such as transformers and cables, also for end-user equipment such as motors.

- In induction motors, under voltages will affect starting torque. When the starting torque is reduced, it may increase the time needed to accelerate the motor. In some cases the motor may not accelerate at all. Over voltages will increase starting torque, decrease power factor and increase starting current that causes greater voltage drop in the supply system and increases the voltage.
- The energy input and consequently the heat output of resistance heaters vary approximately as the square of the voltage, e.g. a 10% drop in voltage will cause approximately 20% drop in heat output.
- Voltage variation affects light output and lifetime of incandescent lamps significantly. Light output of fluorescent lamps vary approximately in direct proportion to the applied voltage [43]. Compared to the incandescent lamps, the lifetime of fluorescent lamps is less affected by voltage variation [1].
- Electronic equipment are sensitive to the voltage variation. They may perform less efficient due to under voltage. The equipment will also be more sensitive to voltage dips.

There is distinction between single-phase measurements and three-phase measurements. Anyway, in this thesis the single-phase measurements are considered, so the voltage magnitude is extracted by using the waveform of only one phase. This may be a phase voltage or a line voltage; however, the calculations for phase voltages and line voltages are the same. To model the effect of a certain load on the voltage, the power system is represented through a Thevenin source in Figure 2.3, consists of an ideal voltage source (E, the no-load voltage) and a constant impedance (Z the source impedance) which are not physical quantities. However, the values can often be approximated by physical quantities, for instance, the impedance of a transformer and the voltage on primary side of the transformer.

2.2.3 Voltage Unbalance

When voltages of a three-phase system are not identical in magnitude or the phase differences between them are not exactly 120 degrees, voltage unbalance occurs [44, 45]. Voltage unbalance is mainly due to unbalance in the load currents and unbalance in the supplying network. Current unbalance in low-voltage networks is due to the load diversity. The load unbalance is partially due to the

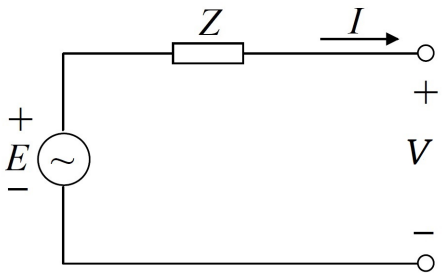

Figure 2.3: Thevenin equivalent of the power grid.

natural variation between single-phase loads in the three-phases and partially due to large individual single-phase loads. Variation over time of individual loads implies that there would never be perfect balance between the load currents even if the loads are equally distributed over the three-phases. This issue is mainly in low voltage networks; however, in medium and higher voltage networks where loads are usually three-phase, the voltage unbalance can be the result of capacitor bank anomalies, such as a blown fuse in one phase of a three-phase bank. In addition to unbalanced load currents, balanced current flowing through unbalanced impedances also cause voltage unbalance.

Three-phase transmission system is balanced as the vectors of voltage and the magnitude of current in all phases are equal and spaced 120° apart [46]. When a single-phase load is connected to such a balanced system, unequal voltage drops occur in different phases that cause unbalance in the power system. The percentage value of the voltage unbalance can be calculated as [47, 48]:

$$V_u = 100\ \frac{V_{dmax}}{V_{avg}} \tag{2.1}$$

Where V_u is voltage unbalance as percentage, V_{dmax} maximum voltage deviation from average voltage and V_{avg} average voltage.

The unbalance can also be derived from the magnitude of connected load and the utility system fault level:

$$V_u = 100\ \frac{S_L}{S_{SC}} \tag{2.2}$$

where S_L is line to line load in VA, and S_{SC} three-phase short circuit fault level in VA.

Unbalanced voltages cause a flow of negative sequence currents in the three-phase equipment connected to the electric power network. The currents magnitude can be as:

$$I_2 = 100\ \frac{V_u}{Z_u} \tag{2.3}$$

where I_2 is negative sequence current as percentage and Z_2 equipment negative sequence impedance as percentage.

In a three-phase system, the voltages are not exactly balanced even in normal operation. A set of three-phase voltages contains three components, called symmetrical components [49]; zero-sequence voltage, positive-sequence voltage, and negative-sequence voltage. The positive-sequence voltage is the amount of voltage contributing to the power flow from generators to motors. The negative-sequence voltage is an indication of the amount of unbalance in the system. The negative sequence unbalance

due to a single-phase load is equal to the ratio between the apparent power of the load and the fault level of the supply. Even if a feeder supplies identical loads equally spread over the phases, a negative sequence current will result. Three-phase equipment that are normally connected phase to phase (or phase to neutral without ground connection, in motor start case) will be affected only by the negative-sequence. The three-phases of an overhead transmission line have slightly different inductances and capacitances resulting in a coupling between positive- and negative-sequence voltages and currents. The zero-sequence voltage does not cause any change in load currents, so normally it is not considered in characterizing the voltage unbalance. The presence of zero-sequence voltage indicates a connection to earth, and it is a measure for the amount of current not returning through the phase conductors.

The voltage unbalance has recently become a major concern for PQ due to its effects on the load and the source. For instance, nonlinear loads such as static converters fed from unbalanced supplies, produce uncharacteristic low frequency harmonics, which increase the ratings of filters, switches, etc [50]. AC electric machines, when supplied by unbalanced voltage sources, generate large negative sequence current components due to the low negative sequence impedance, which increase the machine losses and reduce the net torque [51] Voltage unbalance leads to unbalanced currents (over currents) for three-phase equipment such as rectifiers and rotating machines. It could become a concern for the connection of induction and synchronous generators to low- and medium voltage networks.

2.2.4 Voltage Fluctuations and Flicker

Voltage fluctuations are cyclical variations of the voltage envelope or a series of random voltage changes of up to $\pm 10\%$ of the nominal value [22, 44, 52]. Voltage fluctuations affect the performance of the equipment and cause instability of the internal currents and voltages of electronic equipment. When the voltage level falls outside of this range, a device may not be able to start or operate fairly. It may malfunction or may be damaged. Frequency fluctuations outside tolerance value of $\pm 5\%$ are usually unsafe for equipment which are considered to be sensitive to voltage level or fluctuations [53]. There should be a balance between power generation and power demand or load. The frequency tends to drop from nominal value if demand is more than generation, and if demand is less then the frequency increases. Thus, change or disconnection of of large load, also fault on transmission line or turning on/off of large generator in the power grid may result in frequency fluctuations.

The main source of voltage fluctuation are Industrial loads such as arc furnaces, resistance welders, start-up of drives, etc. Loads that consume large amounts of power, for instance arc furnaces, change the currents at many different time scales. They are typically connected directly to the transmission system and cause light flicker over large areas. Step voltage changes due to the connection or disconnection of large loads or capacitor banks can also cause voltage fluctuations that can affect many consumers. Some domestic equipment can cause voltage fluctuations is refrigerator. When pump starts to circulate the cooling liquid a voltage drop occurs. Loads for which the current varies rapidly and continuously, will cause voltage variations.

The voltage fluctuation which sometimes called voltage flicker, is a series of non-periodic phenomena with smaller amplitude and faster continuous variation in voltage magnitude [54]. It is the ratio of the voltage difference between two adjacent steady-state voltages separated by at least one voltage variation characteristic to the nominal voltage. The main result of voltage flicker is light flicker, the fluctuations in the frequency range 1 to 20 Hz which is a visual phenomenon perceived by eyes. Flicker intensity is a quantity used to quantify voltage fluctuation and light flicker. The value of intensity quantity is an objective measure of the severity of the light flicker due to a certain voltage fluctuation. for a standard incandescent lamp, the flicker severity equal to 1 corresponds to a severity level that is experienced

as uncomfortable by 95% of persons [55]. We can deal with the flicker intensity as a variation, just like voltage magnitude variation. It can be plotted as a function of time, and probability density and distribution functions can be obtained. There are also some other loads that will be negatively affected by fast fluctuations in the voltage amplitude at their terminals, for example, accelerating or decelerating moments for motors, fdefecting electronic equipment and components for telecommunication and so on that the fluctuation of the supply voltage passes through to their electronic parts [56]. An example of small voltage fluctuations that cause problems other than light flicker is small speed variations in the motor driving a weaving machine that results small color variations in the final cloth.

2.3 Waveform Distortion

A steady-state deviation from an ideal sine wave of power frequency is defined as waveform distortion [22, 44, 57]. It includes all deviations of the voltage or current waveform from the ideal sine wave. According to this definition, waveform distortion concerns the voltage quality and current quality. However, variations in magnitude and frequency cannot be considered as waveform distortion. Since the voltage quality is how the network affects the customer or the load, and current quality is how the customer or load affects the network; distorted voltages which are typically created by generators, affect the customer equipment and distorted currents results from loads affect the network components. Anyway, in some cases such as capacitor banks, voltage distortion also affects network components. Transformer voltage and current distortions may lead to additional heating, increase in audible noise and cause additional losses. However, the current distortion has more effect because the current distortion is higher than the voltage. There are five primary types of waveform distortion [58].

DC Offset: Offsetting of a signal from zero is DC offset, and it is the presence of a DC voltage or current in an AC power system. Main source of DC offset in the power systems can be an asymmetry of electronic power converters or geomagnetic disturbance. Incandescent light bulb life extenders may consist of diodes that reduce the rms voltage supplied to the light bulb by half-wave rectification. The Direct Current flow in transformers cause magnetic saturation, increased heating and loss of transformer life. DC current may also cause the electrolytic erosion of grounding electrodes and other connectors.

Harmonics: Harmonics are sinusoidal voltages or currents with frequencies that are integer multiples of the nominal frequency at which the supply system operates. Harmonic occurrence is due to increased use of nonlinear loads which cause sine waveform distortion. The total distorted waveform will be a combination of the fundamental frequency sine wave and the various harmonics, so any distorted waveform can be decomposed into a sum of the fundamental frequency and the harmonics, and can be written as [6, 44]:

$$y(t) = Y_{DC} + \sum_{h=2}^{n} Y_h \sqrt{2} \cos(h\omega t - \Phi_h), \tag{2.4}$$

where Y is sinusoidal component (voltage or current), h is the harmonic order, ω is angular frequency ($2\pi \times 50Hz$), and Φ is phase shift for the h^{th} harmonic. The value of n for a continuous signal is ∞, but for a discrete signal it is determined by the sample frequency which the highest frequency in a discrete signal is half of the sample frequency. Fourier methods can be used for analyzing harmonic distortion [59]. It is much easier to determine the system resonance to an input that is sinusoidal. Harmonic distortion levels are described by the complete harmonic spectrum with magnitudes and phase angles of each individual harmonic component. The Total Harmonic Distortion (THD) is the most common measure of harmonic content. It is a measure of the effective value of the harmonic components of a distorted waveform in both current and voltage waves, but it usually refers to voltage

waveform distortions. Meanwhile, it is not a good measure of heat generation in transformers because it can not calculate core losses accurately. The THD is the rms of the harmonics expressed in percentage of the fundamental component:

$$THD = \frac{1}{V_1}\sqrt{\sum_{h=2}^{\infty} {V_h}^2}. \tag{2.5}$$

Nonlinear loads and power electronic controllers are the major source of harmonics. Some negative effects of harmonics are

- Extra losses and heating in rotating machines, transformers and capacitors
- Overvoltages due to resonance
- Interference with ripple control systems used in Demand Side Management (DSM)
- Noise on telephone lines which cause communications interference

Interharmonics: The voltage or current waveform also contains frequency components that are not a multiple integer of the PS frequency. To measure interharmonics we need to measure waveform over a longer period rather than one cycle. The main sources of interharmonics are static frequency converters, cycloconverters, induction furnaces and arcing devices. Interharmonics can affect power line carrier signaling and cause visual flicker in display devices such as cathode ray tubes. Harmonic distortion is a wide subject and will be discussed in a separate section.

Notching: A periodic voltage disturbance introduced by power converters when current is commutated from one phase to another during normal operation. During notching, the line voltage will be reduced by a momentary short circuit that exist between the two commutating phases. Notching can result in multiple zero voltage crossing which can cause digital clocks to run fast as their design is based on two crossing per cycle. Notching can be analyzed by Fourier series as it is a steady state phenomenon, that gives the harmonic spectrum of the affected voltage. However, notching is treated as a special case as the frequency components associated with notching can be high and outside the range of measuring equipment normally used for harmonic analysis. Notching can be characterized by its depth (average depth of the line voltage notch from the sinusoidal waveform at the fundamental frequency), width (the duration of the commutation process), area (the product of notch depth and width) and position where notch occurs on the sinusoidal waveform.

Noise: Defined as unwanted electrical signals with broadband spectral content less than 200 kHz [60] superimposed on the power system voltage or current in phase conductors, or found on neutral conductors or signal lines. The main sources of noise are power electronic devices, control circuits, loads with solid-state rectifiers and switching power supplies. Noise disturbs electronic devices such as microcomputer and programmable controllers. Using filters, isolation transformers and line conditioners can mitigate the noise problem.

2.3.1 Transients

Transients in the power system are undesirable and short duration voltage or current event that produce distortions [25, 44]. Transient component is the component of voltage and current due to the transition between two steady states within a limited duration [1]. Their main characteristic components are amplitude, rise time, amplitude spectral density, duration, frequency of occurrence and capability of energy delivery. Transients are associated with disturbances caused by faults, load variations, switching operations or lightning strikes. They can have effects on system performance or cause failures to

the power equipment. The term surge is often considered synonymous with transient. Transient can cause two types of stress in power network; Overvoltages, which can cause insulation breakdown or flash-overs (insulation failure through air) and overcurrents, which can damage power equipment due to excessive heat dissipation. Based on their origin, transients can be external (atmospheric) such as lightning, or internal (switching actions) such as switching operations, faults and load variations. Further, transients can be impulsive or oscillatory in terms of wave shape of a current or voltage [61].

Impulsive transients are sudden frequency change in the steady-state condition of voltage, current, or both that are unidirectional in polarity. They are basically described by their rise and decay times, for instance, a 1.2×50 µs 2 kV impulsive transient nominally rises from zero to its peak value of 2 kV in 1.2 µs and then decays to half its peak value in 50 µs [62]. Lightning is the most common cause of impulsive transients which happens within a short duration between 0.1 µs and 1.0 ms [63]. It can strike any place in the power system and produce lightning surge currents that can flow from the power system into the loads, and may cause flash-overs of the utility lines and damage equipment. To protect the system equipment and loads against these surges, lightning arresters are used which provide an easy pass to earth for the lightning surges. The impulsive transients shape for the reason of high frequencies can be changed quickly by circuit components and may have different characteristics when viewed from different parts of the power grid [61].

Oscillatory transients Are sudden frequency change in the steady-state condition of voltage, current, or both that includes both positive and negative polarity values. An oscillatory transient includes voltage or current that its instantaneous value changes the polarity very quickly. Transients are described by their spectral content, duration, and magnitude [58, 60] as shown in Table 2.2.

Table 2.2: Typical characteristics of transients .

Categories	**Spectral content**	**Duration**	**Voltage magnitude**
Impulsive transients:			
Nanosecond	5 ns rise	$<$ 50 ns	
Microsecond	1 µs rise	50 ns - 1 ms	
Millisecond	0.1 ms rise	$>$ 1 ms	
Oscillatory transients:			
Low frequency	$<$ 5 kHz	0.3 - 50 ms	0 - 4 pu
Medium frequency	5 - 500 kHz	20 µs	0 - 8 pu
High frequency	$<$ 0.5 - 5 MHz	5 µs	0 - 4 pu

Medium-frequency transients can also be due to the system response to an impulsive transient. Back to back capacitor energization causes oscillatory transient currents in the tens of kilo Hertz, and cable switching causes oscillatory voltage transients in the same frequency range.

Low frequency transients are often occur on utility sub-transmission and distribution systems. Their most common cause is capacitor bank energization, that usually results in an oscillatory voltage transient with a primary frequency generally between 300 and 900 Hz. The peak magnitude is normally 1.3 to 1.5 pu with a duration of between 0.5 and 3 cycles, but in some cases it can be reached up to 2 pu [61]. Oscillatory transients below 300 Hz of principal frequencies, generally associated with ferroresonance and transformer energization, can also occur on the distribution system when the system responds by resonating with low frequency components in the transformer inrush current or when unusual conditions result in ferroresonance. High frequency transients are mainly the result of a local system response to an impulsive transient.

Chapter 3

Classical Methods and Analysis

3.1 Fourier Transform

Generally speaking, the intention of any transform is to change the domain of a signal from one variant to another in order to investigate specific properties. There are two equations which deal with the changes between time and frequency domains; The *analysis equation* which takes a function in its time domain and converts it into a frequency domain, and the *synthesis equation* which takes a function in its frequency domain and brings it back to the time domain.

Fourier Transform (FT) is one of the most commonly used techniques in periodic and linear time-invariant signal analysis to change the time domain to the frequency domain. It is bijective, which means that there is a one-to-one correspondence between the functions from time to frequency domains and vice versa. FT decomposes any signal into a series of sinusoidal functions. Sinusoidal functions are unique in meaning that they contain a clear physical meaning in terms of frequency. For example if we have a signal which is a combination of two signals $z(t) = x(t) + y(t)$, the FT can decomposes it to its constituent frequencies and the original signals ($x(t)$ and $y(t)$) can be recovered. It decomposes a signal into different frequencies, same as a prism that refract light up into different component colors. FT is widely used not only in signal processing/analysis but also in image analysis eg. edge detection, image filtering, image reconstruction, and image compression. The analysis equation or FT of a signal $x(t)$ in its time domain is defined as [64, 65]:

$$X(\omega) = \int_{-\infty}^{\infty} x(t) e^{-j\omega t} dt, \tag{3.1}$$

where X(ω) represents frequency domain. For going back to time domain from frequency domain and recover the the signal $x(t)$, Inverse Fourier transform (IFT) or synthesis equation is used:

$$x(t) = \frac{1}{2\pi} \int_{-\infty}^{\infty} X(\omega) e^{j\omega t} d\omega. \tag{3.2}$$

The relation between the time domain and frequency domain of a signal established by FT can be writen as $x(t) \leftrightarrow X(\omega)$, where the double-headed arrow represents the bijective characteristic of the mapping. While the Fourier series exists for all periodic functions, the FT only exists for signals that are absolutely integrable, i.e. the integral of the absolute value over the range -∞ to +∞ must be finite, that is:

$$\lim_{\tau\to\infty}\int_{-\tau}^{\tau}|x(t)|\,dt<\infty. \tag{3.3}$$

Impulse function is an important function that leads to mathematical difficulties. From mathematics point of view the impulse is not a function because it is not defined at the point of application, but in signal processing impulse function or the Dirac delta function is used frequently and the difficulties can be handled by the concept of generalized functions.

FT is a very common used technique that can be used in many engineering, science and technology applications. This transform method has several important properties which are useful for signal processing applications. These properties can be used to determine the FT of a signal without the need to apply the analysis or synthesis equations [66, 67]. Convolution theorem [1] which allows us to break problems apart into manageable pieces, is very useful [68].

FT preserves amplitude, frequency and phase information of the signal to transform the signal into frequency domain. Preserving phase information by FT means that the signal can transformed back from frequency domain to time domain. FT is a powerful analytical method, generally applicable for linear systems, but inadequate for non-linear and non-stationary signals. The signal cannot be analyzed simultaneously in both time and frequency domain by using FT because it represents the signal's overall frequency content and does not contain any information showing how frequency changes over time [69–71]. This is the main drawback of FT for analyzing non-linear and non-periodic signals in the time domain.

3.1.1 The Discrete Fourier Transform (DFT)

Fourier series play an important role in the analysis of continuous-time signals. In many cases we have to calculate the Fourier integral or coefficients on the basis of a given sampling of the signal. Therefore, a transformation is required to transform a discrete-time signal or sampling directly into the frequency domain. This transformation is called discrete transform. For getting periodic discrete-time signals we need to sample a periodic continuous-time signal with period T using a sampling frequency $\omega_s = N\omega_0$, where N is an integer and $N > 0$, and $\omega_0 = 2\pi/T$ is the fundamental frequency of signal $f(t)$.

The Discrete Fourier Transform (DFT) of $x(n)$ is defined by [72, 73]

$$X(k)=\sum_{n=0}^{N-1}x(n)e^{-j2\pi kn/N},\quad \text{for}\quad k=0,1,2,...,N-1. \tag{3.4}$$

The summation in Equation (3.4) is performed over N samples of $x(n)$.

To find the relation between the DFT and FT of discrete-time signals, we consider a discrete-time signal $x(n)$ with limited time duration which is not zero only within $0 \le n \le N_0 - 1$.

The DFT is considered as samples of the FT of discrete-time signals in frequency taken at $\Delta\omega = 2\pi/N$, which is corresponding to N frequency samples [74] within the period $-\pi \le \omega < \pi$. Since we have $X(k) = X(e^{j2\pi k/N})$ and $\omega = k\Delta\omega = 2\pi k/N$,

$$X(k) = X(e^{j\omega}). \tag{3.5}$$

The relation between the DFT and the Fourier series coefficients is [12]: $X(k) = TX_k$. We can recover

[1] The FT of a convolution is the point-wise product of Fourier transforms, and the Fourier transform of the point-wise product of two functions is the convolution of the FT of each one of the two functions.

a periodic discrete-time signal $x(n)$ from its spectrum $X(k)$ through Inverse Discrete Fourier Transform (IDFT):

$$x(n) = \frac{1}{N} \sum_{k=0}^{N-1} X(k) e^{j2\pi kn/N}, \quad \text{for} \quad n = 1, 2, ..., N-1. \tag{3.6}$$

The DFT formula is used to calculate N complex-valued coefficients from a length N real or complex-valued signal. It can calculate the frequency spectrum of a signal. DFT has similar properties to the Fourier transform of continuous-time signals. Another similarity with the Fourier theory of continuous-time signals is the convolution product, which is called cyclical convolution in the case of periodic discrete-time signals. There are several ways to calculate DFT. Fast Fourier Transform (FFT) is another approach for calculating the DFT. While FFT produces the same result as the other methods, it significantly reduces the computation time [75]. If we want to calculate a DFT of signal on the N point, it would need to perform N^2 operations, while the FFT reduces the number of operations needed for the same N point data set from N^2 to $Nlog2(N)$. In other words, the FFT is $N/log2(N)$ faster than the DFT.

3.1.2 The Short-time Fourier transform (STFT)

The FT provides frequency information which is the average of the entire time domain. However, we don't know *when* these frequencies occur in the transform. To retrieve this hidden time information, Dennis Gabor introduced the short-time Fourier transform (STFT) which is also known as *time dependent Fourier transform* [76]. The STFT is one of the most common methods for spectral analysis of time-varying signals that preserves both time and frequency information of signals. The basic idea behind STFT is to apply the FT to a portion of the original signal obtained by sliding window function $w(t)$ that will localize and truncate the analyzed signal $x(t)$.

In analyzing non-stationary voltage and current disturbance data, estimating the frequency contents of data as a function of time is one of the main interests. For power system disturbances especially for short-duration events, it requires some nontrivial methods to describe precisely the amplitude and phase-angle jump as a function of time. To extract such information, a suitable way is to apply time–frequency signal decomposition where the time-evolved signal components are obtained in different frequency bands. Among many other methods, discrete STFT is a time–frequency decomposition method which is used for the time–frequency decomposition of non-stationary signals, since the use of Fourier transform alone is not adequate. For a signal $x(n)$, the complex signal component in the frequency band at time instant n can be obtained from the discrete STFT, defined as [77]

$$X(e^{j\omega}, n) = \sum_{m=-\infty}^{\infty} w(m)\, x(n-m) e^{-j\omega m}, \qquad \omega \in \{-\pi, \pi\}, \tag{3.7}$$

where $w(n)$ is a window function that selects a section of finite length R from the input sequence $x(m)$. The main purpose of the window is to select a reasonably stationary segment which is called *short time stable* from the input sequence by using sliding window function, instead of considering the entire signal, then apply the DFT [78]. Hence, the faster changes of input sequence with time, requires the shorter window in order to ensure an approximately stationary segment. The STFT depends upon the length, size and shape of window function. The width of the window function determines the sufficient time or frequency resolution [79–81], i.e, a narrow window (short segment) provides good time resolution, but poor frequency resolution, whereas long segments provide good frequency resolution, but poor time resolution. There is also leakage risk when dividing the signal into smaller

parts (sub-windows). Smaller windows result in higher leakage in the lower frequencies.

Discretizing the frequency variable to $\omega = (2\pi/N)k$, for $k = 0, 1, ..., N-1$, allow us to compute the spectra corresponding to each of the length N input sequences as a DFT, which can be computed very effectively by means of a Fast Fourier Transform algorithm. In order to simplify the Equation (3.7), since the term $j(2\pi/N)$ is constant we define the notation $W_N = e^{j(2\pi/N)}$ and replace the $X(e^{j(2\pi/N)k}, n)$ with the short hand notation $X(k, n)$:

$$X(k,n) = \sum_{m=0}^{N-1} w(m)\, x(n-m) W_N^{km}, \qquad k = 0, 1, 2, ..., N-1. \tag{3.8}$$

The STFT can be considered as a special case of Discrete Time Fourier Transform (DTFT) which is usually implemented by employing a DFT with a sliding window as follows:

$$[X(0) \quad X(1) \quad ... \quad X(N-1)] = DFT_N[x(n-L+1)w(0) \quad x(n-L+2)w(1) \quad ... \quad x(n)w(L-1)], \tag{3.9}$$

where N is the number of frequency bands, n indicates the time, and DFT_N indicates the N-point DFT, and $L = N$ often used. However, if $L < N$ is selected, then the windowed data in the right side of (3.9) should first pad zeros to the length N before applying the DFT.

The DTFT and DFT are defined for steady state where the frequency spectrum is periodic, with period 2 π or equivalently fs (the sample frequency). They are based on global time-domain information and compute only a single spectrum. Whereas, the STFT computes the frequency spectrum from several segments utilizing the windowing technique that moves the time-window along the time-axis to select another length N section, and compute another DFT. Thereafter the time-window is moving again and computes next DFTs [1].

The window function tapers down the input segments towards each end, similarly to the windows used to reduce spectral leakage. In order to compensate the loss of data and reduce artefacts caused by the windowing, the input segments are allowed to overlap with $0 < K < N$ samples which gives more points in the time domain, without any impact on time or frequency resolution. So the window is advanced by $L = N - K + 1$ samples for each new time-frame. Hence, the time index must be modified to $n = lL$, where $L = N - K$ [82]:

$$X(k,lL) = \sum_{m=0}^{N-1} w(m)\, x(lL-m) W_N^{km}, \qquad k = 0, 1, 2, ..., N-1. \tag{3.10}$$

The larger overlap K results less frequency spectrum changes from one time-frame to the next. The output of the STFT $X(k, lL)$ is a function of both time and frequency, so the STFT spectrum retains both time and frequency information.

The problem that the standard FT can analyze only in the frequency domain rather than the time domain is solved by STFT; however, it has also shortcoming because the resolution of STFT is determined by a fixed windowed function whose form and shape don't change. So, we need to choose a different windowed function in order to change the resolution. STFT is effective for analyzing segment-wise stationary signals or approximate-stationary signals, but non-stationary signals that change dramatically, require high time resolution. STFT cannot balance the demand of both time resolution and frequency resolution. For a non-stationary signal analysis to reflect local time-varying spectrum features of the signal, we need a method that can realize time-frequency localization.

3.1.3 The Spectrogram

A spectrogram is the squared magnitude of the STFT [83]. It is a visual representation of the STFT's spectrum which has three dimensional quantity. The vertical y-axis represents frequency, horizontal x-axis represents the time, and the ammplitude will be normal to the page represented by colors. The spectrogram will be used to estimate the evolution of a nonstationary signal frequency along time. It utilises successive windowed Fourier analysis in which the window moves along several positions of the signal over time. In Matlab, an application called *Signal Analyzer* computes the spectrogram. To construct the spectrogram of a signal, below steps are followed:

- Divide the signal into possibly overlapping segments with equal-length which must be short enough that the signal's frequency content does not change significantly within a segment.
- Window each segment and compute its spectrum to get the STFT.
- Display the power of each spectrum segment-by-segment in decibels. Then outline the magnitudes side-by-side as an image with magnitude-dependent color map.

In Signal Analyzer, the length of the segments and the amount of overlap between adjoining segments can be controlled using *Time Resolution* and *Overlap*. By default, the length of segment is chosen as a length based on the entire length of the signal, and overlap will be 50 %. The Signal Analyzer sets the time resolution as $[N/d]$ samples, where N is the signal length and d is a divisor which depends on N; The longer signal (more samples), the greater divisor which increases by the power of 2.

3.2 Wavelet Transform

Wavelet transform (WT) is a great tool for signal analysis in both the time and frequency domain at the same time. It was developed as an alternative to the STFT to overcome problems related to its frequency and time resolution properties. Unlike STFT which uses fixed window width, the WT uses a windowing technique with variable window size. If the width of the window can vary with frequency so that the window always covers the same number of periods, the time localization would be enabled to be sharper for more rapidly varying signals. This leads to the idea of a family of analyzing waveforms constructed from translations and dilations of a prototype waveform called *mother wavelet* or simply a *wavelet* $\Psi(t)$, for which $\Psi \in L^2(\mathbb{R})$ satisfies the admissibility condition [84, 85] $\int_{-\infty}^{\infty} \Psi(t)dt = 0$. This means that Ψ must be an oscillatory function with zero mean and non zero-frequency component. The wavelet is thus defined as [86–88]

$$\Psi_{a,b}(t) = \frac{1}{\sqrt{|a|}}\Psi\left(\frac{t-b}{a}\right), \quad a, b \in \mathbb{R},\ a \neq 0, \tag{3.11}$$

where a is the scaling (or dilation) parameter that measures the degree of compression or scale, and b is the translation parameter which determines the time location of the wavelet. If $|a| < 1$, the wavelet (3.11) is the compressed version of the mother wavelet which corresponds mainly to higher frequencies, and time-widths of wavelets are adapted to their frequencies. This is the main advantages in signal processing and time-frequency signal analysis. Generally, the solution is rough in the time domain, but good in the frequency domain . Furthermore, by decreasing the scale a, the time domain decreases which leads to the finer time resolution, whereas the frequency domain increases (the frequency resolution becomes coarser). The expansion of a function $x(t)$ in terms of wavelets defined as *Wavelet Transform*:

$$W(a, b) = \int_{-\infty}^{\infty} x(t)\Psi_{a,b}(t)dt. \tag{3.12}$$

WT compared with STFT, yields an adaptable time–frequency window, i.e. the window becomes automatically narrower when observes a high-frequency signal, and becomes wider when observes a low-frequency signal. The resolutions is varied with scale, so that a high frequency resolution is best at low frequencies, whereas a high time resolution is best at high frequencies. Therefore, there is trade-off between frequency resolution and time resolution which is known as *time-frequency uncertainty principle*, i.e., increasing the frequency resolution decreases the time resolution, and vice versa.

In the WT, both the time domain and frequency domain can be localized; the time domain via translations of the mother wavelet, and the frequency (scale) domain via dilations. The wavelet is irregular in shape and compactly supported, which is a suitable tool for analyzing transient signals. The compact support means, when a wavelet is multiplied with a signal which is windowed by the wavelet, only the part of the signal that is covered by the wavelet will be extracted. The compactly supported characteristic enables temporal localization of a signal features, while the irregularity makes it appropriate for the analysis of signals with discontinuities or sharp changes. On the power system, its main application in the field of analyzing and processing transient signals include analysis of power quality disturbance signals, noise reduction of electric signals, power equipment fault diagnosis, data compression, relay protection, and fault location [89]. There are both continuous WT (CWT) and discrete WT (DWT); however, in this thesis the CWT will be discussed.

3.2.1 Continuous Wavelet Transform (CWT)

The CWT method was modified as alternative way to solve a resolution problem from the STFT. The width of the window can change with changes made to each spectral component. The CWT of signal $x(t)$ is defined as

$$W(a,b) = \int_{-\infty}^{\infty} x(t) \frac{1}{\sqrt{|a|}} \Psi^* \left(\frac{t-b}{a} \right) dt = \langle x(t), \Psi_{a,b}(t) \rangle \tag{3.13}$$

where a and b are real-valued, Ψ is the mother wavelet, and * denotes a conjugation. The input $x(t)$ is a time-continuous signal and the basis function $\Psi(t)$ (bandpass signal) is a continuous function. Referring to Equation (3.11), the CWT formula can be written on the more compact form:

$$W(a,b) = \int_{-\infty}^{\infty} x(t) \Psi^*_{a,b}(t) dt. \tag{3.14}$$

The scale parameter a stretches or compresses the wavelet along the time axis, and the position parameter b determines the time domain center of the analysis of $x(t)$. It represents time-shift (translation) along the time axis, in a similar manner to moving the window along the time-axis in the STFT. This transform produces a time-scale rather than the time-frequency signal representation.

To establish a relationship between the WT and the STFT, we will choose the basic wavelet $\Psi(t)$ in the form

$$\Psi(t) = w(t) e^{-j\omega t} \tag{3.15}$$

where $w(t)$ is a window function and ω is a constant frequency. Substituting (3.15) into (3.13) turns out a CWT form suitable for a direct comparison with the STFT [12].

$$W(a,b) = \int_{-\infty}^{\infty} x(t) \frac{1}{\sqrt{|a|}} w^* \left(\frac{t-b}{a} \right) e^{-j\omega \frac{t-b}{a}} dt. \tag{3.16}$$

The CWT could be considered as a kind of analysis of signal $x(t)$ that uses a set of wavelets with different analysis widths, which adopt themselves to change the analysis resolutions according to

different frequency scopes requirements.

Chapter 4

The Empirical Mode Decomposition and Hilbert Huang Transform

In the power systems, signal oscillations are essentially non-linear and non-stationary. Therefore, selecting methodology for analyzing such signals is a challenging task [90]. The Fourier analysis is the primary method for analysis of data since it was introduced, and continues to be widely used for the analysis due to its intrinsic ability and simplicity. The main restrictions of this method is the linearity, and the data be precisely periodic or stationary, otherwise erroneous result can be obtained. Since most of PQ signals are non-stationary, Fourier transform methods are not applicable for this purpose. An adaptive method for analyzing non-linear and non-stationary signals is the Hilbert Huang Transform (HHT) which is an empirically based data analysis method. High time resolution is the main advantage of the HHT method over other PQ decomposition methods. In addition, it provides intuitive visual information of the frequency and amplitudes contained in the signal. The HHT consists of two processes [91]: The key part, Empirical Mode Decomposition (EMD) is applied to decompose a signal to obtain the signal components called *Intrinsic Mode Functions* (IMFs) [92] which have meaningful instantaneous frequencies and amplitudes. Once the IMFs are obtained, the Hilbert Transform (HT) process is then applied to each IMF to obtain the instantaneous frequencies, amplitudes and phases. The combination of the EMD and HT which is introduced as HHT provides a novel time-frequency-energy representation of a given signal.

4.1 Empirical Mode Decomposition

Empirical Mode Decomposition (EMD) is a method that handles both non-linear and non-stationary data. This method which was developed by Norden E. Huang *et al. 1998* [93], is an empirical nonlinear analysis tool for complex, non-stationary signals. EMD can be applied in many engineering fields, such as PQ analysis, geophysical and seismic signals analysis, signal and image processing, financial applications, mechanical fault diagnosis, etc. This method decomposes any non-stationary time series into a finite set of oscillatory components represented as IMFs. The principle of this method is to empirically identify these intrinsic oscillatory modes by their characteristic time scales in the signal, and then decompose the signal accordingly. The instantaneous energy associated with various time scales is identified by decomposition in order to extract the IMFs. The instantaneous frequency then can be calculated from the IMFs by using the Hilbert Transform to localize any event by time and by frequency.

4.1.1 Intrinsic Mode Functions (IMFs)

As mentioned, the EMD decomposes a signal into IMFs. Each IMF resulting from EMD process has to satisfy the following conditions [94]:

(a) In the complete data set, the number of extrema and the number of zero-crossings must either equal or differ at most by one.

(b) The mean value of the envelope defined by local maxima and minima must be zero.

The second condition implies that an IMF is stationary which simplifies its analysis. However, an IMF may have amplitude modulation as well as changing frequency. A signal that satisfies the IMF conditions allows instantaneous frequency and amplitude to be clearly defined. The number of IMFs varies from signal to signal.

4.1.2 Sifting process

The EMD algorithm extracts the IMFs through a process called *sifting process* [95]. Most of the riding waves, i.e. oscillations with no zero crossing between extrema, can be eliminated through sifting process. The sifting process starts to separate the signal $x(t)$ into the fine-scale oscillation $h(t)$ which is the first IMF and the residual $r(t)$ that may replace the original signal to go through the next sifting process. The process will be repeated iteratively as long as the residue signal to be processed have at least 3 extremas for which the scale has become very large, then the EMD process is completed. The last waveform remaining from the process is not an IMF, but it is the trend of the original signal.

The sifting process could be described as follows:

1. Identify the local maxima points and local minima poinnts of the given signal $x(t)$.
2. Connect the maxima points using cubic splines to obtain the upper envelope $e_{max}(t)$. Similarly, connect the minima points to obtain the lower envelope $e_{min}(t)$.
3. Calculate the mean as average of upper and lower envelopes, $m(t) = 1/2[e_{max}(t) + e_{min}(t)]$.
4. Extract the local oscillation mode, $h(t) = x(t) - m(t)$.
5. If $h(t)$ does not satisfy the criteria to be an IMF, repeat steps (1) to (3) by setting $x(t) = h(t)$ until the criteria for an IMF is satisfied.
6. Calculate the residue $r_i(t) = x(t) - h_i(t)$ and check if $r_i(t)$ is a monotonic function; if it is not, repeat the overall process by setting $x(t) = r_i(t)$ and increase i by one. However, if $r_i(t)$ is a monotonic function, the process is completed.

Figure 4.1 depicts how the sifting process could be executed on the signal $x(t)$ from step (1) to step (3) in order to identify the mean as average of upper and lower envelopes. In step (5), an appropriate stopping criterion avoids over-improving $h(t)$ which can lead to significant information loss [96, 97]. In the practical implementation, the stop criterion should be taken in consideration in order to get ideal components. The stop criterion for $h(t)$ is to judge whether it is an IMF or not. However, in realistic implementation it is not easy to keep the mean equal to zero. The sifting process (IMF extraction) ends when the range of the envelopes mean $m(t)$ is lower than 1% (0.001) of h_i (candidate IMF). Iteration process ends when the residue $r(t)$ is 10 % or lower of the $x(t)$. Stop rule makes the sifting process stop when the absolute values of the candidate IMFs are smaller than tolerance level tol, i.e. $|hi(t)| < tol$ for all t. We have to determine stop a criterion sifting process in order to guarantee that the IMF components retain enough physical sense of both amplitude and frequency modulations. This

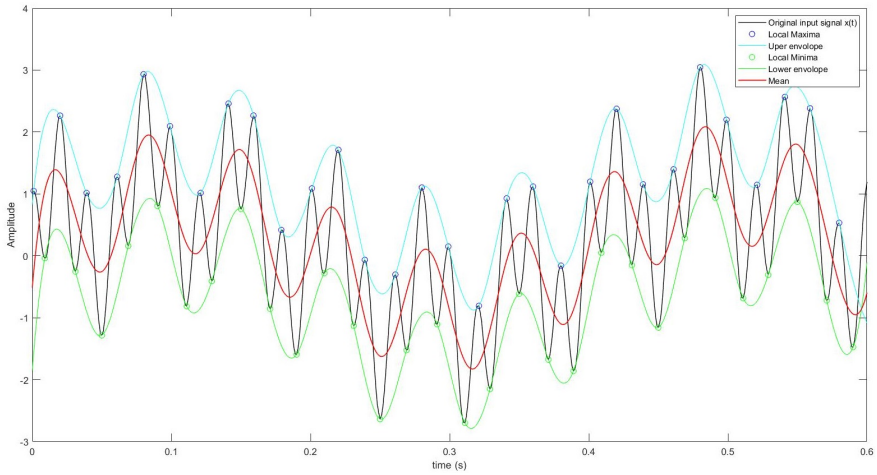

Figure 4.1: Illustration of sifting process from step 1 to 3 to identify the mean $m(t)$.

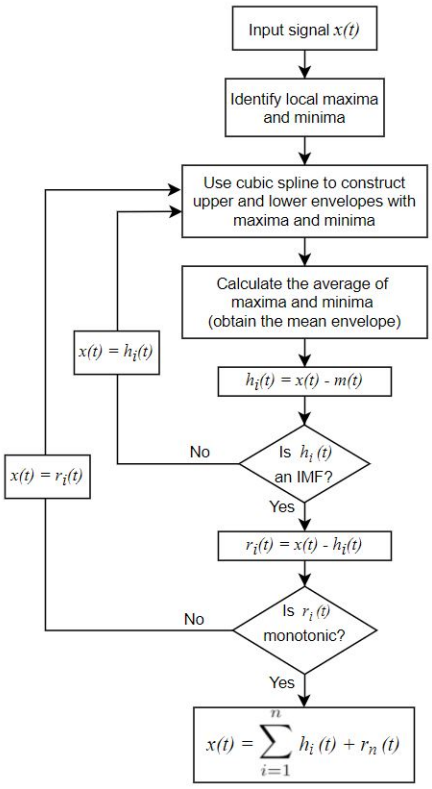

Figure 4.2: Flow chart of EMD process.

can be accomplished by limiting the size of the standard deviation (SD), which is computed from the two consecutive sifting result as [98, 99],

$$SD = \sum_{t=0}^{T} \frac{|h_{1(k-1)}(t) - h_{1k}(t)|^2}{h_{1(k-1)}^2(t)} < tol. \tag{4.1}$$

During the sifting process, the first IMF contains the highest frequency components of the signal. Thereafter, the subsequent IMFs contain progressively lower frequency components existed in the original signal. If we obtain n orthogonal IMFs during the sifting process, the original signal may be

reconstructed as

$$x(t) = \sum_{i=1}^{n} h_i(t) + r_n(t), \tag{4.2}$$

where $h_i(t)$ is IMF and $r_n(t)$ is the last residual. The extracted IMFs are symmetric and have a unique local frequency; however, different IMFs do not exhibit the same frequency at the same time. A flowchart shown in Figure 4.2 is describing the process of the EMD algorithm.

To demonstrate how the sifting process of EMD algorithm works for IMF extraction, consider a signal $x(t)$ shown in Equation 4.3 and Figure 4.3 consisting of four components of frequencies 1 Hz, 10 Hz, 15 Hz and 20 Hz, sampled for 1 second.

$$x(t) = 0.3\,t + sin(\frac{\pi}{2}\,10t) + sin(2\pi 15t) + cos(5\pi 20t). \tag{4.3}$$

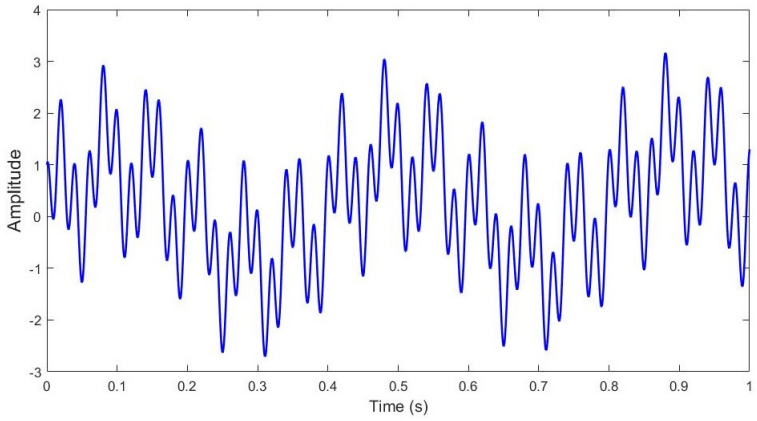

Figure 4.3: The signal $x(t)$ composed of four different signals from 5 Hz to 20 Hz frequencies.

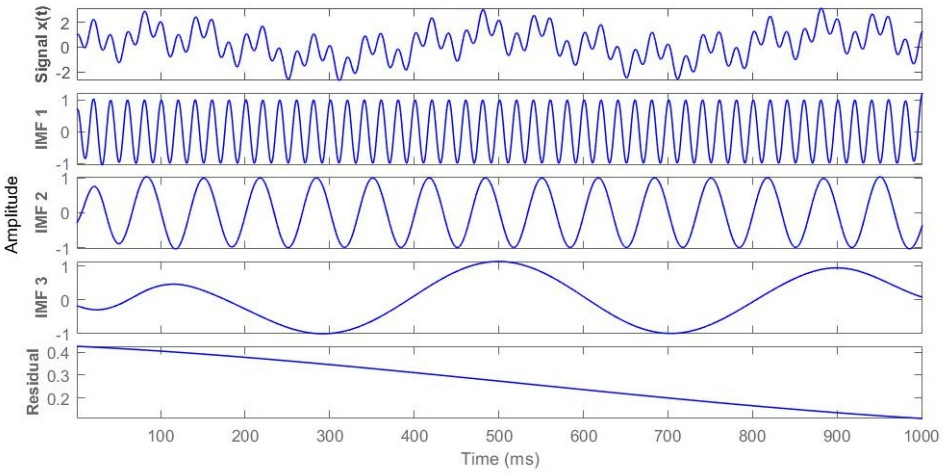

Figure 4.4: The signal $x(t)$ is decomposed into its IMF components and residual, using the EMD algorithm.

Applying the EMD algorithm, the signal $x(t)$ is decomposed into 3 IMFs and a residual as shown in Figure 4.4. The IMFs contain different frequencies as they are decreasing from first IMF to the last; i.e. the first IMF1 has the highest frequency and the last has the lowest. After IMF3 the remaining

residual is a constant or monotonic function that can not be decomposed further.

4.2 Hilbert Transform

After the IMFs have been extracted Hilbert transform (HT) is applied on each IMF to calculate the instantaneous frequency. The HT of a function $x(t)$ is defined as:

$$H[x(t)] = \frac{1}{\pi} \int_{-\infty}^{\infty} P \frac{x(\tau)}{t-\tau} d\tau, \tag{4.4}$$

where P indicates the Cauchy principal value.

The HT of a real signal x is an analytic signal $z = x + j * y$, where x is the original signal and the imaginary part $j * y$ is a version of x with a phase shifted by $\pi/2$. Note that the Hilbert transformed signal x has the same frequency and amplitude as the original signal x. The analytic signal can be used to determine the instantaneous frequency, amplitude and phase of the original data. For a given signal $x(t)$, the analytic signal $z(t)$ is defined as:

$$z(t) = x(t) + H[x(t)] = x + jy = a(t)e^{j\theta(t)}. \tag{4.5}$$

For a pure sinusoid, the instantaneous frequency, amplitude and phase are constant. The analytic signal of a pure cosine wave contains its sine version, e.g. the analytic signal of $x(t) = A\cos(\omega t + \theta)$ is presented as

$$z(t) = A\cos(\omega t + \theta) + j\,A\sin(\omega t + \theta) = Ae^{j\omega(t)+\theta}. \tag{4.6}$$

The instantaneous frequency $\omega(t)$, amplitude $a(t)$ and phase $\theta(t)$ of the $z(t)$ can be calculated as follows:

$$\omega(t) = \frac{d\theta}{dt}, \tag{4.7}$$

$$a(t) = \sqrt{x^2 + y^2} \tag{4.8}$$

and

$$\theta(t) = \arctan\left(\frac{y}{x}\right). \tag{4.9}$$

The advantages of HT for PQ signal analysis can be listed as follow:

- The HT can represent the instantaneous frequency and amplitude of a measured signal, so it solves a typical demodulation problem.
- In comparison to the Fourier analysis, which assumes that a signal is a sum of a number of sine waves, the HT allows a complex demodulation analysis of the form of a single but modulated sine wave.

After implementing the HT on each IMF component, the original signal can be presented as the real part $\mathbb{R}$ in the following form [91]:

$$x(t) = \mathbb{R}\left\{\sum_{j=1}^{n} a_j(t)\, exp\left[i\int \omega_j(t)\mathrm{d}t\right]\right\}. \tag{4.10}$$

This equation represents the HHT, where $a_j(t)$ indicates the instantaneous amplitude and $\omega_j(t)$ the instantaneous frequency of the jth IMF, with j = 1,..., n and n denotes the total number of IMFs.

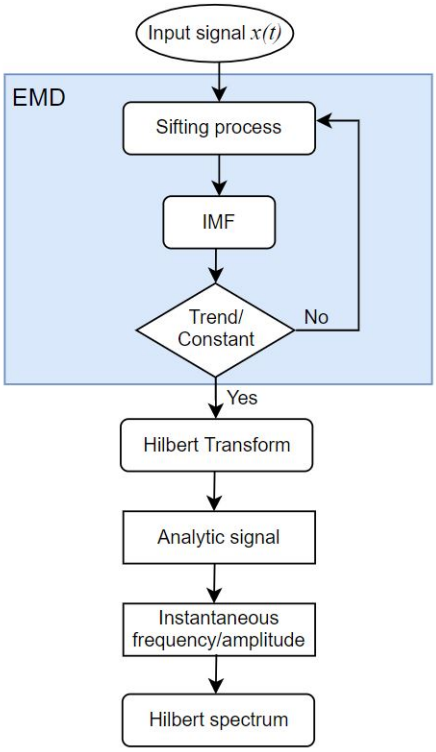

Figure 4.5: Flow chart of HHT.

Notice that the residue r_n has been omitted because it is either a monotonic function or a constant. Equation 4.10 gives both the frequency and amplitude of each component as functions of time, while the same data expanded in a Fourier representation would contain both a_j and ω_j as constants. With the IMF expansion, the amplitude and the frequency modulations are also separated, therefore, in the Fourier expansion the limitation of the fixed frequency and constant amplitude has been overcome with a variable frequency and amplitude representation. This time-frequency distribution of the amplitude is designated as the Hilbert amplitude spectrum $H(\omega, t)$, or simply *Hilbert spectrum*. With this definition, we can also define the marginal spectrum $h(\omega)$ as

$$h(\omega) = \int_0^T H(\omega, t)\, dt, \tag{4.11}$$

where T is the length of the window of signal analysis. The marginal spectrum defines the total amplitude (or energy) contribution from each frequency value. In the example below, the Hilbert spectrum of an arbitrary signal is demonstrated. Signal $x(t)$ represented in Equation 4.12 is composed of two sine waves comprise different frequencies of 15 Hz and 40 Hz within time duration of 4 seconds.

$$x(t) = \begin{cases} \sin(2\pi 15t): & 0 < t \leq 2 \\ \sin(2\pi 40t): & 2 < t \leq 4 \end{cases} \tag{4.12}$$

In Figure 4.6 a magnified view of the signal $x(t)$ from Equation 4.12 depicts how the frequency changes after 2 second, but we do not know the frequency range. In order to get the frequency information, the Hilbert spectrum and Fourier transform of the signal is represented in Figure 4.7 and Figure 4.8.

The Fourier transform represents the signal in the frequency domain. In the FT the frequencies contained in the signal are obtained, however, the time information is missing and there is no idea of

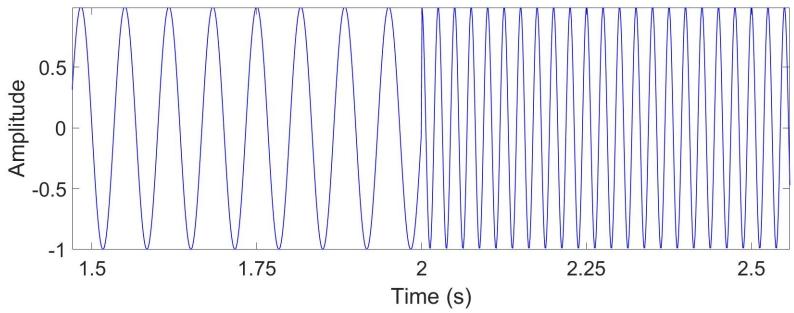

Figure 4.6: The synthetic signal $x(t)$ with instantaneous frequency

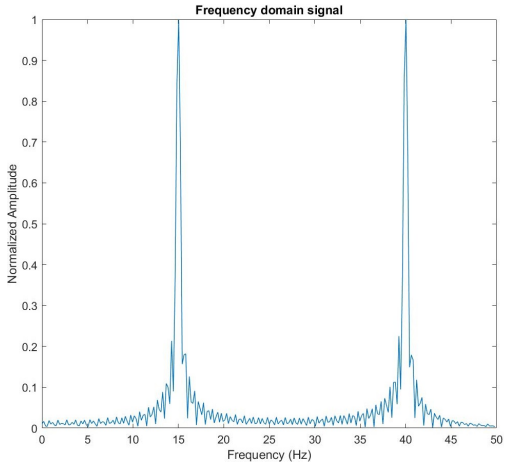

Figure 4.7: Fast Fourier Transform of signal $x(t)$.

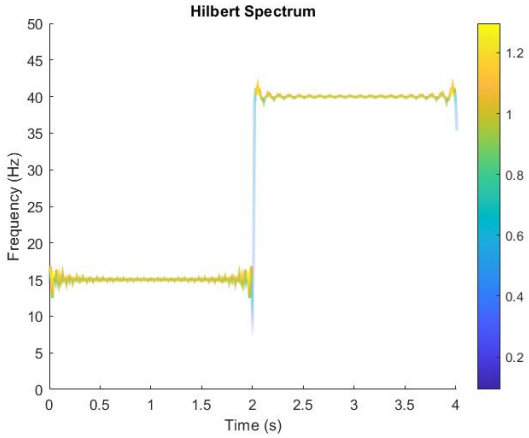

Figure 4.8: Hilbert spectrum of signal $x(t)$ indicates frequency changing time.

signal duration and the time of frequency change. Whereas in Hilbert spectrum, the signal frequency is clearly showed in respect of time. According to the signal specification, the frequency is low in beginning and rises after indicated time spot, and in addition, the frequency change time is visible. Some frequency oscillation in the starting and ending of Hilbert spectrum is due to Gibbs phenomenon [93].

4.3 Analysis of power quality disturbance

A composite signal $s(t)$ containing harmonics and transient presented below is considered to be analyzed using time-frequency analysis methods [79].

$$s(t) = \begin{cases} \sin(2\pi 50t) + 0.4\sin(2\pi 200t) : & 0 \leq t < 0.3s \\ \sin(2\pi 500t)e^{(-30(t-0.1))} : & 0.1 \leq t < 0.16s \end{cases} \tag{4.13}$$

The signal is composed of various frequencies and has a duration of 0.3 s long. As shown in Figure 4.9, an oscillatory transient is superimposed on it with period of 60 ms which decays exponentially over time.

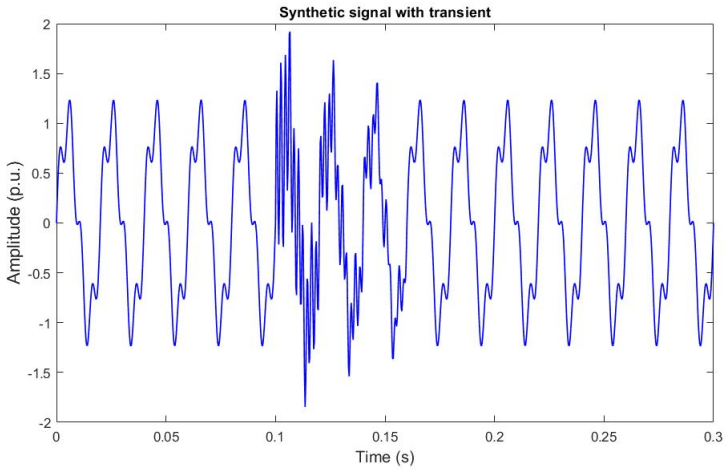

Figure 4.9: The synthetic signal $s(t)$ contains transient.

The signal is decomposed and analyzed by STFT, CWT and HHT. Figure 4.10 represents the STFT spectrum referred to as a *spectrogram*, magnitude Scalogram plotted by CWT and Hilbert spectrum of the the signal. Now one can observes the frequency components which are consist of 50 Hz, 200 Hz and 500 Hz, depicted in all plots. In the spectrogram Figure 4.10 (a), the transient period and its effect on the other frequencies are not represented distinctly. The Scalogram in Figure 4.10 (b) depicts the transient event along with the signal magnitude more accurately. The transient start and end time is clear and the components magnitude are distinct. Nevertheless, the frequency resolution is coarse, so it is difficult to identify the exact frequency value. The Hilbert Spectrum in Figure 4.10 (c) represents the transient event, time and effect on other frequency components very precisely. Additionally, the frequency resolution is very high, so the components are precisely distinguishable.

The EMD method is applied to decompose the signal into intrinsic oscillatory components (IMFs). The result of decomposition illustrated in Figure 4.11 depicts three IMFs and residual extracted from the synthetic signal. Most frequency content lies in the first three mode of oscillations (IMFs) [100].

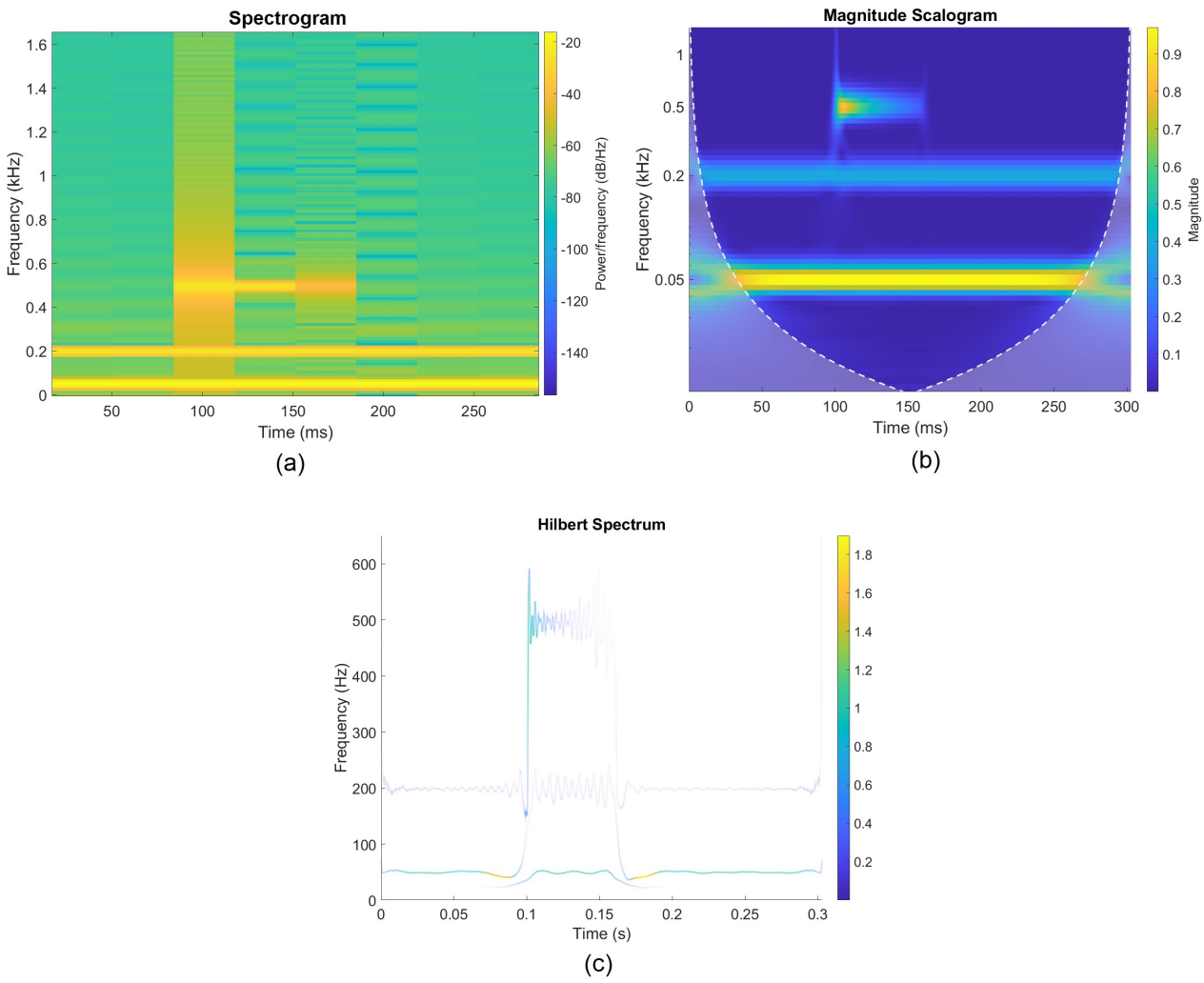

Figure 4.10: Frequency components of signal $s(t)$: (a) spectrogram using STFT , (b) CWT magnitude scalogram and (c) Hilbert Spectrum.

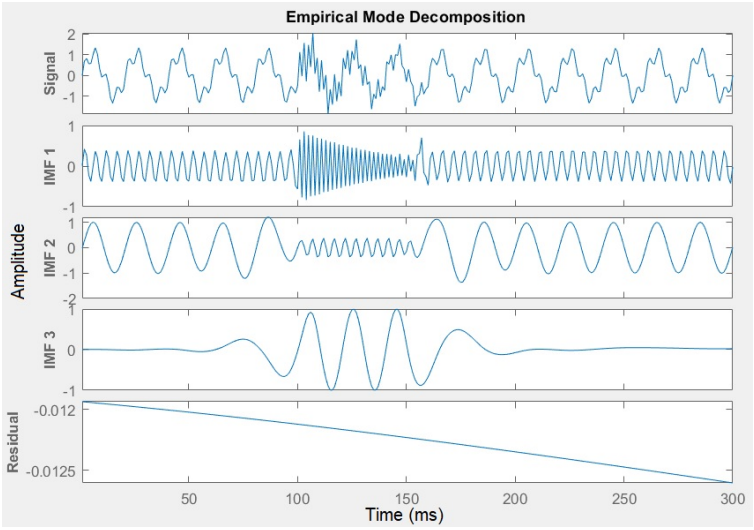

Figure 4.11: Decomposition of synthetic signal using EMD. The first plot on the top is the data, the following 3 plots are the IMFs and the last one is the residue.

Once the IMFs are obtained the Hilbert transform is used to obtain the associated instantaneous frequency and amplitude as shown in Figure 4.12. In the decomposition process by EMD, the highest

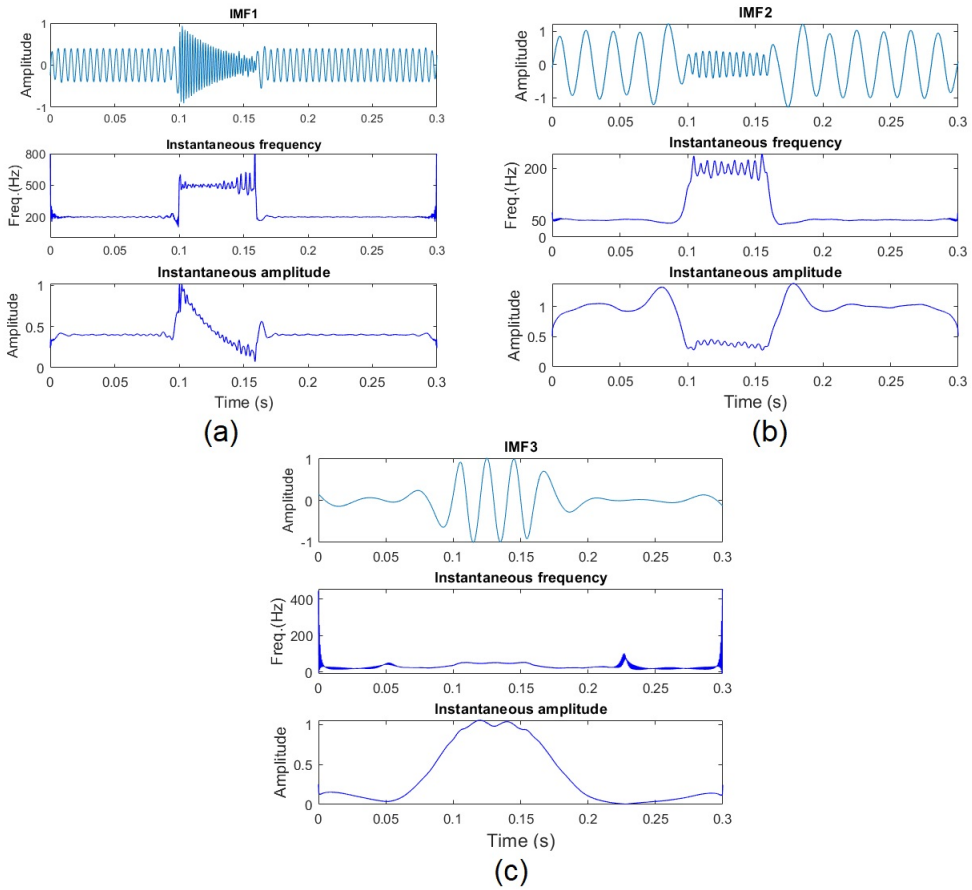

Figure 4.12: Instantaneous frequency and amplitude of: (a) IMF1, (b) IMF2, (c) IMF3, obtained by HHT.

frequency component of the signal will be captured by IMF1, the next highest frequency component will be captured by IMF2 and so on. Additionally, the waveform in the IMF consists of three segments. Segment 1 starts from 0s to to 0.1s, segment 2 from 0.1s to 0.18s and segment 3 from 0.18s to 0.3s. The IMF1 captures the highest frequency component of each segment, i.e. 200 Hz at segment 1, 500 Hz at segment 2 and 200 Hz at segment 3. The waveform of IMF1 and the associated instantaneous frequency and amplitude are shown in Figure 4.12(a). Thereafter, IMF2 captures the lower frequency component of each segment; 50 Hz at segment 1, 200 Hz at segment 2 and 50 Hz at the last segment as shown in Figure 4.12(b). IMF3 captures the lowest frequency component of each segment. Since there is no lower than 50 Hz frequency in the signal, no segment with frequency lower than 50 Hz is detected. In Figure 4.12(a) the exponential sinusoidal waveform which indicates the transient, is captured in second segment of IMF1. Also the instantaneous amplitude of IMF1 shows a waveform decays exponentially in segment 2.

4.3.1 Evaluation and Discussion

For PQ analysis of a non-linear and non-stationary signal affected by a disturbance three time-frequency analysis algorithms are implemented and evaluated; The Fourier Transform, Wavelet Transform and Hilbert Transform. For this purpose, the synthetic signal $s(t)$ with fundamental frequency of 50 Hz is considered as illustrated in Figure 4.9.

In order to analyse non-stationary signals, FT encounters limitation for frequency analysis over time. Although this limitation is solved by the improved version of FT, ST FT, there is still deficiency in using this method for non-stationary signals analysis because STFT has a fixed resolution which is determined by a fixed windowed function whose form and shape don't vary. Looking at the Figure 4.10(a), it can be seen that the PQ disturbance is not well localized in the Spectrogram plot. It is difficult to understand when exactly the transient started and ended. The frequency range also spread widely. Power level of the frequencies present in the signal is indicated by varying colors according to the color code bar on the right. Let's see what will happen when we reduce the windowing size of the function used in the Spectrogram. As seen in Figure 4.13 reducing the size of the window enhances the time resolution, but on the other hand degrade the frequency resolution and the frequency values are not precisely determined. To increase frequency resolution, the width of the window function should be enlarged, but consequently, it affects the time resolution. That is to say, it is showing the trade-off between the time and frequency resolutions. The STFT cannot balance the demand of both time resolution and frequency resolution. The time and frequency uncertainty of the events is still high. Additionally, one can not evaluate the amplitude of the component signals.

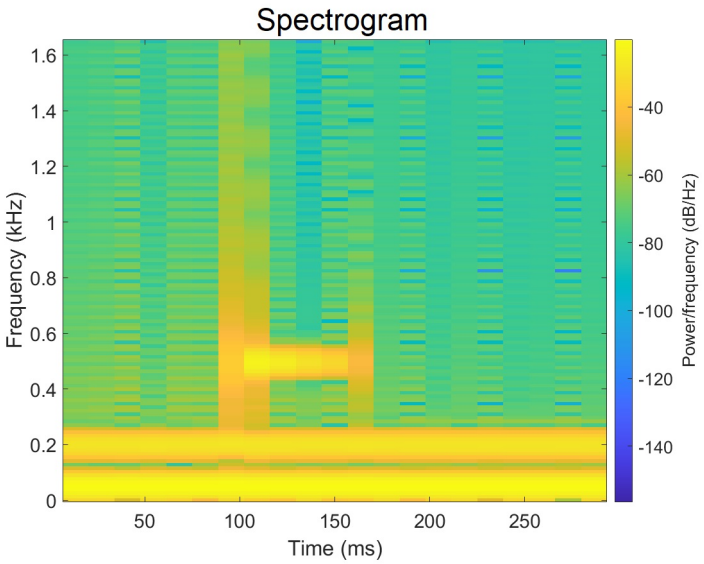

Figure 4.13: Frequency spectrum of signal $s(t)$ using STFT with enhanced time resolution.

Let us apply the Wavelet Transform (WT) to analyze the signal. The WT based on windowing technique with variable-sized regions is a useful method for spectral analysis of signals. Therefore, its time-frequency resolution is better than the STFT. The Continuous Wavelet Transform (CWT) will help to obtain a joint time-frequency analysis of the signal. In Matlab, cwt function is used for this purpose which uses Morse wavelets by default if we don't specify which wavelet to be used. CWT function determines the minimum and maximum scales for analysis automatically based on the wavelet's energy spread. The magnitude of the wavelet coefficients returned by the function are color

coded. As seen in Figure 4.10(b), the time-frequency visualization is enhanced in Scalogram by CWT. Now the transient event is well localized in time and frequency and the magnitude or amplitude of the component signals can be evaluated according to the color cod bar on the right of the plot. The white dashed lines denote the Cone Of Influence (COI). The gray shaded area outside of dashed lines indicates the affected area by edge-effect artifacts in the scalogram. The effects in the scalogram arise from areas where the stretched wavelets extend beyond the edges of the observation interval. The wavelet will be compressed when facing high frequency according to the scale parameter to capture high frequency components and will be expanded to capture low frequency components of the signal. It is why the shaded region is observed expanded at the bottom and shrinks upwards, as the frequency rises upward on the vertical axis. The unshaded region inside dashed lines, represents a reliable time-frequency information of the signal, while the shaded region outside the dashed lines the information would be considered suspectedly due to the potential edge effects.

The CWT, however, still has shortcoming in the adaptivity since the mother function has to be chosen prior to the analysis. It yields good time resolution but poor frequency resolution at high frequencies, and good frequency resolution but poor time resolution at low frequencies. It is effective specifically when the signal has low frequency components for long duration and high frequency components for short durations. Even though wavelets simplify by the sectioning the signal and the application of localized form of spectral analysis, the Inconsistency of wavelet shapes as basis functions introduces some intricacy and a wide variety of analysis results. We also notice that the small deviations of frequencies are not distinguishable and the frequency representation shows like a stationary behavior.

Now the The HHT method will be considered. This method is a well-suited technique for analyzing stationary and non-stationary signals which requires no prior assumption of the signal, so it is adaptive to any unknown signals. The method is especially effective for decomposing non-stationary signals that spectral content changes with respect to time, and often found in power quality waveforms. HHT contains two processes; first the EMD is used to decompose the signal to be analyzed into IMFs which have meaningful instantaneous frequencies and amplitudes. During the decomposition, the IMFs are extracted from the highest frequency component to the lowest, I.e. the first IMF holds the highest frequency and the last IMF holds the lowest one. When a composite signal is decomposed into IMFs, Hilbert transform is applied to each IMF in order to extract the instantaneous frequency and amplitude. As depicted in Figure 4.10(c), the Hilbert spectrum with higher time-frequency resolution can reflect all frequency components of the signal $s(t)$ and give a clear view of these components changing over time. Thus, the local information of the signal, such as instantaneous frequency, can be observed precisely. Table 4.1 indicates a comparative summary of Fourier, wavelet and HHT analyses [101].

Table 4.1: Comparison of power quality spectral analysis techniques.

Feature	**STFT**	**CWT**	**HHT**
Basis	Priori	Priori	Adaptive
Nonlinear	No	No	Yes
Nonstationary	No	Yes	Yes
High frequencies discovering	Medium	High	Very high
Spectrum resolution	Low	Medium	High
Visual representation	Poor	Good	Good
Processing time requirement	Low	Medium	High
Theoretical base	Theory	Theory	Empirical

4.3.2 Mode mixing problem

Although the EMD has been proposed as an adaptive time–frequency data analysis method for non-stationary signals, it still suffers some deficiencies [102]. One of its major deficiency is the frequent appearance of mode mixing which is often due to the signal containing close frequency components [103] or a consequence of signal intermittency. The intermittence that causes serious aliasing in the time–frequency distribution, also obscures the physical meaning of individual IMF. Mode mixing is defined as a single IMF either consisting of oscillations of dramatically disparate scales, or a component of a similar scale residing in different IMFs [104].

Since EMD is adaptive to extrema distribution and uses the extrema information to separate intrinsic oscillatory modes, changes in extrema locations and values due to some disturbance may lead to significantly different results in which the extracted modes sometimes appear unexpected. References [91, 103] describe the sifting process to identify the extrema in the case of mode mixing in more details. To illustrate the mode mixing problem of the EMD algorithm, a simulated synthetic signal $x(t) = \sin(t) + 0.1\sin(20t)$ is considered. The signal contains a fundamental sinusoidal wave of low frequency with unit amplitude, and intermittent oscillations of high frequency that exists only during certain time spans as shown in Figure 4.14. Decomposing the signal performing EMD, it is observed that the obtained two IMFs are distorted significantly. As seen in the figure, the IMF 1 is a mixture of both the low frequency fundamental wave and the high frequency intermittent oscillations. The IMFs are also affected at both ends. Thus, both IMFs obtained through EMD process, fail to reveal the characteristics of the signal $x(t)$ accurately. When the mode mixing problem occurs, an IMF can cease to have physical meaning by itself, suggesting erroneously that there may be different physical processes represented in a mode. In this example, the mode mixing is due to signal intermittency. This

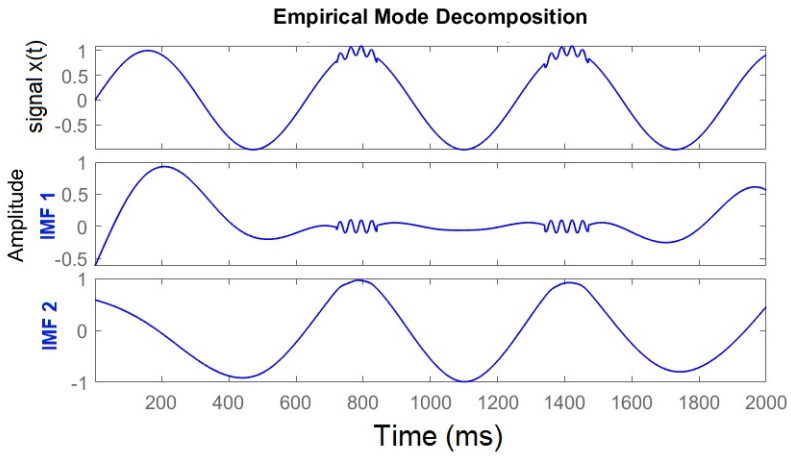

Figure 4.14: The decomposition result using EMD: the input signal $x(t) = \sin(t) + 0.1\sin(20t)$ plotted in the top panel, IMF 1 in the middle and IMF 2 in the bottom panel.

implies that the EMD results can be sensitive to noise contained in signal. If the decomposition is insensitive to noise of small finite amplitude and can bear little quantitative (no qualitative) change, the decomposition would be usually considered robust. Otherwise, the decomposition would be unstable and the EMD may not be reliable. To overcome the mode mixing issue, a noise-assisted data analysis (NADA) technique, referred to as the Ensemble EMD (EEMD), is proposed. This method defines the true IMFs as the mean of an ensemble of trials in which each trial consists of the decomposition results of the signal and a normally distributed white noise with a finite amplitude.

4.4 Ensemble Empirical Mode Decomposition(EEMD)

EEMD, a noise-assisted data analysis method proposed by Wu and Huang *et al.* 2009 [104], represents an improvement over the EMD. It defines the true IMF components as the mean of an ensemble of trials, each consists of the signal plus a distributed white noise of finite amplitude. In this approach, ensemble of white noise-added signal is sifted, and the mean is treated as final true result. The white noise with finite, but not infinitesimal, amplitude is applied to force the ensemble to extrude all possible solutions in the sifting process. It provides a uniform reference frame in the time–frequency space. Therefore, the added noise collates the portion of the signal of comparable scale in one IMF. The EEMD principle is that the added white noise would populate the whole time–frequency space uniformly. When signal is added to this uniformly distributed white noise background, the components of signal of different scales are automatically projected onto proper scales of reference established by the white noise.

In the decomposition process, the added noise is averaged out with sufficient number of trials, so the only persistent part that survives the averaging process is the component of the original data, which is then treated as the true and more physical meaningful result. Since different white noises are added to the signal in each trial in the decomposition process, each individual trial may produce very noisy results. However, the noise in each separate trial is different, so it can be decreased or even completely canceled out in the ensemble mean of enough trials. The ensemble mean is then treated as the true physical result because the only persistent part will be the signal as more and more trials are added in the ensemble. The EEMD method has higher time-frequency resolution ratio to decompose complex disturbances and extract characteristic value. It does not require preset basis function. Therefore, it is not only suitable for stationary signals, but also for non-stationary signals. The concept of EEMD is based on following observations [91]:

1. A collection of white noise cancels each other out in a time-space ensemble mean; therefore, only the signal can survive and persist in the final noise-added signal ensemble mean.
2. White noise of finite magnitude is required to force the ensemble to exhaust all possible solutions; it makes the different scale signals reside in the corresponding IMFs, and render the resulting ensemble mean more meaningful.
3. The decomposition with true and physically meaningful result is not the one without noise; it is designated to be the ensemble mean of a large number of trails consisting of the noise-added signal.

   Based on the principle and observations above, the EEMD algorithm contains the following steps:

1. Add a white noise series with the given amplitude to the signal being analyzed, i.e.

$$x_m(t) = x(t) + n_m(t), \tag{4.14}$$

   where $x_m(t)$ represents the noise-added signal of the mth trial, and $n_m(t)$ indicates the mth added white noise series.

2. Decompose the noise-added signal $x_m(t)$ into IMFs using the EMD method.
3. Repeat Step (1) and Step (2) again and again, but with different white noise series each time.
4. Calculate the ensemble means of corresponding IMFs of the decompositions as the final result.

Figure 4.15 illustrates the decomposition process by EEMD [105].

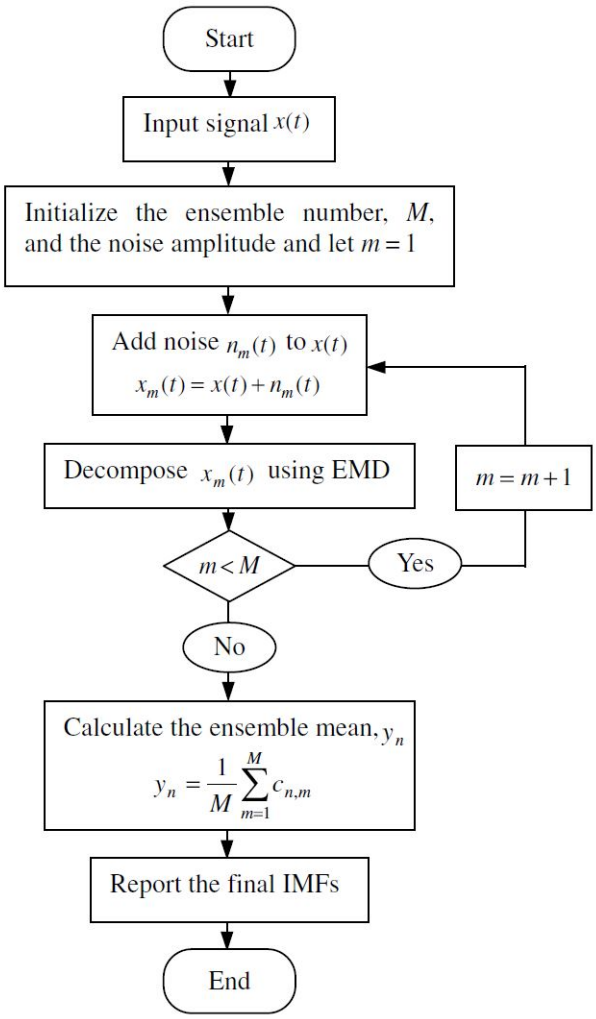

Figure 4.15: Flow chart of EEMD.

To perform the EEMD method, the number of ensembles and amplitude of the added white noise are two considerable parameters. The amplitude of noise is not necessarily small, but the ensemble number of the trials has to be large in order to cancel out the added noise. Equation 4.15 represents the relationship among the amplitude of added white-noise, the ensemble number and the effect of the added white noise [104]:

$$e = \frac{a}{\sqrt{M}}, \tag{4.15}$$

where a is the amplitude of the added noise, M is the number of ensembles and e is the final standard deviation of error, which is defined as the difference between the input signal and the corresponding IMFs.

The EEMD will be effective if the amplitude of added noise is not too small because it introduces the change of extrema that the EMD relies on. Furthermore, by increasing the number of ensembles, the effect of the added noise can be reduced to a quite small even negligible level. To illustrate the performance of EEMD the example in Figure 4.14 is used. As described in the previous section, the EMD method is unable to accurately decompose composite signals that are mixture of intermittent high frequency oscillations residing on a low-frequency sinusoidal signal. To overcome this issue, the EEMD is implemented and the decomposition result is shown in Figure 4.16. This time the signal is

decomposed into the components accurately. The plot reveals fundamental signal in panel IMF 5, and intermittent signal in IMF 3 panel. As illustrated, the mode mixing problem of EMD is eliminated significantly by the EEMD method. This demonstrates that the EEMD can extract the oscillating modes more accurate and is not influenced by mode mixing. Thus, the EMD improves the capability of extracting signals in the data and represents a major improvement of the EMD method.

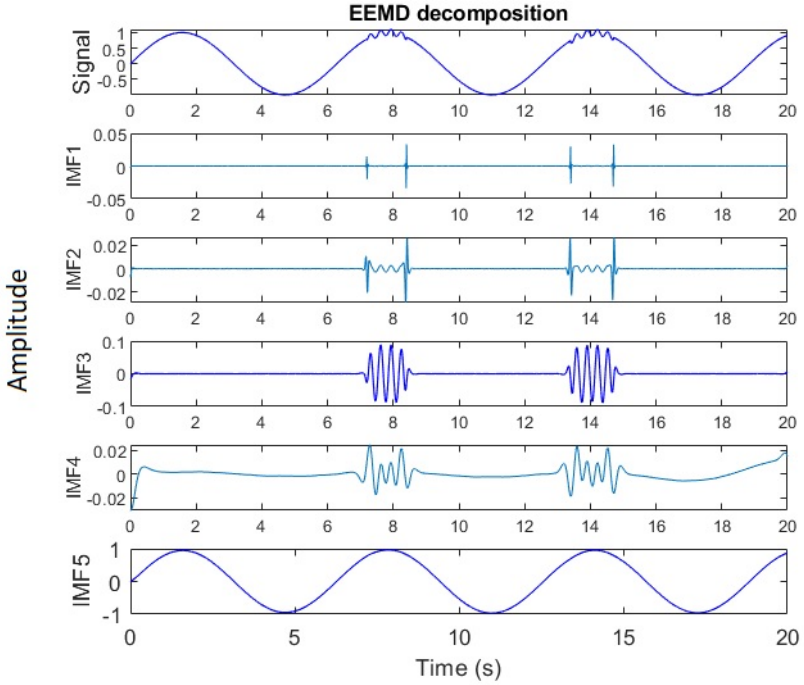

Figure 4.16: Decomposition result using EEMD, The input synthetic signal $x(t) = \sin(t) + 0.1\sin(20t)$ is plotted in the top panel, the fundamental signal in the bottom panel and the intermittent signal in the middle panel IMF3.

Chapter 5

Analysis of Power Grid Data

In the previous chapter the data analysis algorithms have been applied on the simulated synthetic signal. The signal has been decomposed and analyzed using the STFT, CWT and EMD methods. In this chapter a real-world data related to power quality will be analyzed by those methods. The aim of the analysis is to detect time-variant frequency content and localize in the affected signal. Then the time-frequency data analysis methods are utilized to discover PQ disturbance such as transient and exhibit it on time-frequency plots.

The dataset is provided by the Federal University of Technology Paraná in Brazil [106]. It is a recording from an experiment in Laboratory for Innovation and Technology (LIT) in Embedded Systems. The dataset was conceived and engineered to provide data for evaluation and development of Non-Intrusive Load Monitoring (NILM) System, and is available to the public interested in research in NILM as well as other topics. The data is composed of voltage and current waveforms collected in a real environment on a variety of single and multiple loads. The loads were connected to a single-phase 127 V power grid with fundamental frequency of 60 Hz in the lab, and had been switched on and off individually to generate PQ samples. The aggregated data has duration of about two hours which is very large. Therefore, they have segmented and converted it to binary format in order to reduce its size, in addition Matlab scripts are provided to convert the data to *.mat* files. The dataset used for the thesis work is further segmented to a 2 second time span from 726 s to 728 s where a prominent PQ event has occurred as can be seen in Figure 5.1.

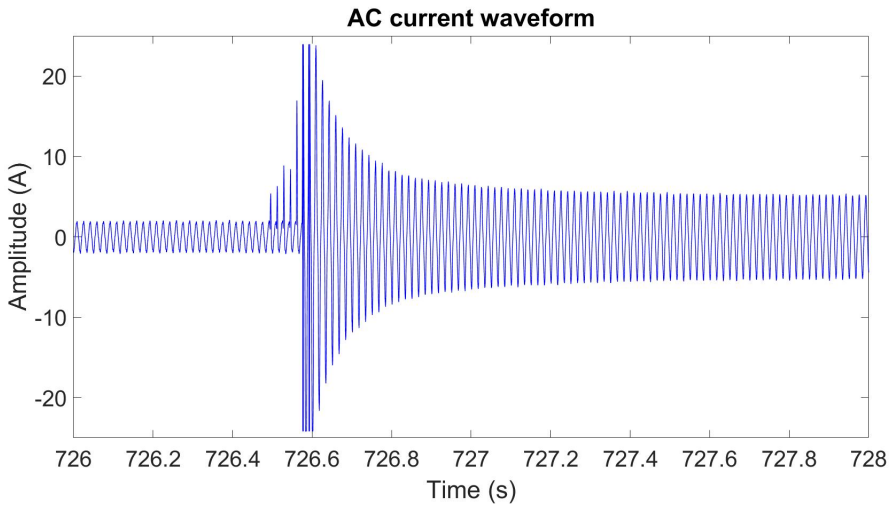

Figure 5.1: Current waveform of an AC power single-phase with 60 Hz fundamental frequency.

Looking at the corresponding voltage waveform of the circuit, we notice that the voltage is also affected when the load connected to the grid is switched on. Figure 5.2 depicts the current and voltage waveforms in the same plot. As seen, the voltage magnitude fluctuates simultaneously with the current magnitude when transient occurs. The fact that the transient distorted the current waveform much

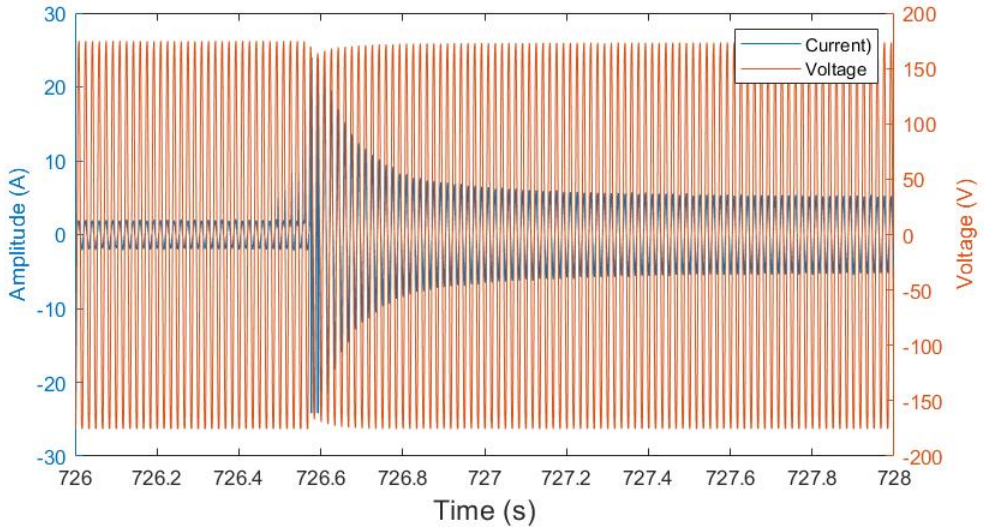

Figure 5.2: Voltage and Current waveform of an AC power showing magnitude variation when a load is switched on.

more severe than the voltage transient is normal for many electronic loads. Such a load contains a small capacitor at the grid side of the power supply, for example, as part of an EMC filter. A small amplitude with fast oscillation in voltage will lead to a large variation in current. The prominent distorted current waveform clearly indicates the presence of electronic load [1].

Considering the time domain representation of the signal, we can see a distinct signal variation at around 726.6 s. However, the event characteristic such as frequency cannot be identified at the time domain representation. Therefore, we need time-frequency analysis methods for further investigation.

5.1 Data analysis using STFT

In this section the PQ signal related to the dataset will be analysed using the short-time Fourier transform (STFT). The STFT which is a sequence of Fourier transforms of a windowed signal provides both the time and frequency information for situations in which frequency components of a signal vary over time. The time and frequency resolution is controlled by the size of window, however, there is a trade-off between frequency and time resolution. That is to say that by choosing a narrow-width window we obtain good resolution in the time domain but a poor resolution in the frequency domain, and vice versa. spectrogram is a visual representation of the spectrum of signal frequencies over time in STFT. The spectrogram of the current signal is shown in Figure 5.3 choosing a narrower window size.

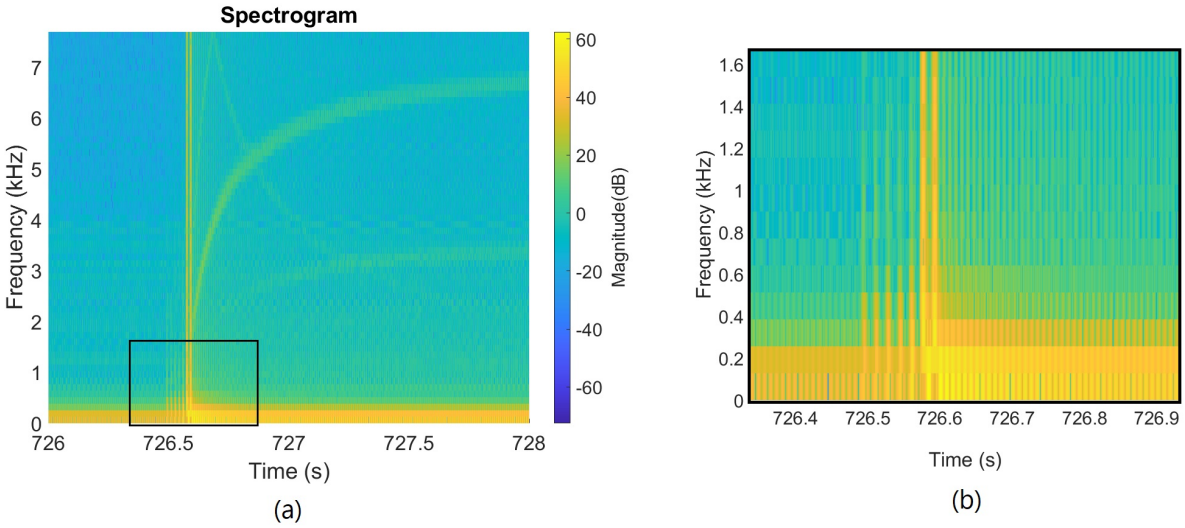

Figure 5.3: Time-frequency representation of the current signal using STFT, (a) spectrogram obtained by Hamming window with a shorter segment length of 120 samples, (b) magnified view of rectangle area.

The figures depict frequency contents of the signal. It also provides information about when the frequency changes happened or an event occurred with respect to time. Nevertheless, there is an issue that one can not identify the exact frequency even if the frequency spectrum is zoomed in, still it can be observed in a wide range as can be seen in the Figure 5.3(b). We can only estimate the frequencies range, also some close frequencies are mixed and spread on the range. Moreover, it is hard to recognize the frequency magnitude before and after transient. The transient can be observed explicitly, however, one cannot distinguish harmonics in this figure. Although the frequency resolution can be increased by selecting a longer window segment, on the other hand it will affect the time resolution As seen in Figure 5.4. Now the frequency resolution is improved and the frequency components such as odd order harmonics are distinct, yet the time resolution is impaired. The frequency can be identified but it is not very well localized. So, the exact time of frequency changes are not identifiable, and any change in the signal components will be observed on the width of the whole window segment. One of the issue in the spectrogram is that some short oscillations or small changes in the time domain will not be captured by the wider window segment. Additionally, the limit of transient frequency is not specified as it exceeds over 7 kHz.

By defining the window size, the frequency or time resolution can be maintained. The shorter the window size the better time resolution but the poor frequency resolution. And contrarily, the longer the window segment, the better frequency resolution but the coarser time resolution is obtained.

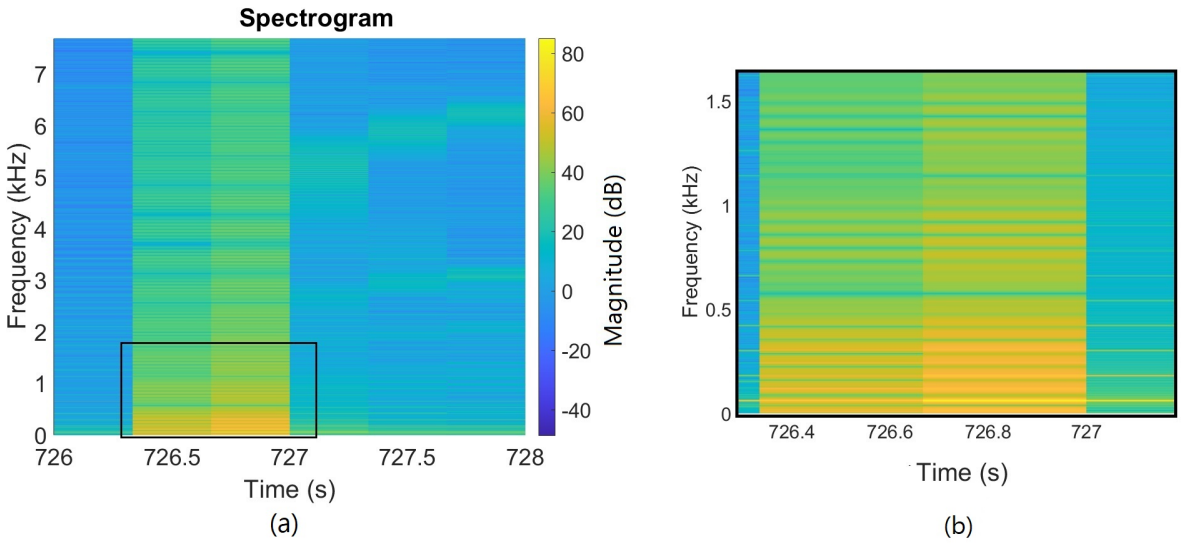

Figure 5.4: Time-frequency plot of the current signal using STFT with wider window size; (a) spectrogram obtained by Hamming window in which the signal is divided into eight segments, (b) magnified view of rectangle area.

5.2 Data analysis using CWT

The main shortcoming of STFT is using the fixed window that cannot afford good localization both in time and frequency domains simultaneously. So, there is always trade off between the time and frequency resolution. To overcome the insufficiency of the STFT, Continuous Wavelet Transform (CWT) is used. The CWT favorable for analyzing transient behavior, rapidly changing frequencies, and slowly varying behavior. The aim of CWT is to decompose signals according to the basis functions to provide good resolution both in frequency and time domains.

As described in the chapter 3, the CWT in which data analysis is based on a basis function or wavelet Ψ, compares the signal to shifted and compressed or stretched versions of the wavelet. Stretching or compressing a function is related to dilation or scaling parameter. At lower (small) scale, the wavelet is compressed which has higher frequency, therefore the fast oscillations or high frequencies could be captured. While at higher (long) scale when the wavelet is stretched and its frequency is low, the lower frequencies will be captured. The time domain localization is related to translation or position parameter at which the wavelet is sliding along the time axis. To visualize the Wavelet coefficients, the scalogram is used. For spectral analysis of a current waveform, the CWT is applied and its scalogram is shown in Figure 5.5. As can be seen in the scalogram we have a clear view of the signal spectrum. Both the time and frequency resolution are maintained and power density is also well represented by color map according to the magnitude color bar on the right. Thus, we can easily evaluate the signal magnitude before and after the event when a load is connected to the grid. In Figure 5.6 both the original current waveform and the scalogram obtained by CWT are plotted for the purpose of illustration of transient effect and current magnitude variation. As can be seen the current amplitude at any point can be identified simply. The effect and power level of the transient is evident as well. Furthermore, a frequency component of the signal at third harmonic can be observed after the event, whereas this cannot be identified easily in spectrogram using a short window length.

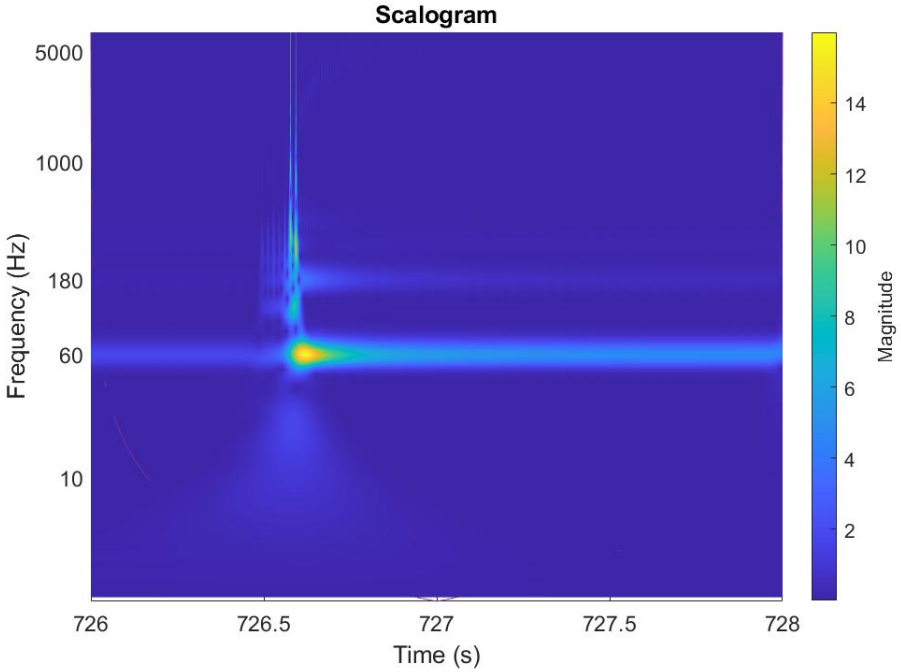

Figure 5.5: Time-frequency representation of the current signal using CWT with Morse wavelet.

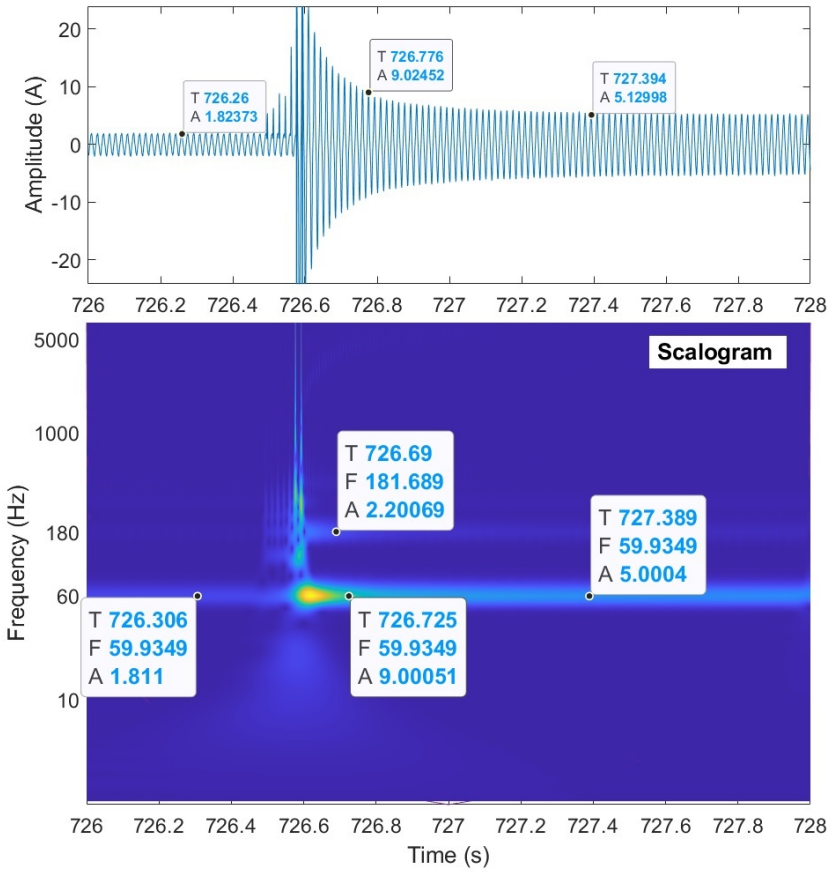

Figure 5.6: Transient event and the current magnitude variation.

5.3 Data analysis using HHT

The Hilbert Huang Transform (HHT) is a suitable method for analyzing stationary and non-stationary signals. This method is adaptive which requires no initial assumption of the signal. The HHT consists of two processes; First the Empirical Mode Decomposition (EMD) is used to decompose the signal to obtain the signal components represented in the Intrinsic Mode Functions (IMFs). The amplitude information of the IMFs can be evaluated in this process, but for acquiring the frequency information next process is required. Hence, the HTT can be applied to to the extracted IMFs in order to obtain instantaneous frequencies which can then be calculated to localize any event by time and frequency information.

5.3.1 EMD application

In this section the EMD is applied to decompose the data into its oscillatory components, then HTT is used to analyze the signal components. As described previously, the EMD which is the key part of the HHT method, can be used as a powerful tool for analyzing transient and nonlinear and non-stationary signals. It can decompose any complicated data into a finite and often small number of components based on the local characteristic time scale of the data. The components known as IMFs, form a complete and nearly orthogonal basis for the original signal. The IMFs are extracted through a sifting process in the EMD algorithm. Sifting is used iteratively to separate different oscillatory riding components of the signal, starting with the fastest and ending with the slowest component. The IMFs contain frequencies ranging from the highest to the lowest ones of the signal. The original signal can be recovered by adding all the IMFs. Applying the EMD method on the current signal, 9 IMFs and a residual are obtained as shown in the Figure 5.7.

The signal is decomposed into different oscillatory components (IMFs). The plot reveals the transient event and other oscillations with their magnitudes. Looking closely at the plot, IMF 1 exhibits the characteristic of transient, and IMF 4 the characteristic of original signal. However, there are fluctuating instantaneous frequency and amplitude which implicates that the IMF contains mixed frequency component due to the mode mixing issue.The computed IMFs can be used by HTT to obtain the instantaneous frequency and amplitude information as shown in the Figure 5.8. The plot reveals frequency components around 7 kHz and the current amplitude around 60 A in the first IMF. The lower frequency components with the corresponding lower amplitudes are plotted in the following IMFs. IMF 1 depicts the characteristic of amplitude at the transient event, and IMF 4 represents the instantaneous amplitude of original signal. However, it is not yet easy to understand the frequency characteristics.

In order to get a better perception of the instantaneous frequencies of IMFs, we use the Hilbert Spectrum of each IMF. As already mentioned, IMF 1 and IMF 4 carry estimated information of the signal components. Since the first IMF contains the highest frequency, it is assumed to contain the transient, and IMF 4 carries the fundamental frequency (60 Hz) with oscillations around it before and after transient event.

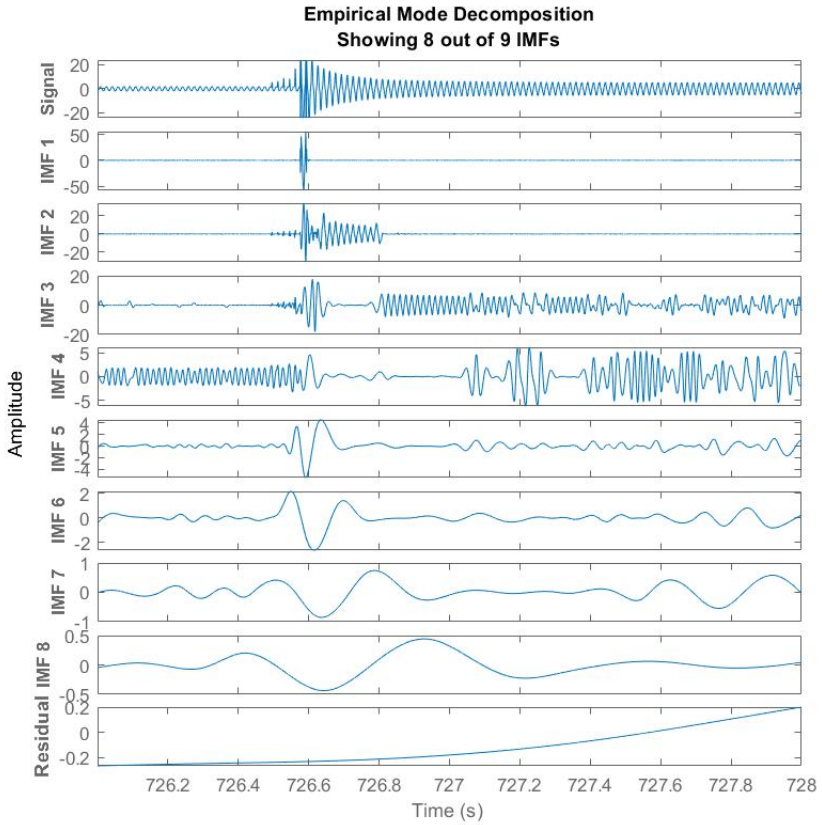

Figure 5.7: Decomposition of the signal performing EMD. The top panel indicates the original data, following panels are the IMFs, the last panel depicts the residue.

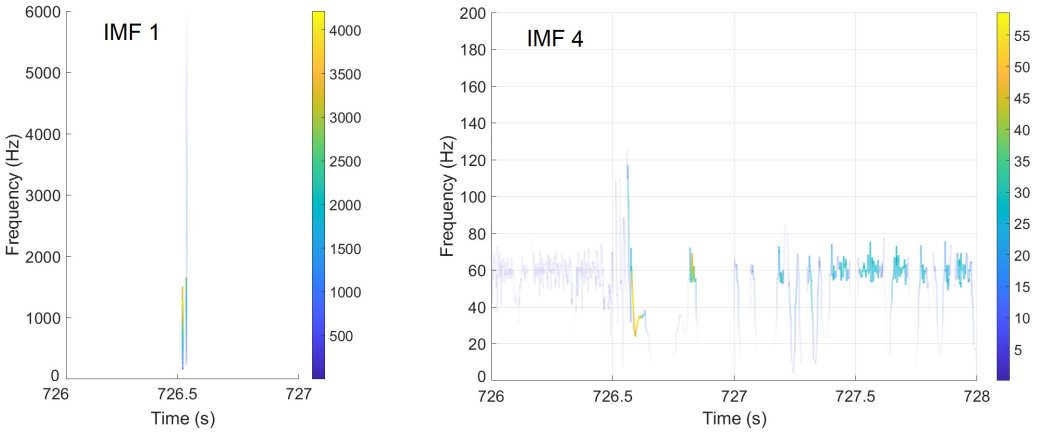

Figure 5.9: Hilbert spectrum of IMF1 (left) and IMF5 magnified (right).

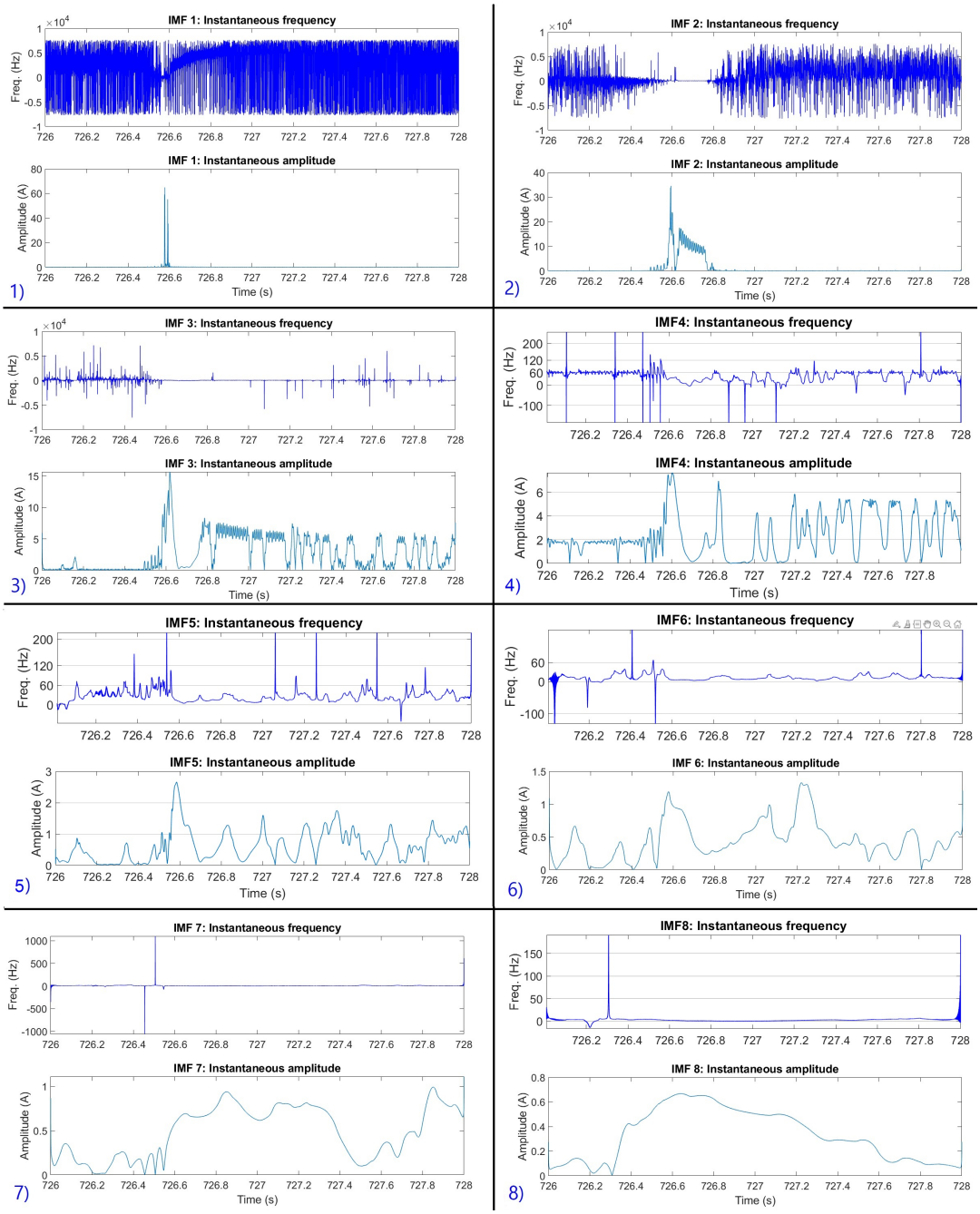

Figure 5.8: Instantaneous frequency at the top, and instantaneous amplitude at the bottom for each IMF.

5.3.2 EEMD application

In the previous section the power grid data was decomposed into 10 IMFs performing the EMD algorithm. The result demonstrated a relatively improvement, however, it is not optimal. There still exists some difficulties in the extracted features of the signal due to some phenomenon. As mentioned in section 4.3.2, one of the major shortcoming of EMD is the effect of mode mixing. This phenomenon occurs when the oscillations with disparate time scales are preserved in one IMF, or the oscillations with the same time scale are sifted into different IMFs. To overcome this drawback, a noise-assisted EMD algorithm, referred to ensemble empirical mode decomposition (EEMD) is proposed. EEMD provides a better scale separation capability than the standard EMD method. The EEMD consists of

adding different series of white noise into the signal in several trials. The added white noises spread uniformly over the entire time-frequency space. So, the processed signal seems to be a projection over white noise background. Since the added noise is different in each trial, the resulting IMFs don't exhibit any correlation with the corresponding IMFs from one trial to another. The results achieved by performing the EEMD depend on the choice of the ensemble number and the amplitude of added noise. If the number of trials is adequate, the added noise can be eliminated by ensemble averaging of the obtained IMFs related to the different trials. For our work, different number of ensemble and amplitude of added noise are used. The ensemble numbers are selected from 100 to 5000, while the standard deviation of the added noise selected from 0.05 to 0.3. By increasing the number of ensemble while reducing the amplitude of noise, smoother components are obtained. Figure 5.10 illustrates the decomposition result of EEMD algorithm. It can be seen that the IMF 1 to 3 exhibit characteristic of transient, IMF 4 shows characteristic of signal after event, and IMF 5 before event.

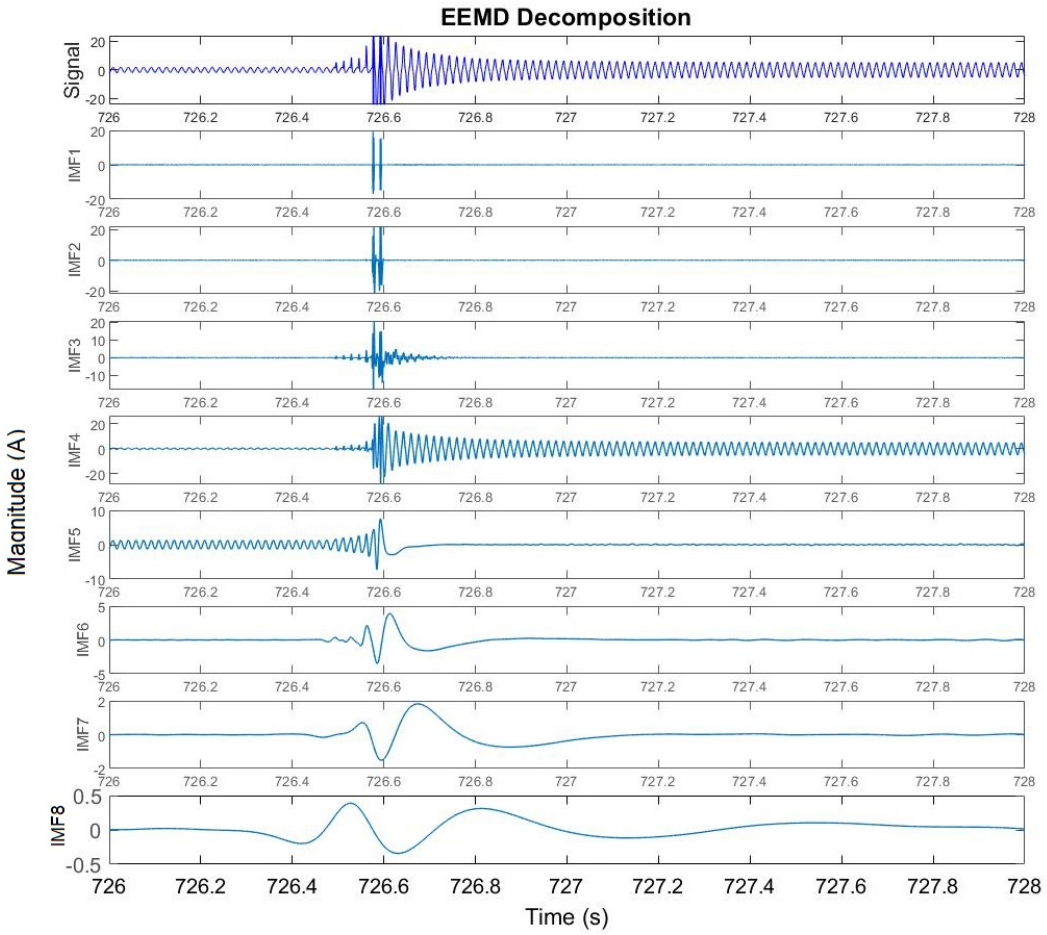

Figure 5.10: Decomposition of the signal performing EEMD with noise amplitude standard deviation of 0.1 and 5000 ensembles. The top panel indicates the original data, following panels are the IMFs.

For an enhanced presentation of the signal characteristic by instantaneous amplitude and frequency the HHT is performed on IMF 1, IMF 4 and IMF 5 as can be seen in Figure 5.11 and Figure 5.12.

The Hilbert spectrum of IMF 4 that is zoomed in, depicts the lower frequency contents of the signal. Frequency contents before event which are of lower magnitude, can not be clearly seen because of the color map.

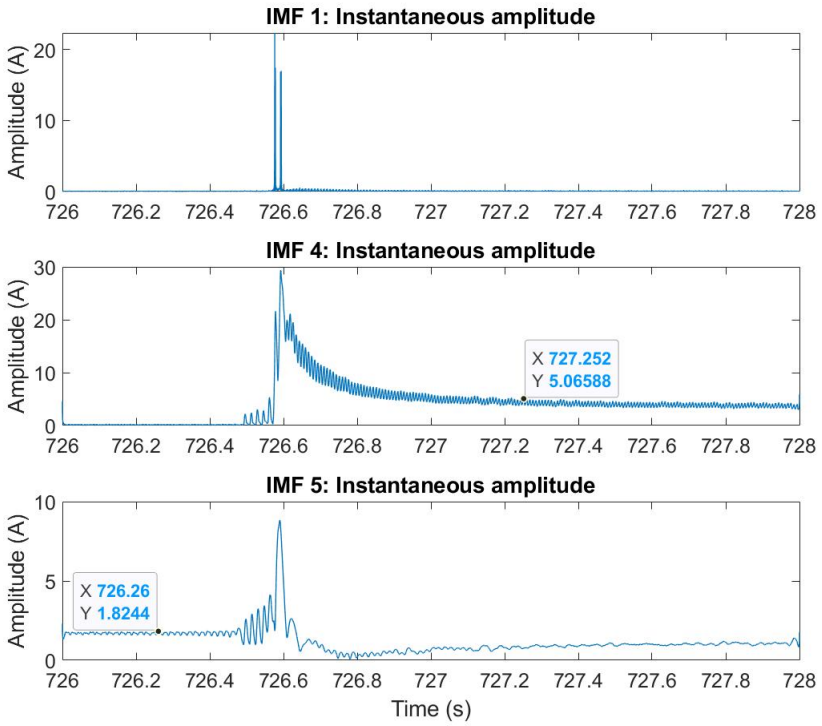

Figure 5.11: Instantaneous amplitude of the signal. Transient amplitude captured in IMF1 in the top panel, amplitude of the signal after event in the middle panel and amplitude after event in bottom panel.

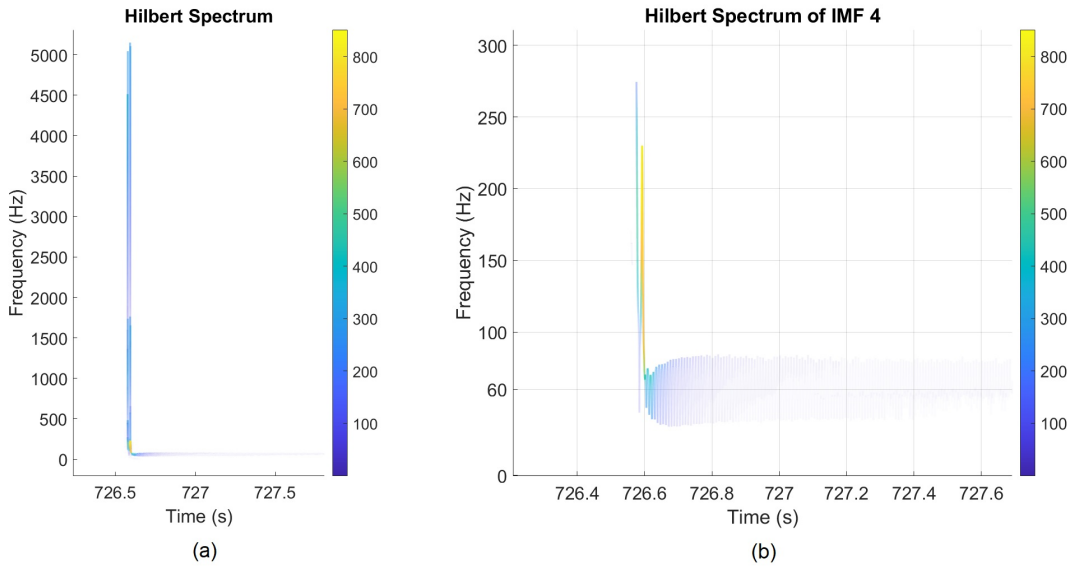

Figure 5.12: Hilbert spectrum of: (a) all IMFs, (b) IMF 4 magnified.

Chapter 6

Discussion

In this chapter we discuss the effectiveness and shortcoming of different techniques for analysis of Power Quality (PQ) problems. There are several PQ events as described in Chapter 2. Transients are common events in the grid that contain a damped oscillation with frequencies ranging from few hundred hertz up to the megahertz. High-frequency transients may be more dangerous that may cause damage to equipment. The origin of transients are switching transients, lightning, and other faults. In this thesis however the switching transients which is a common PQ event at the power consumer end is considered. The switching transients originates in the grid due to energizing of capacitor banks. Transients at equipment terminals could be due to switched mode power supplies.

To help identify PQ problems, measuring instruments are required to collect data. The PQ data for this work is generated in the Laboratory for Innovation and Technology (LIT) in University of Technology Paraná in Brazil. The original signal which was recorded in a real environment. It is composed of voltage and current waveforms with fundamental frequency of 60 Hz and mains voltage of 127 V. Since most of the PQ disturbances (PQDs) are non-linear and non- stationary, proper time-frequency analysis methods are required to decompose the data and identify the PQD.

In the previous chapter three different time-frequency analysis methods have been applied to the PQ signal. All of them demonstrated that they are capable of detecting the PQ event. However, there are some pros and cons when utilizing these methods for individual task. Although basic Fourier Transform is limited to stationary signals, the STFT can be used for non-stationary signal analysis. Its main drawback is that it has a fixed resolution which depends on the chosen window size. Therefore, there is trade off between time and frequency resolution. Enhancing resolution in the time domain will cost resolution in the frequency domain, and vice versa. As illustrated in Figure 5.3, the STFT detected the event in the time series and decomposed the signal into its frequency components. It yielded good time domain localization, consequently lost the frequency resolution. Choosing a wider window size in Figure 5.4 however enhanced the frequency resolution, on the other hand degraded the time resolution. So, the STFT failed to maintain time and frequency resolution simultaneously.

Alternatively, the Wavelet Transform overcomes the time-frequency resolution shortcoming of the STFT by using scaled and dilated versions of the basis function. As it has been seen in Figure 5.5 the transient event is exhibited very clearly by scalogram using CWT. The method yielded a better overview of the signal components and evaluated as favorable tool for analyzing transient behavior, and sudden and slow transition positions. Nonetheless, the CWT is not adaptive; i.e. we shall choose a suitable wavelet in different scenarios. Additionally, it is not good for computing instantaneous

frequencies in details.

Lastly, the EMD which is a data driven technique considered a well suited for PQ signal analysis. As it does not require initial assumption of the signal, it is adaptive to any unknown signals. Furthermore, applying the HHT to the extracted components provided details on instantaneous frequency and amplitude. We observed small oscillations around the fundamental frequency component in IMF 4 in the Hilbert spectrum. Although this method is most suitable for decomposing nonstationary signals, yet it suffers some shortcomings such as mode mixing issue when it is applied to a signal that contains relatively high level of noise. The noise content of the signal which usually has high frequency might mix with a high frequency component of the signal in the same IMF. As it can be seen in the Figure 5.7, IMF 3 and IMF 4 indicate fluctuating frequency and amplitude which implies that the IMFs contain mixed frequency signal. Consequently, applying Hilbert Transform on these IMFs will produce unsatisfactory results. To resolve the mode mixing problem, the ensemble EMD (EEMD) which is an extended version of EMD, can be used. (EEMD) defines the true IMFs as the mean of an ensemble of trials. Each trial consists of the decomposition results (components) of the signal plus a normally distributed white noise that has a constant standard deviation. The EEMD utilizes the statistical characteristics of noise. It contributes to perturb the signal and enable the EMD algorithm to come across a wide range of possible solutions. EEMD mimics a controlled and repeated experiment to produce an ensemble mean for a nonstationary data as the true answer. The added noise in the EEMD decomposition process helps to separate different scales from the input data that actually should not contribute to IMFs. Thus, EEMD can be regarded as a genuine noise assisted data analysis method which is effective in extracting intrinsic scales in a dataset.

Although EEMD alleviates the mode mixing issue, it consums too much time because of the large number of sifting iterations required to achieve the decomposition. Moreover, we might notice that the EMD or EEMD could not extract the harmonics components of the signal explicitly, even though there exist harmonics after the event. Taking the FFT of the signal can expose the harmonics clearly. As it can be seen in Figure 6.1, the prominent harmonics observed are 120 Hz, 180 Hz, 240 Hz and 300 Hz. Accordingly, comparing the EMD with the STFT and CWT in term of computational cost and regarding evaluating the amplitude of the harmonic components, the EMD is no longer a best choice.

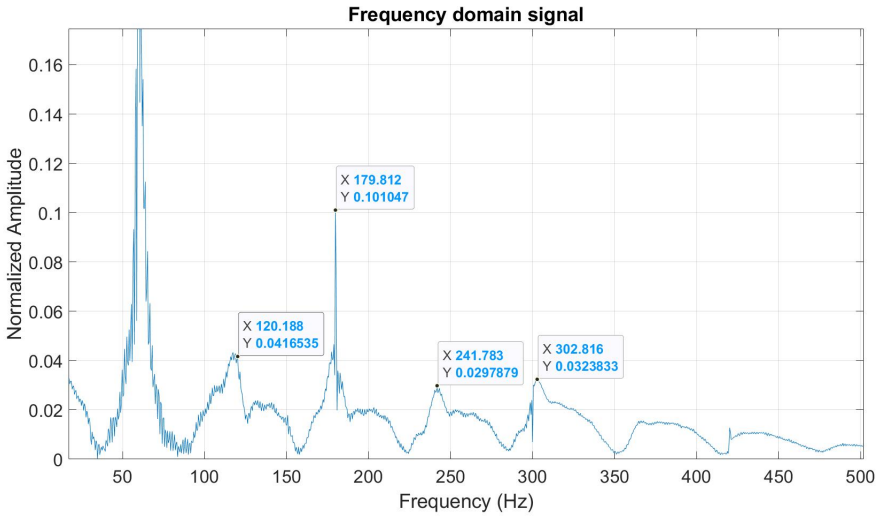

Figure 6.1: Fast Fourier Transform of the current waveform represents frequency components.

Table 6.1 represents the temporal computational cost comparison among the forementioned data

analysis techniques to extract the current waveform signal components. The signal is 2 s long and contains 30769 samples. The algorithms have been executed on a PC Core i5, CPU @ 1.60 GHz, RAM 8 GB. The mentioned computational time for EEMD in the table was calculated for 100 trials. However, choosing higher numbers of ensemble require more time to compute the IMFs, e.g., 5000 ensembles (in our case) require around 650 seconds to execute the EEMD.

Table 6.1: Temporal computation cost of methods for the data analysis. Executing the EEMD takes longer time which depends on number of ensembles. The calculated time mentioned for EEMD is for 100 trails, however, higher numbers of ensembles require longer time.

Executed on PC Core i5, CPU @ 1.60 GHz, RAM 8 GB

Data analysis algorithm	**STFT**	**CWT**	**EMD**	**EEMD**
Computational duration (s)	0.03	0.67	0.09	10.03 *(100 trails)*
Computation with plot (s)	0.65	1.96	2.36	10.77

Chapter 7

Conclusion

Recently, Power Quality (PQ) issue has become a major concern since poor PQ can influence the power grid and cause failure or malfunction to sensitive electrical equipment. In this thesis, the PQ disturbances and techniques for their analysis are investigated. Three different methods that are suitable for analyzing non-stationary signals, have been carried out, and their effectiveness and performance are discussed. As a real PQ signal, a low voltage power grid data containing voltage and current waveforms, has been analyzed.

The traditional Fourier transform (FT) is reported to have difficulties to analyze non - stationary signals, because it cannot provide the signal information in the time-frequency representation. However, short time FT (STFT) can be applied as time-frequency analysis method with a fixed resolution depends on the fixed window size which is chosen priorly. One of its main disadvantages is that it cannot maintain time resolution and resolution frequency concurrently. By choosing the size of window, resolution can be enhanced either in the frequency domain or in time domain. Enhancing resolution in the frequency domain degrades resolution in the time domain, and vice versa. The Wavelet transform (WT) outperforms the STFT in term of the time-frequency resolution and yields an enhanced visual presentation of the signal components. It is designed to analyze the signal using windowing technique with variable-sized segment; therefore, it yields better resolution than the STFT. Continuous WT (CWT) is a favorable tool for analyzing transient behavior. It can provide a more informative time-frequency representation in a situation when the signal is corrupted by transients, whereas the STFT does not have the capability to localize transients to the same degree as the CWT. It is important to be able to localize these transients in addition to characterizing oscillatory components in the signal. However, when using the CWT we shall choose a suitable wavelet in different scenarios. Additionally, it is not good for computing instantaneous frequencies in details. Nevertheless, the CWT has difficulty in the adaptivity since the mother function has to be chosen prior to the analysis.

Empirical Mode Decomposition (EMD) and Hilbert spectrum (HS) analysis has demonstrated to be an effective time–frequency analysis method. The Hilbert–Huang transform (HHT) consists of two processes: First the EMD is executed to decompose a signal adaptively into a finite number of intrinsic mode functions (IMFs). Once the IMFs are obtained, the HT is applied to obtain instantaneous frequency and amplitude. A better perception of a signal component is achieved by visual inspection, so the visual representation obtained by the Hilbert spectrum is a notable quality of HHT over other mentioned techniques, in which the frequency and amplitude variation can be inspected visually in more detail.

The EMD is well suited for analyzing stationary and non-stationary signals and requires no initial assumption of the signal; thus, it is adaptive to any unknown signals. The methods is most suitable for decomposing non-stationary signals often found in PQ waveforms. One of the major drawbacks of EMD method is the phenomenon of mode mixing. It occurs when either a single IMF consisting of components of widely disparate scales, or a component of a similar scale residing in different IMFs. This problem can be alleviated by using ensemble EMD (EEMD). This algorithm works by creating an ensemble of white noise-added signal from the original data. The EMD is applied to each of these signals to produce an ensemble of IMFs which are then averaged to obtain the final IMF which is treated as the true and more physical meaningful answer. Although, the EEMD has been considered to be effective in resolving the mode mixing issues of the noisy signals, it consumes too much time because of the large number of sifting iterations required to achieve the decomposition. It takes even longer time if the number of ensembles increase. Moreover, the EMD/HHT accuracy is degraded when calculating the oscillations of small magnitudes.

In summary, comparing the EMD with the STFT and CWT in term of computational cost and regarding evaluating frequency components of small amplitude, the STFT and CWT outperform the EMD. However, window length, overlap, and basis wavelet parameters restrict the resolution of STFT and CWT; hence, predefined decomposition bases render these two methods less suitable for non-stationary signal analysis. Whereas the EMD with combination of the HT has an important role in signal analysis application by obtaining the instantaneous frequency and amplitude of the IMFs. Even with the mentioned limitations, experiences indicate that the results obtained by the HHT are consistently better than most of the other methods.

References

[1] M. H. Bollen and I. Y. Gu, *Signal processing of power quality disturbances*. John Wiley & Sons, 2006, vol. 30.

[2] A. Gomez-Exposito, A. J. Conejo, and C. Cañizares, *Electric energy systems: analysis and operation*. CRC press, 2018.

[3] A. Larsson, "On high-frequency distortion in low-voltage power systems," Ph.D. dissertation, Luleå tekniska universitet, 2011.

[4] S. Gupta, "Power quality: problems, effects and economic impacts," *Int. J. Electr. Electron. Eng.(IJEEE)*, vol. 1, no. 1, pp. 83–91, 2012.

[5] Z. He, R. Mai, W. He, and Q. Qian, "Phasor measurement unit based transmission line fault location estimator under dynamic conditions," *IET Generation, Transmission & Distribution*, vol. 5, no. 11, pp. 1183–1191, 11 2011.

[6] A. A. Sallam and O. P. Malik, *Electric distribution systems*. John Wiley & Sons, 2018.

[7] P. Kumari and V. K. Garg, "Power quality enhacement using dynamic voltage restorer: An overview," *International Journal of Scientific and Research Publications*, vol. 3, no. 8, pp. 1–8, 2013.

[8] M. Noh and F. H. Binti, "Application of advanced signal processing technique for power quality disturbances detection and classification system," Ph.D. dissertation, Kumamoto University, 2016.

[9] J. Arrillaga, M. H. Bollen, and N. R. Watson, "Power quality following deregulation," *Proceedings of the IEEE*, vol. 88, no. 2, pp. 246–261, 2000.

[10] D. Saxena, K. Verma, and S. Singh, "Power quality event classification: an overview and key issues," *International Journal of Engineering, Science and Technology*, vol. 2, no. 3, pp. 186–199, 2010.

[11] V. Kumar, S. Kumar, A. Benuel, and S. Raj, "Simulation of various power quality disturbances on secondary distribution power system," *Journal of Advanced Research in Dynamical and Control Systems*, vol. 10, January 2018.

[12] L. Stankovic, M. Dakovic, and T. Thayaparan, *Time-frequency signal analysis with applications*. Artech House, 2013.

[13] G. Wang, X. Chen, F.-L. Qiao, Z. Wu, and N. Huang, "On intrinsic mode function." *Advances in Adaptive Data Analysis*, vol. 2, pp. 277–293, 07 2010.

[14] A. Zeiler, R. Faltermeier, I. R. Keck, A. M. Tomé, C. G. Puntonet, and E. W. Lang, "Empirical mode decomposition - an introduction," in *The 2010 International Joint Conference on Neural Networks (IJCNN)*, 2010, pp. 1–8.

[15] R. Faltermeier, A. Zeiler, I. R. Keck, A. M. Tomé, A. Brawanski, and E. W. Lang, "Sliding empirical mode decomposition," in *The 2010 International Joint Conference on Neural Networks (IJCNN)*, 2010, pp. 1–8.

[16] J. Sivasankari, U. Shyamala, and M. Vigneshwaran, "Power quality improvement using hysteresis voltage control of dynamic voltage restorer," *vol*, vol. 2, 2014.

[17] D. Prasad, T. S. Kumar, B. V. Prasanth, K. Sankar *et al.*, "Fuzzy Logic Control of D-Statcom for Power Quality Improvement," *Int. Journal of Engineering Research and Applications*, vol. 3, no. 6, pp. 398–403, 2013.

[18] M. Prathmesh, W. Mahesh, and S. Nilkanth, "Review on power quality enhancement in weak power grids by integration of renewable energy technologies," *International Research Journal of Engineering and Technology*, vol. Vol. 02, 04. 2015.

[19] P. Kumari and V. K. Garg, "Simulation of dynamic voltage restorer using matlab to enhance power quality in distribution system," *Simulation*, vol. 3, no. 4, pp. 1436–1441, 2013.

[20] C. P. Meena, "Power quality problems, effects and solution techniques in electrical power system," *International Journal of Research in Engineering, Science and Management*, vol. 2, 2019.

[21] B. Singh, A. Chandra, and K. Al-Haddad, *Power quality: problems and mitigation techniques*. John Wiley & Sons, 2014.

[22] K. Padiyar, *FACTS controllers in power transmission and distribution*. New Age International, 2007.

[23] M. H. Bollen, "Understanding power quality problems," in *Voltage sags and Interruptions*. IEEE press, 2000.

[24] N. G. Hingorani, "Introducing custom power," *IEEE spectrum, June, 1995*, vol. 32, no. 6, pp. 41–48, 1995.

[25] R. C. Dugan, M. F. Mc Granaghan, S. Santoso, and H. W. *Electric power systems quality*. McGraw-hill, 2004.

[26] H. Kuisti, M. N. M. Lahtinen, K. Eketorp, D. W. E. Ørum, A. Slotsvik, and A. Jansson, *Frequency Quality Report*, Frequency Quality sub-group of Nordic Analysis Group (NAG), 2015.

[27] F. Statnett *et al.*, "Challenges and opportunities for the Nordic power system," *Technical Report*, 2016.

[28] Z. Xu, J. Ostergaard, and M. Togeby, "Demand as frequency controlled reserve," *IEEE Transactions on Power Systems*, vol. 26, no. 3, pp. 1062–1071, 2011.

[29] B. Franken, V. Ajodhia, K. Petrov, K. Keller, and C. Müller, "Regulation of voltage quality," in *9th International Conference" Electric Power, Quality and Utilisation", Barcelona*. Citeseer, 2007.

[30] F. Heistad and W. A. Kristensen, "Prediksjon av feil i det norske strømnettet," Master's thesis, NTNU, 2019.

[31] L. Saarinen, "The frequency of the frequency: on hydropower and grid frequency control," Ph.D. dissertation, Acta Universitatis Upsaliensis, 2017.

[32] J. Hedberg, "Control of Swedish wind power plants meeting future grid codes in a changing power market," *Coden: Lutedx/Teie*, 2015.

[33] X. Luo, J. Wang, J. D. Wojcik, J. Wang, D. Li, M. Draganescu, Y. Li, and S. Miao, "Review of voltage and frequency grid code specifications for electrical energy storage applications," *Energies*, vol. 11, no. 5, p. 1070, 2018.

[34] I. Machado and I. Arias, "Grid codes comparison," Master's thesis, Department of Electric Power Engineering, Chalmers University of Technology, Göteborg, Sweden, 2006.

[35] E. On, "Grid code high and extra high voltage," *Requirements on generating plants*, 2006.

[36] N. Espinoza, "Grid code testing of wind turbines by voltage source converter based test equipment," Master's thesis, Department of Energy and Environment, Chalmers University of Technology, Göteborg, Sweden, 2015.

[37] P. S. Revuelta, S. P. Litrán, and J. P. Thomas, *Active power line conditioners: design, simulation and implementation for improving power quality.* Academic Press, 2016.

[38] W. Christiansen and D. T. Johnsen, "Analysis of requirements in selected grid codes," *Prepared for Orsted-DTU Section of Electric Power Engineering, Technical University of Denmark (DTU)*, 2006.

[39] J. Nömm, S. K. Rönnberg, and M. H. Bollen, "An analysis of frequency variations and its implications on connected equipment for a nanogrid during islanded operation," *Energies*, vol. 11, no. 9, p. 2456, 2018.

[40] C. Tejavoth, M. Trishulapani, V. M. Rao, and Y. Rambabu, "Power quality improvement for grid connected wind energy system using STATCOM-Control scheme," *Power*, vol. 3, no. 7, 2013.

[41] M. Tollardo, "Applications and measurement techniques for a reliable and affordable innovative power quality analysis system," Master's thesis, Department of Industrial Engineering, University of Padua, 2015.

[42] M. H. Bollen, *Overview of Power Quality and Power Quality Standards.* Wiley-IEEE Press, 2000, pp. 1–34.

[43] A. M. Hussain Shareef and K. Mohamed, "Sensitivity of compact fluorescent lamps during voltage sags: An experimental investigation," *WSEAS transactions on power systems*, vol. 5, 2010.

[44] E. Fuchs and M. A. Masoum, *Power quality in power systems and electrical machines.* Academic press, 2011.

[45] M. Gao and K. Awodele, "Investigation of power electronics solutions to power quality problems in distribution networks," in *AFRICON 2015.* IEEE, 2015, pp. 1–6.

[46] T. A. Kneschke, "Control of utility system unbalance caused by single-phase electric traction," *IEEE Transactions on Industry Applications*, no. 6, pp. 1559–1570, 1985.

[47] P. Pillay and M. Manyage, "Definitions of voltage unbalance," *IEEE Power Engineering Review*, vol. 21, no. 5, pp. 50–51, 2001.

[48] L. Moran, P. Ziogos, and G. Joos, "A three-phase solid-state voltage compensator system," *Canadian Journal of Electrical and Computer Engineering*, vol. 15, no. 1, pp. 27–36, 1990.

[49] S. Marx and D. Bender, "An introduction to symmetrical components, system modeling and fault calculation," in *30th Annual Hands-ON Relay School*, 2013.

[50] A. Campos, G. Joos, P. D. Ziogas, and J. F. Lindsay, "Analysis and design of a series voltage unbalance compensator based on a three-phase vsi operating with unbalanced switching functions," *IEEE Transactions on Power Electronics*, vol. 9, no. 3, pp. 269–274, 1994.

[51] R. Woll, "Effect of unbalanced voltage on the operation of polyphase induction motors," *IEEE Transactions on Industry Applications*, 1975.

[52] C. R. Bayliss, C. Bayliss, and B. Hardy, *Transmission and distribution electrical engineering.* Elsevier, 2012.

[53] D. O. Johnson and K. A. Hassan, "Issues of power quality in electrical systems," *International Journal of Energy and Power Engineering*, vol. 5, no. 4, 2016.

[54] D. Kai, L. Wei, H. Yuchuan, H. Pan, and Q. Yimin, "Power quality comprehensive evaluation for low-voltage dc power distribution system," *IEEE 3rd Information Technology, Networking, Electronic and Automation Control Conference (ITNEC)*, 2019.

[55] M. H. Bollen and F. Hassan, *Integration of distributed generation in the power system.* John wiley & sons, 2011, vol. 80.

[56] J. Schlabbach, J. Schlabbach, D. Blume, D. Blume, T. Stephanblome, and T. Stephanblome, *Voltage quality in electrical power systems.* IET, 2001, no. 36.

[57] B. W. Kennedy, *Power quality primer.* McGraw Hill Professional, 2000.

[58] T. Gonen, *Electric power distribution engineering.* CRC press, 2015.

[59] L. L. Grigsby, *Electric power generation, transmission, and distribution.* CRC press, 2016.

[60] E. Fuchs and M. S. Masoum, *Power Quality in Power Systems and Electrical Machines, 2nd Edition.* Academic Press, 2015.

[61] R. C. Dugan, M. McGranaghan, S. Santoso, and H. W. Beaty, "Electrical power systems quality," *Inc., NY, USA*, 2012.

[62] R. E. Brown, *Electric power distribution reliability.* CRC press, 2017.

[63] J. Das, *Transients in Electrical Systems: Analysis, Recognition and Mitigation.* McGraw-Hill Professional Publishing, 2010.

[64] K. Y. Lee, "Electric and magnetic fields," *Electrical Engineering-Volume I*, 2009.

[65] V. Liepins, "Extended Fourier analysis of signals," *arXiv preprint arXiv:1303.2033*, 2013.

[66] P. F. Ribeiro, C. A. Duque, P. M. Ribeiro, and A. S. Cerqueira, *Power systems signal processing for smart grids.* John Wiley & Sons, 2014.

[67] G. Dijk, *Distribution theory: convolution, Fourier transform, and Laplace transform.* Walter de Gruyter, 2013.

[68] M. Mastro, *Financial derivative and energy market valuation.* Wiley Online Library, 2013.

[69] M. Muller, "The Fourier transform in a Nutshell," *Fundamentals of Music Processing, Section 2*, vol. 2, pp. 40–56, 2015.

[70] M. Portnoff, "Time-frequency representation of digital signals and systems based on Short-time Fourier analysis," *IEEE Transactions on Acoustics, Speech, and Signal Processing*, vol. 28, no. 1, pp. 55–69, 1980.

[71] V. S. Yendole and K. A. Dongare, "Power system fault analysis using signal processing technique," *Power*, vol. 6, no. 8, 2018.

[72] D. Sundararajan, *The Discrete Fourier Transform: theory, algorithms and applications.* World Scientific Publishing Co. Pte. Ltd., 2001.

[73] K. V. Rangarao and R. K. Mallik, *Digital Signal Processing: A Practitioner's Approach.* John Wiley & Sons, 2006.

[74] R. J. Beerends, H. G. ter Morsche, J. Van den Berg, and E. Van de Vrie, "Fourier and Laplace transforms," *Cambridge University Press, August 2003.*, 08 2003.

[75] S. Mohammed, *Fourier transform: Signal processing and physical sciences.* Croatia: INTECH, 2015.

[76] A. V. Oppenheim, J. R. Buck, and R. W. Schafer, *Discrete-time signal processing*, 3rd ed. Pearson Higher Education Inc, 3rd. ed., 2010.

[77] S. K. Mitra, "Digital signal processing: A computer-based approach. ed.[sl]," 2011.

[78] M. Müller, *Fundamentals of music processing: Audio, analysis, algorithms, applications.* Springer, 2015.

[79] M. J. Afroni, "Analysis of non-stationary power quality waveforms using iterative empirical mode decomposition methods and SAX algorithm," Ph.D. dissertation, School of Electrical, Computer and Telecommunication Engineering, University of Wollongong, 2015.

[80] M. J. Afroni, D. Sutanto, and D. Stirling, "Analysis of non-stationary power quality waveforms using iterative Hilbert Huang transform and SAX algorithm," *IEEE Transactions on Power Delivery*, vol. 28, no. 4, pp. 2134–2144, 2013.

[81] P. Boggiatto, E. Cordero, M. de Gosson, H. G. Feichtinger, F. Nicola, A. Oliaro, and A. Tabacco, *Landscapes of Time-Frequency Analysis.* Springer, 2019.

[82] G. S, "The short-time Fourier transform," 2017.

[83] B. Boashash, *Time-frequency signal analysis and processing: a comprehensive reference.* Academic Press, 2016.

[84] P. Flandrin, *Explorations in time-frequency analysis.* Cambridge CB2 8BS, United Kingdom: Cambridge University Press, 2018.

[85] L. Debnath, *Wavelet transforms and their applications.* Springer Science & Business Media New York, 2002.

[86] E. W. Hansen, *Fourier transforms: principles and applications.* John Wiley & Sons, 2014.

[87] S. Santoso, E. J. Powers, and W. M. Grady, "Power quality disturbance data compression using wavelet transform methods," *IEEE Transactions on Power Delivery*, vol. 12, no. 3, pp. 1250–1257, 1997.

[88] R. Flores, "Signal processing tools for power quality event classification," Ph.D. dissertation, Electrical Engineering, Chalmers University of Technology, Gothenburg, Sweden, 2003.

[89] Z. He, *Wavelet analysis and transient signal processing applications for power systems.* John Wiley & Sons, 2016.

[90] P. Y. Kovalenko, "The extended frequency-directed EMD technique for analyzing the low-frequency oscillations in power systems," in *2016 International Symposium on Industrial Electronics (INDEL)*, 2016.

[91] N. E. Huang, *Hilbert-Huang transform and its applications*, 2nd ed. World Scientific, 2014, vol. 16.

[92] P. Georgieva, L. Mihaylova, and L. C. Jain, *Advances in Intelligent Signal Processing and Data Mining.* Springer, 2013, vol. 410.

[93] N. Huang, Z. Shen, S. Long, M. Wu, H. Shih, Q. Zheng, N. Yen, C.-C. Tung, and H. Liu, "The empirical mode decomposition and the Hilbert spectrum for nonlinear and non-stationary time series analysis," *Proceedings of the Royal Society of London. Series A: Mathematical, Physical and Engineering Sciences*, vol. 454, pp. 903–995, 03. 1998.

[94] M. J. Afroni, "Analysis of non-stationary power quality waveforms using iterative empirical mode decomposition methods and SAX algorithm," Ph.D. dissertation, Electrical, Computer and Telecommunication Engineering, University of Wollongong, 2015.

[95] R. Shilpa, S. P. Shruthi, and P. Puttaswamy, "Analysis of power quality disturbances using empirical mode decomposition and SVM classifier," *International Journal of Advanced Research in Electronics and Communication Engineering (IJARECE)*, vol. 4, no. 5, 2015.

[96] N. Senroy, S. Suryanarayanan, and P. F. Ribeiro, "An improved Hilbert–Huang method for analysis of time-varying waveforms in power quality," *IEEE Transactions on Power Systems*, vol. 22, no. 4, pp. 1843–1850, 2007.

[97] G. Rilling, P. Flandrin, P. Goncalves *et al.*, "On empirical mode decomposition and its algorithms," in *IEEE-EURASIP workshop on nonlinear signal and image processing*, vol. 3, no. 3. NSIP-03, Grado (I), 2003, pp. 8–11.

[98] T. Yalcin, O. Ozgonenel, and U. Kurt, "Feature vector extraction by using empirical mode decomposition for power quality disturbances," in *2011 10th International Conference on Environment and Electrical Engineering.* IEEE, 2011, pp. 1–4.

[99] J. J. Pan, "EMD/BEMD improvements and their applications in texture and signal analysis," Ph.D. dissertation, Hong Kong Baptist University, 2013.

[100] S. Shukla, S. Mishra, and B. Singh, "Empirical-mode decomposition with Hilbert transform for power-quality assessment," *IEEE transactions on power delivery*, vol. 24, no. 4, 2009.

[101] J. Luque, D. Anguita, F. Pérez, and R. Denda, "Spectral analysis of electricity demand using Hilbert-Huang Transform," *Sensors and Data Analytic Applications for Smart Grid*, vol. 20, 2020.

[102] J. Fleureau, J.-C. Nunes, A. Kachenoura, L. Albera, and L. Senhadji, "Turning tangent empirical mode decomposition: a framework for mono-and multivariate signals," *IEEE Transactions on signal Processing*, vol. 59, no. 3, pp. 1309–1316, 2010.

[103] G. Rilling and P. Flandrin, "One or two frequencies? the empirical mode decomposition answers," *IEEE transactions on signal processing*, vol. 56, no. 1, pp. 85–95, 2007.

[104] Z. Wu and N. E. Huang, "Ensemble empirical mode decomposition: a noise-assisted data analysis method," *Advances in adaptive data analysis*, vol. 1, no. 01, pp. 1–41, 2009.

[105] Y. Lei and M. J. Zuo, "Fault diagnosis of rotating machinery using an improved HHT based on EEMD and sensitive IMFs," *Measurement Science and Technology*, vol. 20, no. 12, p. 125701, 2009.

[106] Universidade Tecnologica Federal do Parana´, Laboratory for Innovation and Technology in Embedded Systems and Energy. (2020) LIT-DATASET. (Accessed on 06.04.2021). [Online]. Available: https://pessoal.dainf.ct.utfpr.edu.br/douglasrenaux/LIT_Dataset/

[107] J. M. Giron-Sierra, *Digital signal processing with Matlab examples, volume 1: Signals and data, filtering, non-stationary signals, modulation.* Springer, 2017.

[108] Neil Po-Nan Li. (2014) Matlab code for 1-D ensemble empirical mode decomposition method. (Accessed on 07.02.2021). [Online]. Available: https://github.com/leeneil/eemd-matlab

[109] Bruna Molinari, Douglas Renaux. (2020) Converting binary data to Matlab file format (LIT_bin2mat.m). (Accessed on 10.04.2021). [Online]. Available: https://pessoal.dainf.ct.utfpr.edu.br/douglasrenaux/LIT_Dataset/Matlab/index.html

Appendix

Matlab codes

MATLAB codes used for the thesis work is presents below. A very useful reference for Matlb programming for students and researchers could be the book; "Digital signal processing with matlab examples, volume 1: signals and data, filtering, non-stationary signals, modulation" [107]. Additionally, references [108] is related to the EEMD function code, and [109] for electrical power data and converting the data from binary to Matlab file (*.mat*) format.

```
% Author: Jan Ali
% Master in Systems Engineering with Embedded Systems
% University of South-Eastern Norway - Kongsberg Campus
% Faculty of Technology, Natural Sciences, and Maritime Sciences
% https://www.usn.no

% Power Grid Noise Analysis
```

Generate a synthetic non-stationary signal

```
% This is a simple code to generate a synthetic signal containing transient
% and harmonics.
% Last edited: 2nd Feb. 2021

% Clear the workspace and command window, and close the existing plots
clc
clear
close all

fs = 3000;                 % sampling frequency
t = linspace(0,0.3,1000);  % time vector

% Unit steps:
ut1=t>=0;   % unitsetp1 takes 1 only when t is greater than equal to 0
ut2=t>=0.1; % unitsetp2 takes 1 only when t is greater than equal to 0.1
ut3=t>=0.18;% unitsetp3 takes 1 only when t is greater than equal to 0.18
ut4=t>=0.3; % unitsetp4 takes 1 only when t is greater than equal to 0.3

t1=ut1-ut2; % t1 takes 1 only when 0<=t<0.1
t2=ut2-ut3; % t2 takes 1 only when 0.1<=t<0.18
t3=ut3-ut4; % t2 takes 1 only when 0.18<=t<0.3

% Signal segments:
s1 = sin(2*pi*50*t) + 0.2*sin(2*pi*200*t);
s2 = sin(2*pi*50*t) + 0.2*sin(2*pi*200*t) + sin(2*pi*500*t).*exp(-30*(t-0.1));
s3 = sin(2*pi*50*t) + 0.2*sin(2*pi*200*t);

% Composite signal:
s = s1.*t1 + s2.*t2 + s3.*t3; % combining signal segments

plot(t, s); % plot signal in respect to time
title('Synthetic signal');      % set title for the plot
xlabel('Time (s)');             % set lable for x axis
ylabel('Amplitude (A)');        % set y axis lable

% Alternative for combining signal segments:
s = s1.*(t>=0 & t<0.1) + s2.*(t>=0.1 & t<0.18) + s3.*(t>=0.18 & t<0.3);
```

Load the dataset

```
% Following code is used to load, segment and plot an electrical power current waveform
% which is generated in the Laboratory for Innovation and Technology (LIT)
% in University of Technology Paraná in Brazil. the waveform is of 900 s
% length, but a segment of 2 s is selected from 726 s to 728 s
% where a prominent PQ event has occurred.
% https://pessoal.dainf.ct.utfpr.edu.br/douglasrenaux/LIT_Dataset/index.html
%
% Author: Jan Ali
% Last edited: 10 th Apr. 2021

clc
clear
close all

load('LIT_Dataset\Matlab_Data\Natural\7\7H2A2B2C2K2F2D2\Waveform70001.mat');
fs = 15384; % sampling frequency
x = iHall(length(iHall)/900*726:length(iHall)/900*728);
% Select part of signal (current waveform ) where transient occured
t = (0:length(x)-1)/fs; % segment time
t = t + 726; % segment time offset (in this case segment is from 276 s to 278 s)

% Plotting the data against the related time interval

plot(t,x, 'b', 'LineWidth', 0.8);
xlabel('Time (s)','FontSize',12); ylabel('Amplitude (A)');
v = vGrid(length(vGrid)/6300*5083:length(vGrid)/6300*5093); % select corresponding
% voltage signal
hold on;
yyaxis right;
plot(t, v);
title('AC voltage and current waveform');
ylabel('Voltage (V)');
legend('Current)','Voltage');
hold off;
```

Fast Fourier Transform (FFT)

```
% This code performs fft to present the the signal (x) in the frequency domain
% Author: Jan Ali
% Last edit: 24th Jan. 2021

fs = 15384;             % sampling frequency
ts = 1/fs;              % sampling period
t = 0:ts:0.3-ts;        % time vector
n = length(x);          % length of signal
nf = 2^nextpow2(n);     % define a new signal length as the next power of 2
ff = fft(x, nf);        % compute the fft
sf = ff(1:nf/2);        % eliminate the symmetry
sf = sf/max(sf);        % normalize DFT Sample points
xf = fs*(0:nf/2 -1)/nf; % assign x axis to frequency
```

```
plot(xf, abs(sf));
xlabel('Frequency (Hz)'); ylabel('Normalized Amplitude');
title('Frequency domain signal');
```

Short Time Fourier Transform (STFT)

```
% This code executes the stft and plots the spectrogram.
% spectrogram(x,window,noverlap,nfft,fs)
% window: divides the signal into segments, default is Hamming window
% noverlap: No of overlap, samples of overlap between adjoining segments,
% default is 50% overlap between contiguous segments
% nfft: NFFT sampling points to calculate the DFT
% fs: sample rate

% Author: Jan Ali
% Last edited: 28. Apr. 2021

[s,f,t] = spectrogram(x,120,100,120,fs);
% Output the STFT of the input signal, cyclical frequencies
% and time instants at which the spectrogram is computed

spectrogram(x,120,100,120,fs,'yaxis'); % plot the spectrogram
t = linspace(0,2,length(t)) + 726;
ax = newplot; % assign new plot
surf(t,f/1e3,20*log10(abs(s)),'edgecolor','none'); % areate surface plot
view(0,90); % shading interp;
axis tight;
cb = colorbar(ax); % color bar for power distribution indication
cb.Label.String = 'Power(db)';
title('Spectrogram')
xlabel('Time (s)','FontSize',14), ylabel('Frequency (kHz)');

% Using the default values of the preceding optional arguments for
% a wider window segment to enhance frequency resolution:
spectrogram(x,[],[],[],fs,'yaxis')
```

Calculating the power spectrum density (psd)

```
% This code performs fft function and computes the psd of signal (s)
% to outputs as Power/Frequency (dB/Hz

% Author: Jan Ali
% Last edited: 7th Mar. 2021

N= length(s);
xdft = fft(s);
xdft = xdft(1:N/2+1);
psdx = (1/(fs*N)) * abs(xdft).^2;
psdx(2:end-1) = 2*psdx(2:end-1);
freq = 0:fs/length(x):fs/2;
plot(freq,10*log10(psdx))
```

```
grid on
title('Periodogram Using FFT')
xlabel('Frequency (Hz)')
ylabel('Power/Frequency (dB/Hz)')
```

Continuous Wavelet Transform (CWT)

```
% This is the Matlab builtin function for cwt
% to decompose the signal and output its components.
% Author: Jan Ali
% Last edited: 12th Mar. 2021

[wt,perd,coi] = cwt(x,fs); % Output the WT,
% time periods, and cone of influence
% by specifying sampling frequency

[cfs,frq] = cwt(x); % Obtain the wavelet coefficients and frequencies

% Create frequency ticks and tick labels in powers of 2:
[minf,maxf] = cwtfreqbounds(numel(x),600);

cwt(x,fs) % plot scalogram
% Determine the minimum and maximum wavelet bandpass frequencies:
t = linspace(0,2,length(cfs)) + 726;
ax = newplot;
surf(ax,t,f,abs(cfs));
view(0,90); shading interp;
ax.YScale = 'log';
ax.YDir = 'normal';
axis tight
cb = colorbar(ax);
cb.Label.String = 'Magnitude';
hold on
plot(ax,t,coi,'w--');
xlabel('Time (s)');
ylabel('Frequency (Hz)');
set(findobj(gcf,'type','axes'), 'FontSize',12);

% Compare computational efficiency:
tic; cfs = cwt(x); toc % calculate computed time using cwt
tic; cfs = wt(fb,x); toc  % calculate computed time using filber bank
```

Hilbert Huang Transform (HHT)

```
% This is the Matlab builtin emd program performing the
% Empirical Mode Decomposition algorithm for IMF extraction
%
% Author: Jan Ali
% Last edited: 12th Mar. 2021
```

```
% Implement EMD to the current waveform to extract IMFs and residue:

[imf,residual,info] = emd(x,'Interpolation','pchip','Display',1);
% imf: Matrix (NxM) of IMF components
%Current IMF  |  #Sift Iter  |  Relative Tol  |  Stop Criterion Hit
%      1      |        3     |      0.18644   |  SiftMaxRelativeTolerance
%      2      |        3     |     0.044223   |  SiftMaxRelativeTolerance
%      3      |        2     |      0.18689   |  SiftMaxRelativeTolerance
%      4      |        1     |      0.15219   |  SiftMaxRelativeTolerance
%      5      |        2     |      0.06122   |  SiftMaxRelativeTolerance
%      6      |        2     |     0.085096   |  SiftMaxRelativeTolerance
%      7      |        2     |     0.078174   |  SiftMaxRelativeTolerance
%      8      |        2     |      0.01957   |  SiftMaxRelativeTolerance
%      9      |        2     |     0.066682   |  SiftMaxRelativeTolerance
%Decomposition stopped because maximum number of intrinsic mode functions was extracted.

emd(x); % execute emd and plot the signal components

% Assign time axis according to the actual time interval:
ds = 30769; % data samples
a=(726:2/10:728); % corresponding ticks for 2 s
xticks(0:ds/10:ds); % X ticks
xlabel('Time','FontSize',14);
% yticks([m n]) % in case of tick y axis, m and n are numbers

% Applying HHT to IMF:
hht(imf,fs);

% For better view, limit the frequency range:
hht(imf,fs,'FrequencyLimits',[0 5500]);

% Align time axis:
a = linspace(726,728,11); % Cutomize the xticklabels
ax = gca; %fetches handle to EMD plot
ax.XLim(1) = 0; %adjusting x-axis to start from 0
ax.XTickLabel = num2cell(a);

% Instantaneous frequencies of over all IMFs:
instfreq(x,fs,'Method','hilbert');
```

Performing the Hilbert transform on the IMF1 to IMF9

```
ht1=hilbert(imf(:,1));
ht2=hilbert(imf(:,2));
ht3=hilbert(imf(:,3));
ht4=hilbert(imf(:,4));
ht5=hilbert(imf(:,5));
ht6=hilbert(imf(:,6));
ht7=hilbert(imf(:,7));
ht8=hilbert(imf(:,8));
ht9=hilbert(imf(:,9));
```

Calculating the instantaneous amplitudes (envelope)

```
inst_amp2 = abs(ht1);
inst_amp1 = abs(ht2);
inst_amp3 = abs(ht3);
inst_amp4 = abs(ht4);
inst_amp5 = abs(ht5);
inst_amp6 = abs(ht6);
inst_amp7 = abs(ht7);
inst_amp8 = abs(ht8);
inst_amp9 = abs(ht9);
```

Calculating the instantaneous frequencies

```
inst_f1 = diff(unwrap(angle(ht1)))/(1/fs*2*pi);
inst_f2 = diff(unwrap(angle(ht2)))/(1/fs*2*pi);
inst_f3 = diff(unwrap(angle(ht3)))/(1/fs*2*pi);
inst_f4 = diff(unwrap(angle(ht4)))/(1/fs*2*pi);
inst_f5 = diff(unwrap(angle(ht5)))/(1/fs*2*pi);
inst_f6 = diff(unwrap(angle(ht6)))/(1/fs*2*pi);
inst_f7 = diff(unwrap(angle(ht7)))/(1/fs*2*pi);
inst_f8 = diff(unwrap(angle(ht8)))/(1/fs*2*pi);
inst_f9 = diff(unwrap(angle(ht9)))/(1/fs*2*pi);
```

Plot the IMFs and their Instantaneous frequencies and amplitudes

```
% IMF1
subplot(3,1,1), plot(t,imf(:,1),'LineWidth', 0.8);
title('IMF1'), ylabel('Amplitude');

subplot(3,1,2), plot(t(1:(length(t)-1)), inst_f1,'LineWidth', 0.8);
title('Instantaneous frequency'), ylabel('Freq. (Hz)');

subplot(3,1,3), plot(t,inst_amp1,'LineWidth', 0.8);
title('Instantaneous amplitude'), ylabel('Amplitude');
xlabel('Time (s)');
set(findobj(gcf,'type','axes'), 'FontSize',14);

% IMF2
subplot(3,1,1), plot(t,imf(:,2),'LineWidth', 0.8);
title('IMF2'), ylabel('Amplitude');

subplot(3,1,2), plot(t(1:(length(t)-1)), inst_f2,'LineWidth', 0.8);
title('Instantaneous frequency'), ylabel('Freq. (Hz)');

subplot(3,1,3), plot(t,inst_amp2,'LineWidth', 0.8);
title('Instantaneous amplitude'), ylabel('Amplitude'), xlabel('Time (s)');
set(findobj(gcf,'type','axes'), 'FontSize',14);

% IMF3
subplot(3,1,1), plot(t,imf(:,3),'LineWidth', 0.8);
title('IMF3'), ylabel('Amplitude');
```

```
subplot(3,1,2), plot(t(1:(length(t)-1)), inst_f3,'LineWidth', 0.8);
title('Instantaneous frequency'), ylabel('Freq. (Hz)');

subplot(3,1,3), plot(t,inst_amp3,'LineWidth', 0.8);
title('Instantaneous amplitude'), ylabel('Amplitude'), xlabel('Time (s)');
set(findobj(gcf,'type','axes'), 'FontSize',14);

% IMF4
subplot(3,1,1), plot(t,imf(:,4),'LineWidth', 0.8);
title('IMF4'); ylabel('Amplitude');

subplot(3,1,2), plot(t(1:(length(t)-1)), inst_f4,'LineWidth', 0.8);
title('Instantaneous frequency'), ylabel('Freq. (Hz)');

subplot(3,1,3), plot(t,inst_amp4,'LineWidth', 0.8);
title('Instantaneous amplitude'), ylabel('Amplitude'), xlabel('Time (s)');
set(findobj(gcf,'type','axes'), 'FontSize',14);

% IMF5
subplot(3,1,1), plot(t,imf(:,5),'LineWidth', 0.8);
title('IMF5'), ylabel('Amplitude');

subplot(3,1,2), plot(t(1:(length(t)-1)), inst_f5,'LineWidth', 0.8);
title('Instantaneous frequency'), ylabel('Freq. (Hz)');

subplot(3,1,3), plot(t,inst_amp5,'LineWidth', 0.8);
title('Instantaneous amplitude'), ylabel('Amplitude'), xlabel('Time (s)');
set(findobj(gcf,'type','axes'), 'FontSize',14);

% IMF6
subplot(3,1,1), plot(t,imf(:,6),'LineWidth', 0.8);
title('IMF6'), ylabel('Amplitude');

subplot(3,1,2), plot(t(1:(length(t)-1)), inst_f6,'LineWidth', 0.8);
title('Instantaneous frequency'), ylabel('Freq. (Hz)');

subplot(3,1,3), plot(t,inst_amp6,'LineWidth', 0.8);
title('Instantaneous amplitude'), ylabel('Amplitude'), xlabel('Time (s)');
set(findobj(gcf,'type','axes'), 'FontSize',14);

% IMF7
subplot(3,1,1), plot(t,imf(:,7),'LineWidth', 0.8);
title('IMF7'); ylabel('Amplitude');

subplot(3,1,2), plot(t(1:(length(t)-1)), inst_f7,'LineWidth', 0.8);
title('Instantaneous frequency'), ylabel('Freq. (Hz)');

subplot(3,1,3), plot(t,inst_amp7,'LineWidth', 0.8);
title('Instantaneous amplitude'), ylabel('Amplitude'), xlabel('Time (s)');
set(findobj(gcf,'type','axes'), 'FontSize',14);

% IMF8
subplot(3,1,1), plot(t,imf(:,8),'LineWidth', 0.8);
title('IMF8'), ylabel('Amplitude');
```

```
subplot(3,1,2), plot(t(1:(length(t)-1)), inst_f8,'LineWidth', 0.8);
title('Instantaneous frequency'), ylabel('Freq. (Hz)');

subplot(3,1,3), plot(t,inst_amp8,'LineWidth', 0.8);
title('Instantaneous amplitude'), ylabel('Amplitude'), xlabel('Time (s)');
set(findobj(gcf,'type','axes'), 'FontSize',14);

% IMF9
subplot(3,1,1), plot(t,imf(:,9),'LineWidth', 0.8);
title('IMF9'), ylabel('Amplitude');

subplot(3,1,2), plot(t(1:(length(t)-1)), inst_f9,'LineWidth', 0.8);
title('Instantaneous frequency'), ylabel('Freq. (Hz)');

subplot(3,1,3), plot(t,inst_amp9,'LineWidth', 0.8);
title('Instantaneous amplitude'), ylabel('Amplitude'), xlabel('Time (s)');
set(findobj(gcf,'type','axes'), 'FontSize',14);
```

Ensemble empirical mode decomposition

```
% This is the eemd function to implement the
% Ensemble Empirical Mode Decomposition:
% a noise-assisted data analysis method.
% Author: Neil Po-Nan Li.
% Cited in the "Reference" section.
% Writen: 17th Nov. 2014
% Edited: Jan Ali
% Last edited: 28th Mar. 2021

function [modes] = eemd(y, imf, NR, Nstd)

stdy = std(y);
if stdy < 0.01
    stdy = 1;
end
y = y ./ stdy;
siz = length(y);
modes = zeros(siz,imf);

for k = 1:NR
    disp(['Ensemble number #' num2str(k)]);
    wn = (randn(1,siz).*Nstd)';
    y1 = y + wn;
    y2 = y - wn;
    modes = modes + emd(y1,'MaxNumIMF',imf);
    if Nstd > 0 && NR > 1
       modes = modes + emd(y2,'MaxNumIMF',imf);
    end
end

modes = modes .*stdy./(NR);
if Nstd > 0 && NR > 1
```

```
   modes = modes./2;
end

end

%% INPUT:
%   y: Inputted data;
%   Nstd: ratio of the standard deviation of the added noise and that of Y;
%   NE: Ensemble number for the EEMD

load('LIT_Dataset\Matlab_Data\Natural\7\7H2A2B2C2K2F2D2\Waveform70001.mat');
fs = 15384; % sampling frequency
t = (0:length(y)-1)/fs + 726; % Time
y = iHall(length(iHall)/900*726:length(iHall)/900*728); % Select part of signal (current
waveform ) %    where transient occured

imf = 9;                        % number of IMF
NR = 5000;                      % number of ensembles of EEMD
                           % For each ensemble different white noise is added with the
signal
Nstd = 0.2;                     % standard deviation of the added noise

modes = eemd(y, imf, NR, Nstd); % Output IMFs using eemd function

subplot(10,1,1,'align'), plot(t, x,'b');
ylabel('Signal');
title('EEMD Decomposition','fontsize', 14);

for i=1:9
subplot(10,1,1+i,'align'), plot(t, IMF(:,i),'LineWidth',0.7);
y_titre = sprintf('IMF%d',i);
   ylabel(y_titre);
set(gca,'XColor', [0.37,0.37,0.37],'YColor', [0.30,0.30,0.30]);
end

xlabel('Time (s)','Color','k', 'fontsize', 14);
set(gca,'XColor','k','fontsize', 14)

tic;         %   Calculate processing time
modes = eemd(y, 9, 5000, 0.2);
toc
Elapsed time is 192.775861 seconds.
```

Selecting Power Quality (PQ) data

```
%   This MATLAB script is used to select dataset among subsets
%   Author: Bruna Molinari, Douglas Renaux (2020)
%   Cited in the "Reference" section.
%

function [loads] = ChoiceOfLoads(subset)
```

```
    if(strcmp(subset,'Synthetic'))

        loads_1 =
["1A0";"1B0";"1C0";"1D0";"1E0";"1F0";"1G0";"1H0";"1I0";"1J0";"1K0";"1L0";"1M0"; ...
 "1N0";"1O0";"1P0";"1Q0";"1R0";"1S0";"1T0";"1U0";"1V0";"1W0";"1X0";"1Y0";"1Z0"];

        loads_2 =
["2A0B0";"2A0H0";"2A0L0";"2A0M0";"2A0N0";"2A0Q0";"2B0A0";"2B0H0";"2B0L0";"2B0M0";...

"2B0N0";"2B0Q0";"2H0A0";"2H0B0";"2H0L0";"2H0M0";"2H0N0";"2H0Q0";"2L0A0";"2L0B0";...

"2L0H0";"2L0M0";"2L0N0";"2L0Q0";"2M0A0";"2M0B0";"2M0H0";"2M0L0";"2M0N0";"2M0Q0";...

"2N0A0";"2N0B0";"2N0H0";"2N0L0";"2N0M0";"2N0Q0";"2Q0A0";"2Q0B0";"2Q0H0";"2Q0L0";...
                    "2Q0M0";"2Q0N0"];

        loads_3 =
["3B0K0D0";"3D0Q0I0";"3D0Q0N0";"3D0Y0S0";"3E0N0Q0";"3H0P0W0";"3M0R0W0";"3M0R0X0";...

"3M0W0I0";"3N0S0I0";"3P0U0Z0";"3P0Z0H0";"3Q0K0B0";"3Q0X0E0";"3R0E0S0";"3S0E0Y0";...

"3S0I0Y0";"3T0Q0N0";"3T0V0M0";"3U0N0Z0";"3U0R0Y0";"3U0T0H0";"3V0D0M0";"3V0H0X0";...

"3V0M0Q0";"3W0E0H0";"3W0E0T0";"3W0I0Z0";"3X0D0P0";"3X0N0R0";"3Y0P0U0";"3Y0T0E0";...
                    "3Z0P0V0"];

        loads_8 =
["8D0G0P0Q0M0N0H0E0";"8D0M0S0G0H0N0R0E0";"8E0P0I0M0N0H0W0Y0";"8I0E0H0D0M0N0U0Z0";...
                    "8Q0H0N0M0P0E0I0V0";"8X0E0H0I0M0P0N0D0"];

        loads = sort([loads_1; loads_2; loads_3; loads_8]);


elseif(strcmp(subset,'Sim_Ideal')||strcmp(subset,'Sim_Induct')||strcmp(subset,'Sim_Induc
t_Harmo')...

||strcmp(subset,'Sim_Induct_Harmo_SNR_10')||strcmp(subset,'Sim_Induct_Harmo_SNR_30')...
          ||strcmp(subset,'Sim_Induct_Harmo_SNR_60'))

        loads_1 =
["1A0";"1B0";"1C0";"1D0";"1E0";"1F0";"1G0";"1H0";"1I0";"1J0";"1K0";"1L0";"1M0"; ...

"1N0";"1O0";"1P0";"1Q0";"1R0";"1S0";"1T0";"1U0";"1V0";"1W0";"1X0";"1Y0";"1Z0"; ...
                    "1A1";"1B1"];

        loads_2 =
["2Y0G0";"2O0S0";"2Y0X0";"2S0D0";"2J0G0";"2K0X0";"2Z0G0";"2A1J0";"2F0I0";"2R0M0"; ...

"2J0W0";"2I0O0";"2Y0E0";"2V0U0";"2K0B0";"2A0B0";"2N0T0";"2A1F0";"2P0M0";"2A0K0"; ...

"2D0V0";"2Q0O0";"2E0Q0";"2H0R0";"2T0U0";"2N0C0";"2F0Y0";"2E0W0";"2P0A1";"2C0L0"];

        loads_3 =
["3T0P0W0";"3Y0F0J0";"3M0A1E0";"3X0B0J0";"3F0L0Z0";"3D0Y0G0";"3K0P0D0";"3I0G0Q0";...
```

```
"3X0A1S0";"3K0O0U0";"3Z0X0V0";"3H0Q0A0";"3K0I0E0";"3F0U0C0";"3Q0M0S0";"3T0R0A0";...

"3B0I0N0";"3D0L0V0";"3U0A1E0";"3J0C0P0";"3W0L0C0";"3H0N0B1";"3M0O0B1";"3Y0N0B1";...
                    "3R0Z0W0";"3S0H0R0";"3T0B0G0";"3G0O0V0";"3J0V0R0";"3A0Q0K0"];

        loads_4 =
["4Z0A0M0J0";"4M0X0I0T0";"4N0A0E0S0";"4A1E0V0P0";"4F0T0G0W0";"4H0X0E0B1"; ...

"4C0P0R0N0";"4L0B0Q0Z0";"4V0Z0F0B1";"4G0D0O0L0";"4M0Y0W0I0";"4S0B1V0U0"; ...

"4H0Q0P0N0";"4Y0H0I0C0";"4X0R0M0P0";"4B0R0O0S0";"4O0A1F0C0";"4D0B0W0L0"; ...

"4G0X0Q0T0";"4A1B1E0D0";"4A0C0N0Z0";"4Y0N0A1Q0";"4U0O0J0D0";"4Q0H0B0S0"; ...

"4G0L0R0I0";"4U0K0R0Z0";"4M0A0I0K0";"4Y0F0V0K0";"4H0K0T0J0";"4W0U0J0F0"];

        loads_5 =
["5W0Z0I0Q0K0";"5H0U0K0V0B1";"5O0Z0E0D0P0";"5L0U0V0T0H0";"5O0C0A1D0Q0"; ...

"5N0F0M0J0B0";"5A1H0I0R0N0";"5W0X0Z0A0U0";"5R0A1N0L0T0";"5G0N0X0O0U0"; ...

"5A1G0H0Q0C0";"5R0B1S0W0X0";"5V0T0Y0O0A0";"5D0Z0M0L0F0";"5P0R0A0B1I0"; ...

"5B0S0F0D0E0";"5E0F0B0P0G0";"5P0S0M0N0K0";"5D0J0G0V0W0";"5F0I0Q0K0E0"; ...

"5A1C0B1K0Y0";"5R0P0B0T0B1";"5S0B0W0X0Y0";"5Y0V0N0E0J0";"5D0A0Y0H0Z0"; ...

"5J0M0Q0A0U0";"5P0X0J0L0B0";"5W0R0I0E0C0";"5B1O0S0Y0G0";"5L0M0T0U0C0"];

        loads = sort([loads_1; loads_2; loads_3; loads_4; loads_5]);

    elseif strcmp(subset,'Natural')
        loads = ["7H2A2B2C2K2F2D2"];
    else
        disp('Subset not avaiable yet')
        loads = 0;
    end
end
```

Converting binary data to Matlab file format (LIT_bin2mat.m)

```
%   This MATLAB script is used to extract binary data from the LIT-Dataset
%   RAW_Data files and construct MATLAB arrays from this data for further
%   processing. MATLAB arrays are saved in .mat files.
%   Author: Bruna Molinari, Douglas Renaux (2020)
%   Cited in the "Reference" section.
%   Edited by Jan Ali, last edited: 16th Apr. 2021

% 1 - Select a subset:
% Type = char array
%  Options =
%                   º 'Natural'
```

```
%                     º 'Synthetic'
%                     º 'Sim_Ideal'
%                     º 'Sim_Induct'
%                     º 'Sim_Induct_Harmo'
%                     º 'Sim_Induct_Harmo_SNR_10'
%                     º 'Sim_Induct_Harmo_SNR_30'
%                     º 'Sim_Induct_Harmo_SNR_60'

 subset = 'Natural';

% 2 - Build list of loads for this subset
loads_set = ChoiceOfLoads(subset);

% 3 - Reference directory and search path

r_dir = fileparts(mfilename('fullpath'));

cd(r_dir)
cd('C:\Users\latif\OneDrive\Documents\MATLAB\Examples\R2020a\matlab\LIT_Dataset')

addpath(genpath(pwd))


% 4 - Number of loads to change the files
L = length(loads_set);
file_offset_in_loadset = 0;
current_numLoads = "1";

% 5- Loop for all loads in load set
for n = 1:L

    % Determines the amount of strokes (angle variation) in each
    % acquisition.
    [n_t, numLoads] = NumberOfTraces(subset, loads_set(n,:));
    if ~ strcmp(current_numLoads,numLoads)
        current_numLoads = numLoads;
        file_offset_in_loadset = 0;
    end

    for trace = n_t
        % Create one .mat for each database file
        if strcmp(subset,'Natural')
            if (false == CreateStructLIT_nat(subset, loads_set(n,:), trace,
file_offset_in_loadset))
                break;
            end
        else
            CreateStructLIT(subset, loads_set(n,:), trace, file_offset_in_loadset);
        end
    end
    file_offset_in_loadset = file_offset_in_loadset + length(n_t);
end
```

Published with MATLAB® R2020b